CHARLES UNIVERSITY

Faculty of Pharmacy

in Hradec Králové

The Dissertation

Viriyanata Wijaya, M.Sc.

Alkaloids of *Dicranostigma franchetianum* (Prain) Fedde and their selected biological activity

Department of Pharmacognosy and Pharmaceutical Botany

Supervisor: Prof. RNDr. Lubomír Opletal, CSc.

Branch of study: Pharmacognosy and Nutraceuticals

August 2023

The Declaration

I declare that the material contained within this Thesis is original and contains no material which has been accepted for a degree or diploma by either the University or any other institution, except by way of background information and duly acknowledged in the Thesis. To the best of my knowledge and belief, this Thesis contains no material previously published or written by another person except where due acknowledgement is made in the text of the Thesis.

Hradec Králové, August 2023 Viriyanata Wijaya, M.Sc.

Acknowledgements

All praises to Siddharta Gautama as a Buddha who has wisdom and compassion for every Buddhist made me more blessed during and to complete my doctoral studies in the Faculty of Pharmacy, Charles University.

This dissertation was supported by Specific scientific research of Charles University, Faculty of Pharmacy in Hradec Králové (SVV 260 548). It was cofinanced by the Research Programme of the Faculty of Pharmacy called PROGRES Q42 that deals with both traditional and newly discovered medicinal plants and their secondary metabolites.

I would like to say many thanks to all the members of ADINACO research group, especially my supervisor, Prof. RNDr. Lubomír Opletal, CSc. for his guidance throughout my studies, and also Dr. Jakub Chlebek for his advice and critics. I would say a lot gratitude to the Department of Pharmaceutical Botany and in particular, Prof. Lucie Cahlíková, PhD. as head of the department who gave this valuable opportunity to study and carried out research with the help of all of my colleagues, whom I have to mention their names are Eliška Kohelová, PhD. and Jaroslav Jenčo, PhD., who helped me for separation and purification of alkaloids by flash chromatography and HPLC-MS; Marcela Šafratová, PhD. who helped me to measure compounds in GC-MS and ESI-MS; Anna Hošťálková, Kateřina Hradiská Breiterová, and Daniela Hulcová were ready to answer all of my questions during my studies, and other ADINACO's Doctorate students and alumni (Abdullah Al Mamun, Negar Maafi, Latifah Al Shammari, Rudolf Vrabec, Filip Pidaný, Rozálie Peřinová, and Aneta Ritomská) for giving me support and motivation until I finished my studies.

I would not be able to analyse the elucidation of the structure and determine some biological activities without the cooperation of other departments in this faculty and universities. Therefore, I should thank to Prof. Jiři Kuneš, PhD. and Jana Křoustková, PhD. (interpretation of molecular structure by NMR spectra analysis) and other colleagues who helped me determine some biological activities, such as antimycobacterial activity and prolyloligopeptidase inhibition. In addition, I would like to thank Rudolf Vrabec for helping analyse the structure of compounds with *in silico* molecular docking studies.

Furthermore, I would like to thank my deceased grandmother, my parents, my family, and my friends in Indonesia, who motivate and support me in studying in the Czech Republic.

Finally, I would like to thank you for the financial support of the following grants: Specific scientific Research SVV UK 260 548 of Charles University, and by project, "Modernization and Extension of the Doctoral Study Field of Pharmacognosy and Toxicity of

Natural Products" in the study program Pharmacy (reg. No. CZ.02.2.69/0.0/0.0/16_018/0002736).

Table of contents

ABBREVIATIONS

4-HPAA	4-hydroxyphenylacetaldehyde
4'-OMT	4'-*O*-methyltransferase
6OMT	Norcoclaurine 6-*O*-methyltransferase
Aβ	Amyloid-β
AA	Arachidonic Acid
AD	Alzheimer's disease
AhR	Aryl hydrocarbon receptor
AIDS	Acquired immune deficiency syndrome
AMP	Adenosine monophosphate
AMPK	Adenosine monophosphate-activated protein kinase
AP-1	Activator protein-1
APH	Acetyl phenyl hydrazine
AsPC-1	Human pancreas adenocarcinoma ascites metastasis
ATCh	Acetylthiocholine
ATCC	American Type Culture Collection
ATP	Adenosine Triphosphate
BACE-1	Beta-site APP Cleaving Enzyme-1, Beta-secretase-1
BAX	Bcl-2-associated X protein
BBB	Blood-brain barrier
BBE	Berberine bridge enzyme
BBR	Berberine
BCG	Bacillus Calmette Guérin
Bcl-2	B-cell lymphoma-2
BTCh	Butyrylthiocholine
CA	Carrageenan
CAT	Catalase
Caco2	Human colorectal adenocarcinoma cells
CCK-8	Cell Counting Kit-8
CCL-2	Chemokine (C-C motif) ligand 2
CCl_4	Carbon tetrachloride
Cdc25C	Cell division cycle 25C
$CDCl_3$	Deuterated Chloroform
CD_3OD	Deuterated Methanol
CEM/ADR5000	Adryamicin-resistant lymphoblastic leukaemia cells
$CHCl_3$	Chloroform
ChEs	Cholinesterases
Chk	Checkpoint kinase
CheSyn	Cheilantifoline Synthase
CHx	Cyclohexane
CNS	Central nervous system
CNMT	Coclaurine *N*-methyl transferase

COVID-19	Coronavirus disease of 2019
COX	Cyclooxygenase
CPX	Ciprofloxacin
CYP	Cytochrome P-450
DAD	Diode Array Detector
DBOX	Dihydrobenzophenanthridine alkaloid oxidase
DMSO	Dimethylsulfoxide
DOPA	L-dihydroxyphenylalanine
DTNB	5,5'-dithio-bis(2-nitrobenzoic) acid
EC_{50}	Half maximal effective concentration
ELISA	Enzyme-linked immunosorbent assay
EI-MS	Electron Ionization-Mass Spectrometry
EROD	7-ethoxyresorufin-O-deethylase
ESI-HRMS	Electrospray Ionization-High Resolution Mass Spectrometry
Et_2NH	Diethyl amine
Et_2O	Diethyl ether
EtOAc	Ethyl acetate
EtOH	Ethanol
FAD	Flavin Adenine Dinucleotide
G-6-PD	Glucose-6-phosphate dehydrogenase
GC	Gas chromatography
GC/MS	Gas chromatography/mass spectrometry
GPT	Glutamic pyruvic transaminase
GPx	Glutathione peroxidase
GSK-3β	Glycogen synthase kinase-3 beta
*h*AChE	Human acetylcholinesterase
*h*BuChE	Human butyrylcholinesterase
H_2O	Water
H_2O_2	Hydrogen Peroxide
H_2SO_4	Sulfuric Acid
HEK293	Human embryonic kidney 293
HepG2	Human hepatoma cells
HCC	Hepatocellular carcinoma
HCl	Hydrochloric acid
HCT116	Human colorectal cancer cell 116
HIV	Human immunodeficiency virus
HPLC	High Performance Liquid Chromatography
HT29	Human colorectal adenocarcinoma 29
Huh7	Human hepatoma 7
IAs	Isoquinoline alkaloids
IC_{50}	Half maximal inhibitory concentration
ICD	Isocorydine

IL-1β	Interleukin-1β
IL-6	Interleukin-6
IL-10	Interleukin-10
INH	Isoniazid
iNOS	Inducible nitric oxide synthase
κB	Kappa B
KCl	Kalium chloride
Ki	Inhibitory constant
LC	Liquid Chromatography
LDH	Lactate dehydrogenase
LnCaP	Lymph node carcinoma of the prostate
LPS	Lipopolysaccharide
mRNA	Messenger ribonucleic acid
NaCl	Sodium Chloride
m/z	mass-to-charge ratio
MAO-A	Monoamine Oxidase Type A
MAPK	Mitogen-activated protein kinase
MCF-7	Michigan Cancer Foundation-7
MCP-1	Monocyte chemoattractant protein-1
MDA	Malondialdehyde
MDR	Multiple drugs resistant
MeOH	Methanol
MHz	Mega Hertz
MIC	Minimum Inhibitory Concentration
MMP-2	Matrix metalloproteinase-2
MMP-9	Matrix metalloproteinase-9
MS	Mass spectrum/spectrometry
MSH	*N*-methylstylopine 14-hydroxylase
Mtb	*Mycobacterium tuberculosis*
N2a	Neuroblastoma-2a
Na_2CO_3	Sodium Carbonate
NaOH	Sodium Hydroxide
NCS	Norcoclaurine synthase
NF-κB	Nuclear factor-kappa B
NMR	Nuclear magnetic resonance
NO	Nitric Oxide
OADC	Oleic Albumin Dextrose Catalase
ODS-BP	Octadesyl silane-bonded phase
P6H	Protopine 6-hydroxylase
PAF	Platelet Activating Factor
PAMPA	Parallel artificial membrane permeability assay
PAS	Peripheral Anionic Site

PB	Phosphate Buffer
PBS	Phosphate Buffer Saline
PGE2	Prostaglandin E2
PLC	Phospholipase C
PP	Polypropylene
PRF	Platelet Rich Fibrin
p-CDK1	Phospho-cyclin dependent kinase 1
pH	Potential of Hydrogen
POP	Prolyloligopeptidase
Q-TOF	Quadrupole-Time of Flight
RIF	Rifampicin
RNMT	RNA guanine-7 methyltransferase
RP	Reverse phase
SalS	Salutaridine synthase
SCC	Squamous cell carcinoma
SEM	Standard Error of the Mean
SiRNA	Small interfering ribonucleic acid
SQ-20B	Human squamous cell carcinoma-20B
SMT	Scoulerine 9-O-methyltransferase
SOD	Superoxide dismutase
STAT3	Signal transducer and activator of transcription 3
STORR	(S)-Reticuline to (R)-reticuline
STOX	(S)-tetrahydroprotoberberine oxidase
StySyn	Stylopine Synthase
TB	Tuberculosis
TFAA	Trifluoroacetic acid
THBO	Tetrahydroberberine oxidase
THP-1	Human monocytic cell line
TIC	Total Ion Chromatogram
TLC	Thin Layer Chromatography
TNF-α	Tumour necrosis factor-alpha
TNMT	Tetrahydroprotoberberine *N*-methyltransferase
To	Toluene
TXA_2	Thromboxane A2
TYDC	Tyrosine/DOPA decarboxylase
UHPLC	Ultra high-performance liquid chromatography
UV	Ultraviolet
VEGF	Vascular endothelial growth factor
WHO	World Health Organization

LIST OF FIGURES

LIST OF TABLES

1 INTRODUCTION

Based on data from the World Health Organisation (WHO), 80% of people still depend on medicinal plants as primary health care [1, 2]. The knowledge of traditional medicine knowledge (alternative or complementary products) has encouraged further research of medicinal plants to turn to potential medicines and led to the isolation of many natural products that become prominent pharmaceuticals [3].

Natural products are widely identified as something generated in life (for example, wood, silk, bioplastics, cornstarch, milk, and plant extracts), whereas more deeply natural products are identified as any organic compounds synthesised with a living organism through a synthetic or semisynthetic process which less or more alters their biological activities. Phytochemicals are the chemical constituent of plants that are active physiologically in the human body. The main bioactive compounds, called phytochemicals, consist of alkaloids, phenolics (tannin and flavonoids), and terpenes [4].

Alkaloids are one of the largest groups of natural products, so far more than 12.000 alkaloids belonging to different structural types have been isolated and identified from various plant families such as Papaveraceae, Amaryllidaceae, Solanaceaea, Apocynaceae, etc. Many alkaloids still possess prominent places in modern pharmacotherapy. Alkaloids used in medications are often used in life-threatening conditions, for example, paclitaxel (originally isolated from *Taxus brevifolia*, Taxaceae) and its derivatives are applied against ovarian carcinoma, breast cancer, lung, as well as Kaposi´s sarcoma; dimeric alkaloids from Madagascar periwinkle (*Catharanthus roseus*, Apocynaceae) vincristine and vinblastine are frequently used against leucemia and lymphoma. Morphine from opium poppy (*Papaver somniferum*, Papaveraceae) and its derivatives are indispensable for the treatment of severe pain [5, 6].

Among the most numerous groups of alkaloids belongs isoquinoline alkaloids (IAs), which are derived from the amino acids tyrosine. They are widely distributed in plants from the families Papaveraceae, Rutaceae, Berberidaceae, Menispermaceae, Ranunculaceae, and Annonaceae [7-9]. Several species of Magnoliaceae and Convolvulaceae are also rich in these alkaloids and have been intensively investigated for their various biological activities [10]. On the basis of different degrees of oxygenation, intramolecular rearrangements, distribution, and the presence of additional rings connected to the main system, they may be divided into eight subgroups: benzylisoquinoline, aporphine, protoberberine, benzo[*c*]phenanthridine, protopine, phthalide isoquinoline, morphinan, and emetine alkaloids. Among the listed subgroups, protoberberines are the largest group: They constitute 25% of all elucidated structures of

isoquinoline alkaloids, making them the most widespread secondary metabolites containing nitrogen among natural products [11-13].

The genus *Dicranostigma* is a small genus of the Papaveraceae family with eight accepted species native to the Himalayas and western China [14, 15]. Plants of this genus are also known as eastern horned poppies. Some species of *Dicranostigma* have been investigated in several phytochemical and pharmacological studies. Until now, more than 30 isoquinoline alkaloids (IAs) of different structural scaffolds have been identified or isolated from the genus *Dicranostigma* [14, 16-18]. Alkaloids from *Dicranostigma* plants have been intensively investigated for their promising activities, such as anti-inflammatory, antibacterial, antiviral, and hepatoprotective effects [19-21].

Dicranostigma franchetianum (Prain) Fedde is a bushy herbaceous annual plant native to western China. In Europe, the herb is known as a cultivated plant in botanical gardens. So far, 13 IAs have been isolated from this species, including berberine, protopine, chelerythrine, and sanguinarine [22-25].

Important biological activities of IAs, together with the absence of a detailed current phytochemical report on *D. franchetianum*, encouraged us to examine this species in detail within the dissertation thesis.

2 AIMS OF THE DISSERTATION

The main aims of this dissertation were the isolation and identification of isoquinoline alkaloids from the concentrated alkaloidal extract prepared from the fresh aerial part of *Dicranostigma franchetianum* (Papaveraceae). Subsequently, the isolated compounds were screened for various biological activities to identify attractive structures for more detailed studies.

The partial aims were:

- detailed research of the literature that mentions alkaloids of the genus *Dicranostigma* and their biological activity,
- isolation of the wide spectrum of alkaloids from the concentrated alkaloidal extract of *D. franchetianum*,
- determination of their structures based on their physical and chemical properties (NMR, MS, optical rotation, etc.)
- screening of biological activities of isolated alkaloids,
- selection of the most active alkaloids for further detailed biological studies or preparation of semisynthetic derivatives.

3 THEORETICAL PART

3.1 Papaveraceae family

The Papaveraceae plant family consists of approximately 42 genera and approximately 775 known species [3] of flowering plants in the order Ranunculales, informally known as the poppy family species [7]. Plants of this family are distributed throughout the world, occurring in temperate and subtropical climates (mostly in the northern hemisphere), on the other hand, they are almost unknown in the tropics. Most of them are herbaceous plants, but some are shrubs and small trees. The family is well known for its striking flowers, with many species grown as ornamental plants, including the California poppy (*Eschscholtzia californica*, the California state flower), stunning blue Himalayan poppies (*Meconopsis*), several species of *Papaver*, and the wildflower bloodroot (*Sanguinaria canadensis*). Two species are of economic importance for the production of opium alkaloids for pharmaceutical purposes. *Papaver somniferum* is grown legally to obtain morphine and other morphine alkaloids, and *P. bracteatum* is used for the isolation of thebaine. *Papaver somniferum* is also the source of the poppy seeds used in cooking and baking, and the oil of the poppy seeds.

Phytochemically, plants in the Papaveraceae family are characterised by the presence of different types of IAs. The most important IAs are opiate/morphine alkaloids which belong to the large biosynthetic group of isoquinoline alkaloids. The major psychoactive morphine alkaloids are morphine, codeine, and thebaine. Papaverine, noscapine, and approximately 24 other alkaloids are also present in opium but have little or no effect on the human central nervous system (CNS) [9]. Since morphine, as the first alkaloid from *P. somniferum, was* isolated in 1817 by Sertürner, many researchers focused on developing the discipline of natural product isolation, which consequently led to an increasing number of isolated alkaloids rapidly afterwards [26]. Some alkaloids have been extensively used in modern pharmacotherapy as drugs, for example, atropine is used as an antidote against intoxication with nerve agents and insecticides, morphine and its derivatives are still crucial as analgesic substances, noscapine has antimitotic activity against various cell cancers, sanguinarine has antibacterial activity against methicillin-resistant *Staphylococcus aureus*, protopine has anticholinergic effects due to inhibition activity of acetylcholine in the nervous system, and berberine exhibited promising cytotoxic activity with as low side effects as vinblastine and paclitaxel [5, 27-32].

3.2 The tribe Chelidonieae

The Chelidonieae tribe of the Papaveraceae family comprises 8 genera and 23 species and is mainly distributed in the northern temperate zone. The genera belonging to this section are the following: *Sanguinaria*, *Eomecon*, *Macleaya*, *Bocconia*, *Stylophorum*, *Hylomecon*, *Dicranostigma,* and *Chelidonium*. Plants in these genera contain biologically active compounds and many of them have been used as folk medicine for centuries, especially in China and western countries [8]. *Chelidonium majus* has been used as a traditional medicine for bile and liver disorders in both China and Europe for a long history, and its fresh latex has also been used in the treatment of many skin complaints, such as corns, eczema, tinea infections, and skin tumours [33]. Native Americans used *Sanguinaria canadensis* to treat ulcers and sores, croup, burns, tapeworms, fever, diarrhoea, and irregular periods [34]. The further traditional use of Chelidonieae plants is summarised in Table 1.

Table 1. Traditional uses of selected Papaveraceae plants from the Chelidonieae tribe

Plants	Part of the plant used	Therapeutic effects	Main Alkaloids	Ref.
Chelidonium majus L.	Roots, stems, leaves	Analgesic, antispasmodic, cholecystagogic, antibacterial, applicable to cholecystitis and hepatitis	Chelidonine	[8]
Dicranostigma leptopodum (Maxim.) Fedde	Aerial parts	Analgesic, spasmolytic for coronary arteries	Isocorydine	[8]
Stylophorum lasiocarpum (Oliv.) Fedde	Whole plant	CNS depressant may be used as a sedative	Tetrahydrocoptisine	[8]
Eomecon chionantha Hance	Fruit	Analgesic, prolonged sleeping time, antibacterial Antibacterial, local anaesthetic	Chelerythrine Sanguinarine	[8]

3.3 Chemical constituents of the tribe Chelidonieae

So far, more than 170 compounds have been isolated and identified from the plants of the tribe Chelidonieae, including alkaloids, amides, organic acid, aromatics, triterpenoids, steroids, and other constituents. Most phytochemical studies have focused on the isolation and structural identification of isoquinoline alkaloids since they are the main components of this tribe. IAs form one of the largest groups among alkaloids. They can be further classified on the basis of their different chemical basic structures. The most common structural types are benzylisoquinolines, aporphines, protoberberines, protopines, benzophenanthridines, morphinanes and others [35]. According to current knowledge, a total of about 2500 isoquinoline alkaloids are known today, which are mainly synthesised by plants [35].

3.4 Biosynthesis of isoquinoline alkaloids: S-reticuline pathway

The biosynthesis of isoquinoline alkaloids in plants starts with the decarboxylation of tyrosine or L-dihydroxyphenylalanine (DOPA) to obtain 4-hydroxyphenylacetaldehyde (4-HPAA) and L-dopamine, independently, under the catalyzation of tyrosine/DOPA decarboxylase (TYDC) in Figure 1. Furthermore, the condensation of L-dopamine and 4-HPAA are catalysed by norcoclaurine synthase (NCS) to afford (S)-norcoclaurine as the first isoquinoline scaffold in plants. Four additional enzymatic steps, norcoclaurine 6-*O*-methyltransferase (6OMT), (*S*)-coclaurine *N*-methyltransferase (CNMT), (S)-*N*-methylcoclaurine 3'-hydroxylase (CYP80B), and 3'-hydroxy-N-methylcoclaurine. 4'-*O*-methyltransferase (4'OMT) catalyses 6-*O*-methylation, *N*-methylation, 3'-hydroxylation and 4'-*O*-methylation, respectively, resulting in the central intermediate (*S*)-reticuline. Next, internal carbon-carbon, carbon-oxygen phenol coupling, and functional group substitutions as various additional reactions, can lead in the formation of different types of IAs [36].

(*S*)-Reticuline is a general precursor to the majority of benzylisoquinoline alkaloids. The first step carried out in the biosynthesis of benzophenanthridine and protoberberine alkaloids is catalyzed by the FAD-dependent oxidoreductase berberine bridge enzyme, which catalyzes oxidation and methylene bridge formation of (*S*)-reticuline to obtain (*S*)-scoulerine [37].

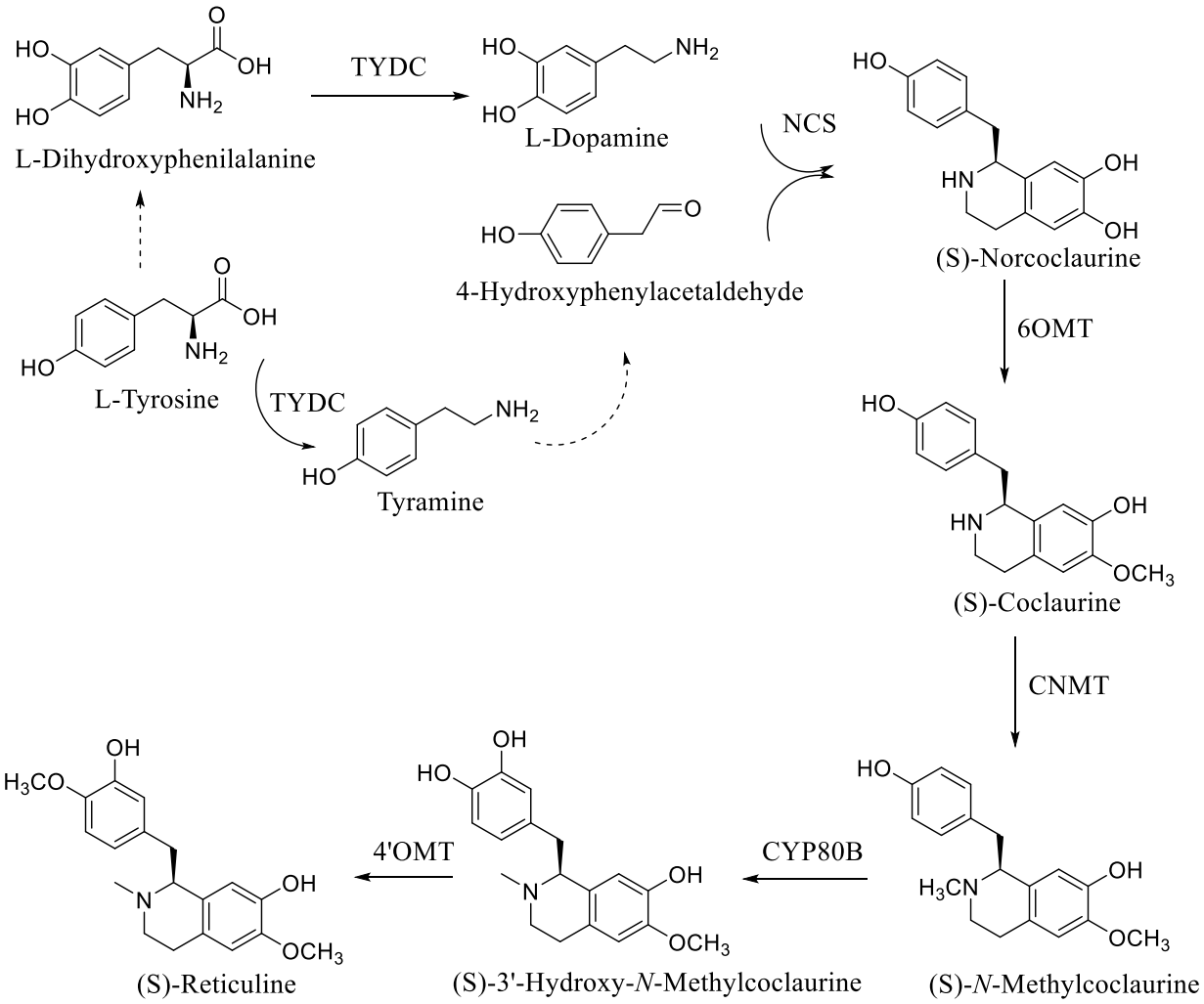

Fig. 1. Biosynthetic pathway of isoquinoline alkaloids

(*S*)-Scoulerine, a key intermediate in the biosynthesis of other structural types of IAs, is created from (*S*)-reticuline under catalysis of the berberine bridge enzyme (BBE). The biosynthesis then continues with the formation of further structural types of IAs: protopine-, benzophenanthridine-, protoberberine-, phtalidisoquinoline-type, and other minor structural types. Within the second branch of biosynthesis of IAs, (*S*)-reticuline is converted to (*R*)-reticuline, and further biosynthetic steps lead to the formation of a morphinane scaffold (Fig. 2) [38].

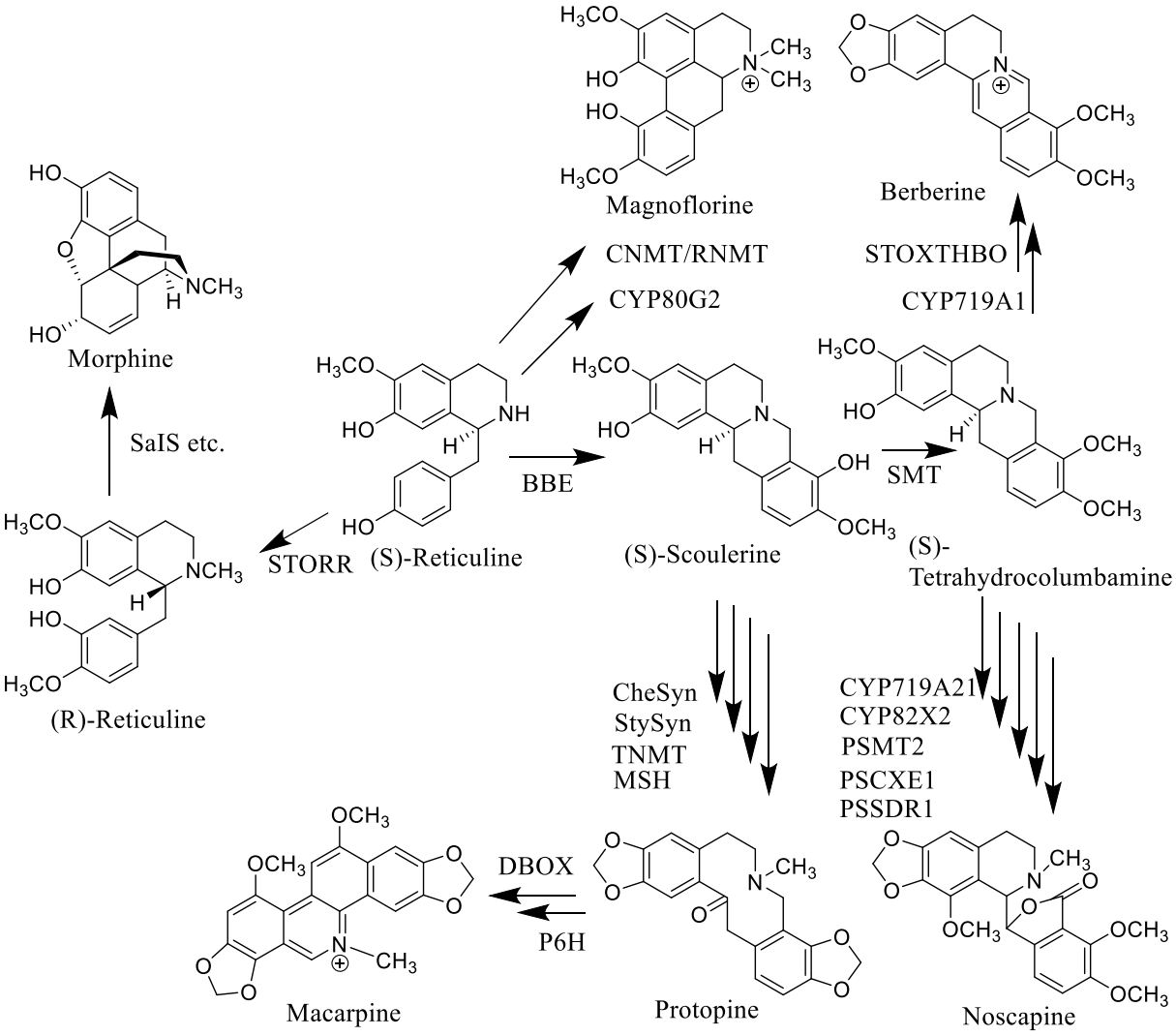

Fig. 2. Overview of the formation of various structural types of isoquinoline alkaloids

3.5 Genus *Dicranostigma* Hooker f. & Thomson (Papaveraceae)

Dicranostigma is a small genus of the Papaveraceae family with eight accepted species native to the Himalayas and western China. Plants of this genus are also known as eastern horned poppies. Although resembling the true horned poppies of *Glaucium*, they have stigmas with two lobes and fruit with only traces of "horns".

The genus *Dicranostigma* has been established by Hooker & Thomson. in 1885 with only a single species *D. lactucoides* [39]. In 1985, Chengyih and Hsuan of the Kunming Institute of Botany described two species of the genus *Dicranostigma, D. platycarpum* and *D. iliensis* [40]. The genus *Dicranostigma* consists of three or four closely similar species, particularly distributed in central and western China, southern Tibet (Xizang), and the dry parts of the Himalayas, Nepal, and northern India [39]. Three species *D. platycarpum*, *D. lactucoides*, and

D. leptopodum are endemic to the Himalayas and adjacent areas, as well as in the Loess Plateau region in China [41].

These plants have been used for a long time in folk medicine to treat various diseases, especially in China. They have been used for the treatment of tonsillitis, hepatitis, sore throat, scrofula, bald scars, scabies, and others [42-44].

So far, three species of *Dicranostigma* have been investigated in several phytochemical and pharmacological studies. So far, more than 30 isoquinoline alkaloids (IAs) from different structural scaffolds (Table 2) have been identified or isolated from the genus *Dicranostigma* [14, 16-18]. Furthermore, alkaloids from *Dicranostigma* plants have also been investigated for their biological activities, such as anti-inflammatory, antibacterial, antiviral and hepatoprotective effects [19-21]. Most of these studies concentrated only on the basic screening of biological activities, and they were not concentrated on the identification of a mechanism of action.

3.5.1 Botany and morphology of phytochemically studied *Dicranostigma* species

3.5.1.1 *Dicranostigma franchetianum*

Dicranostigma franchetianum (Prain) Fedde is a herbaceous annual plant with a height of up to 50 cm and is distributed in western China [22]. It is an erect and branching plant that can form tufts of deeply cut leaves. A pearl-grey blooms from July to October and produces a large profusion of large yellow flowers [45]. In Europe, the herb is known as a cultivated plant in botanical gardens [39].

3.5.1.2 *Dicranostigma lactucoides*

Dicranostigma lactucoides Hook.f. & Thomson is a herb that grows as a biennial or short-lived perennial plant with a height from 15 to 60 cm and a length of roots 10-15 cm [41]. It is described as a small plant with flat rosettes and occurs in the northern Himalayas and the southern Tibetan Plateau; it can grow especially in moraines, river gravels, rocky sites, and stony slopes. *D. lactucoides* is a relatively small plant that has flat rosettes with very glaucous and obtuse-lobed leaves with thickened mucronate tips [39].

3.5.1.3 *Dicranostigma leptopodum*

Dicranostigma leptopodum (Maxim.) Fedde is widely distributed in western (Tibet, Qinghai and Gansu), east through Hebei, Henan, Shanxi and Shaanxi, and southward China through

Sichuan and Yunnan [41]. It flowers between March and July on mountain rocks, grassy slopes, roadsides, and field ridges. *D. leptopodum* is a large plant with tall 1 m that has more coarsely divided leaves and diameter flowers up to 5 cm with deep yellow or yellow - orange coloured. Furthermore, the fruit capsules have 8-14 cm long and are substantially large [39].

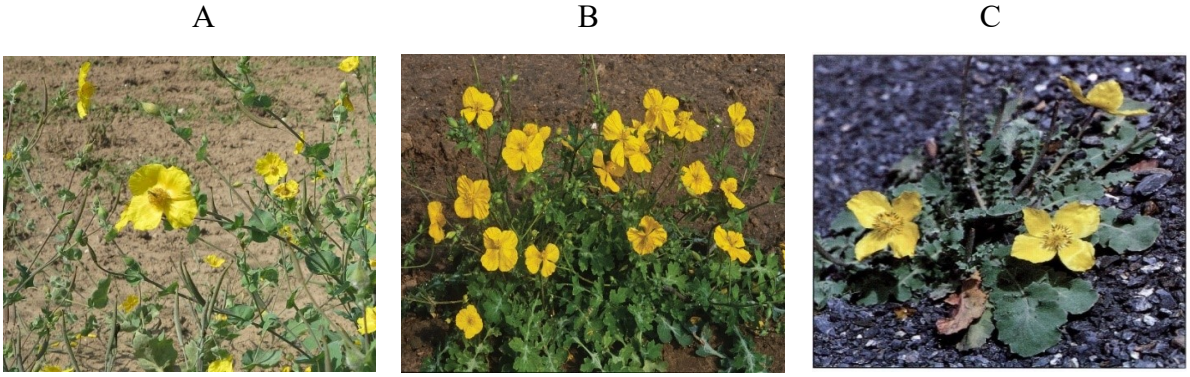

Fig. 3. Phytochemically studied species of the genus *Dicranostigma*: A (*D. franchetianum*), B (*D. lactucoides*)[46], C (*D. leptopodum*)[39].

3.5.2 Phytochemistry of the genus *Dicranostigma*

Altogether 33 IAs were identified or isolated from various parts of three species of *Dicranostigma* (Table 2). The isolated alkaloids belong to various structural types such as aporphine (**1-13**), benzophenanthridine (**14-19**), morphine (**20**), protoberberine (**21-26**), and protopine (**27-33**) types (Table 2, Figs. 4-5). Most phytochemical studies have been performed on *D. leptopodum*. Common separation techniques for the isolation of alkaloids have been used, such as column chromatography using silica gel and aluminium oxide as stationary phase, preparative TLC, and HPLC techniques. The widest spectrum of IAs has been isolated from different parts of *D. leptopodum.* As the main alkaloids have been identified in 1978 menisperine (**3**), magnoflorine (**4**), corytuberine (**10**) and isocorypalmine (**21**) [23]. In further research, five alkaloids have been isolated from this plant and identified as corydine (**1**), dicranostigmine (**2**), isocorydine (**6**), sinoacutine (**20**) and protopine (**31**) [14]. The study and research on the chemical composition of alkaloids from D. leptopodum bald flowers in 2011 resulted in the identification of 11 alkaloids, such as corydine (**1**), dicranostigmine (**2**), isocorydine (**6**), *N*-methylhernovine (**8**), 6-acetonyl-5,6-dihydrosanguinarine (**14**), dihydrosanguinarine (**15**), sinoacutine (**20**), allocryptopine (**28**), protopine (**31**), *cis*-protopinium (**32**), and *trans*-protopinium (**33**) [15]. Otherwise, two quaternary protoberberine alkaloids berberrubine (**24**) and 5-hydroxycoptisine (**26**), were isolated for the first time from the whole plants of *D. leptopodum* [44]. In the same year, other alkaloids were isolated from *D.*

leptopodum by repeated silica gel column chromatography 10-*O*-methylhernovine (**9**), corytuberine (**10**), nantenine (**12**), lagesianine A (**13**), and dihydrocryptopine (**30**). These isolated compounds were carried out with pharmacological activity, especially for cytotoxic tests against some tumour cell lines [19].

Furthermore, eight alkaloids including corydine (**1**), isocorydine (**6**), sinoacutine (**20**), berberine (**23**), berberrubine (**24**), 5-hydroxycoptisine (**26**), allocryptopine (**28**), protopine (**31**) were separated using HPLC chromatography with mobile phase for gradient elution using acetonitrile and 0.2% phosphoric acid solution adjusted to pH 6.32 with triethylamine and optimised by the SinoChrom ODS-BP column [16]. Isocorydione (**7**) and coptisine (**25**) were separated using the high-speed countercurrent chromatography method with purity 86.6 and 97.6 %, respectively [17]. Chelidonine (**16**), one of the benzophenanthridine types, was isolated for the first time using chromatographic column chromatography [42].

Table 2. Alkaloids reported in the genus *Dicranostigma*

	D. franchetianum	***D. lactucoides***	***D. leptopodum***
Aporphine-type			
Corydine **(1)**	[23]		[14, 16, 17, 19, 42, 47]
Dicranostigmine **(2)**			[14, 15]
Magnoflorine **(3)**	[23]	[23, 48]	[23, 49]
Menisperine **(4)**	[23, 24]	[23]	[23]
Glaucine **(5)**			[50]
Isocorydine **(6)**	[22-24]	[51]	[14-19, 23, 42, 47]
Isocorydione **(7)**			[18]
N-Methylhernovine **(8)**			[15]
10-*O*-Methylhernovine **(9)**			[19]
Corytuberine **(10)**	[24]		[19, 23]
Isocorytuberine **(11)**			[16]
Nantenine **(12)**			[19]
Lagesianine A **(13)**			[19]
Benzophenanthridine-type			
6-Acetonyl-dihydrosanguinarine **(14)**			[15]
Dihydrosanguinarine **(15)**			[15, 19]
Chelidonine **(16)**	[24, 25, 52]		[42]
Chelerythrine **(17)**	[23, 24]	[48, 51, 53, 54]	[23, 55]
Chelirubine **(18)**	[23, 24]	[48, 53]	[23]
Sanguinarine **(19)**	[23, 24]	[48, 51, 53, 54]	[23, 50, 55]
Morphine-type			
Sinoacutine **(20)**			[14, 15, 17]
Protoberberine-type			
Isocorypalmine **(21)**			[23]
Stylopine **(22)**	[24, 25, 52]		
Berberine **(23)**	[24]	[23, 53]	[16, 17]
Berberrubine **(24)**			[17, 44]
Coptisine **(25)**	[24]	[23, 53]	[16, 18]
5 – Hydroxycoptisine **(26)**			[16, 17, 44]
Corydaline **(27)**			[15]
Protopine-type			
Allocryptopine **(28)**	[23, 24]	[53]	[16-18, 23]
Cryptopine **(29)**			[55]
Dihydrocryptopine **(30)**			[19]
Protopine **(31)**	[23-25, 52]	[48, 51, 53]	[14, 16-19, 23, 42, 55]
cis-Protopinium **(32)**			[15]
trans-Protopinium **(33)**			[15]

In addition, other types of secondary metabolites, such as hopane triterpenes (dicranostigmone and erythrodiol-3-*O*-palmitate; Fig. 6) have been isolated from the whole parts of *D. leptopodum* [56].

Isocorydine (**6**) has been identified as the main component in a pilot phytochemical study of *D. franchetianum* [22]. Other alkaloids present at higher concentrations in this plant are protopine (**31**), chelidonine (**16**), and stylopine (**22**) [25, 52]. Allocryptopine (**28**), berberine (**23**), coptisine (**25**), sanguinarine (**19**), chelerythrine (**17**), chelirubine (**18**), menisperine (**4**) and corytuberine (**10**) were isolated from aerial parts and roots within an ongoing study [23, 24].

Separation of the alkaloidal extract from the upper parts of *D. lactucoides* resulted in isolation of berberine (**23**), coptisine (**25**), magnoflorine (**3**), and menisperine (**4**) [23]. Another study of isocorydine (**6**), sanguinarine (**19**), chelerythrine (**17**), and protopine (**31**) have been

identified as the main components of this plant [51]. The roots of *D. lactucoides* have been found to be a rich source of quaternary benzophenanthridine alkaloids chelerythrine (**17**) (about 3.43% of the dried roots) [48].

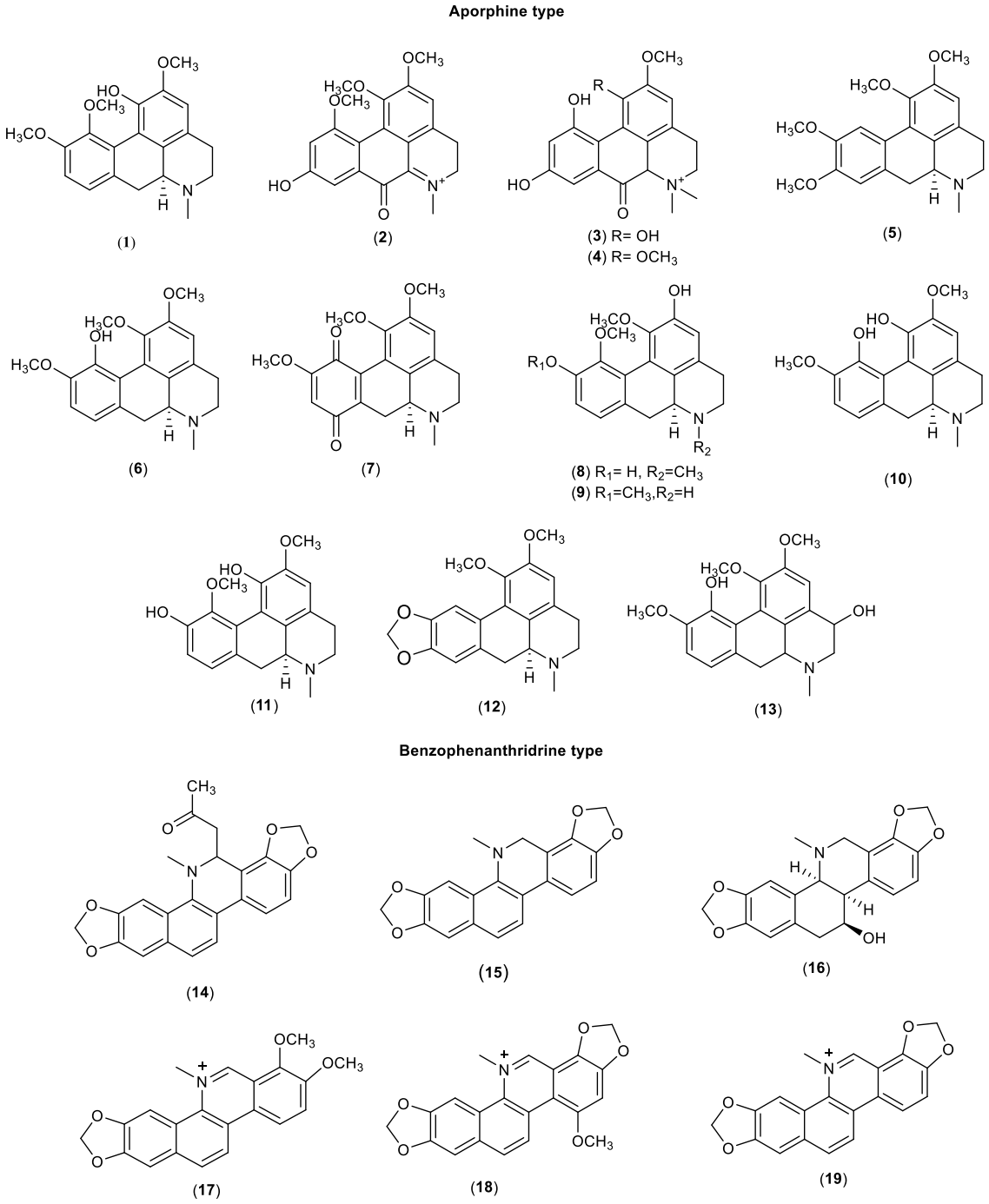

Fig. 4. Isoquinoline alkaloids of the aporphine and benzophenanthridine type isolated or identified in *Dicranostigma* species

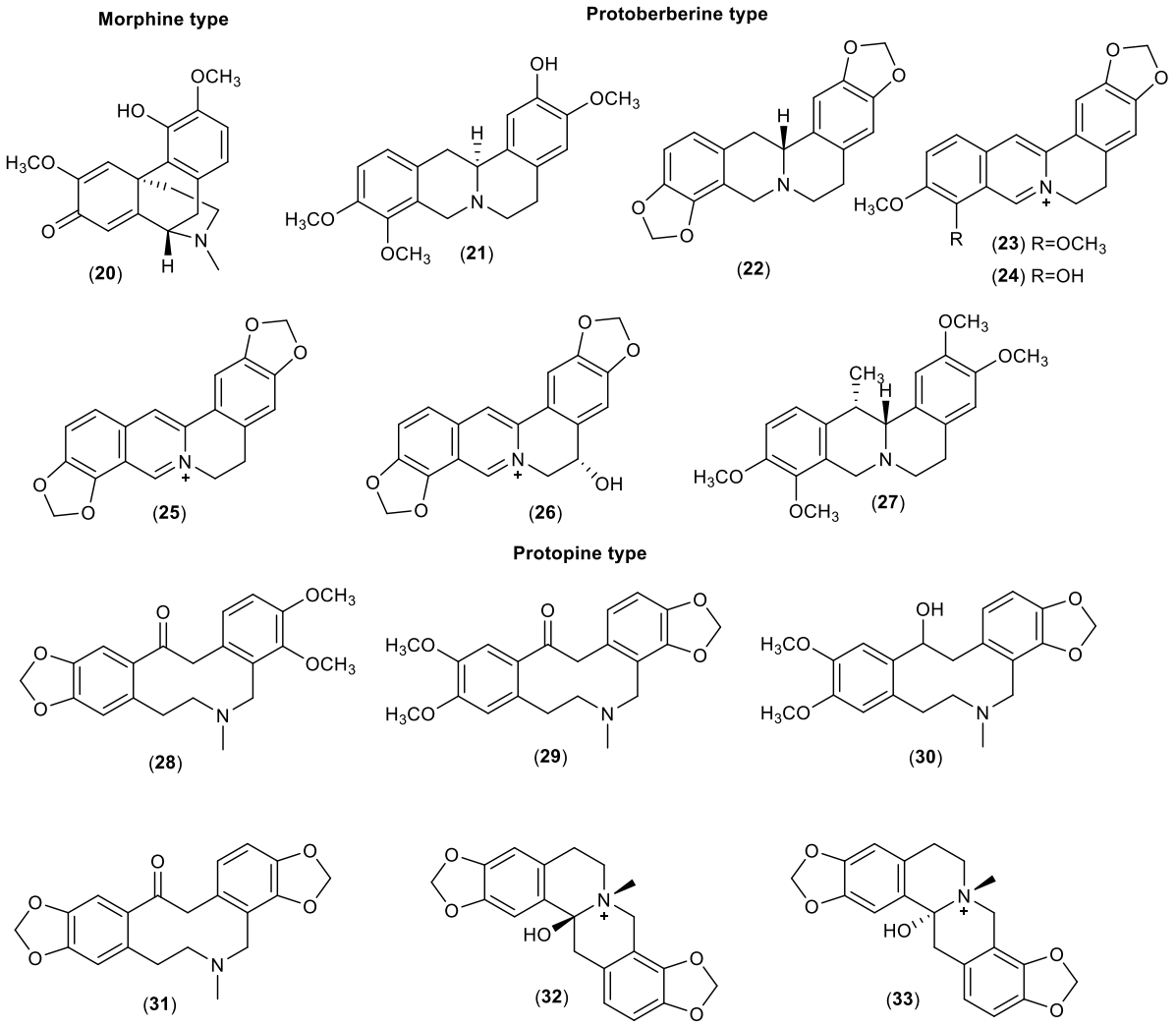

Fig. 5. Isoquinoline alkaloids of protoberberine, protopine, and morphine type reported in *Dicranostigma* species

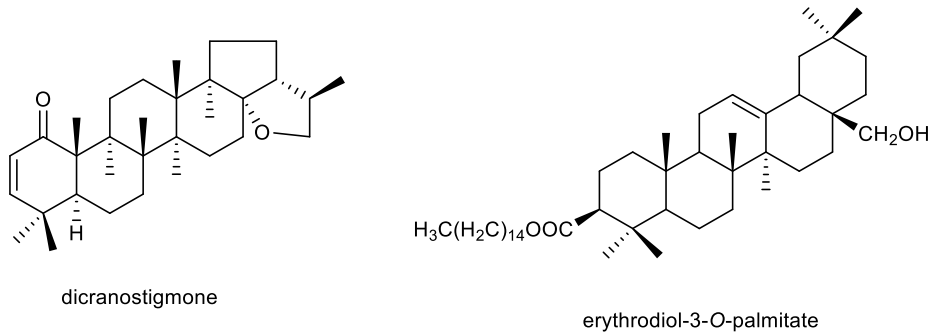

Fig. 6. Structures of hopane triterpene isolated from *D. leptopodum*

3.5.3 Biological activities of the isoquinoline alkaloids isolated from *Dicranostigma* species

Because the plants of the genus *Dicranostigma* have not been studied too intensively, compared to other more extensive genera of the Papaveraceae family, from a phytochemical point of view, the alkaloids isolated directly from the plants of the genus *Dicranostigma* have not been studied too much. On the other hand, several alkaloids that occur in the genus *Dicranostigma* have been isolated from other plants in the Papaveraceae family and subjected to the study of their biological activity. In the following section, we summarise the biological activity of extracts and alkaloids prepared and isolated directly from plants of the genus *Dicranostigma.*

The extract, essential oil, and pure alkaloid of *Dicranostigma* species showed a wide spectrum of biological activities, including cytotoxicity, anti-inflammatory, antibacterial, hepatoprotective, and anti-hemolysis effects [23, 57, 58]. Plants of the genus *Dicranostigma* are recognised as a rich source of quaternary benzophenanthridine alkaloids. These compounds are known to have a wide range of biological activities, including antimicrobial, antifungal, anti-inflammatory, antitumor activities and others [59, 60].

3.5.3.1 Biological activity in connection with the potential treatment of Alzheimer´s disease

Since Alzheimer's disease is the most common cause of dementia, the search for more potent drugs for its therapy is urgently needed [61]. AD is a multifactorial progressive disorder of the CNS characterised by memory loss, disorientation, deficits in cognitive functions, and behavioural abnormalities [62, 63]. According to the World Alzheimer's Disease Report, approximately 50 million people worldwide are currently suffering from AD. Due to the ageing population in western countries, the number of sufferers is expected to increase in the coming years by double in 2030 and more than triple by 2050. In addition to personal and family trauma, the stress of caregiving is a global cost estimated at US $305 billion in 2020, expected to increase to US $2 trillion by 2030 [64-66]. Natural compounds, especially alkaloids, are still attractive sources for identification and further development as new drugs [67].

Alkaloids isolated directly from *Dicranostigma* plants have not yet been tested for inhibition of enzymes involved in the pathogenesis of AD. As a result of the focus of the work, the biological activities of isoquinoline alkaloids that occur in these plants but were isolated from other plants of the Papaveraceae family for biological studies will be summarised here.

Berberis vulgaris is generally considered a rich source of the quaternary protoberberine alkaloid berberine (**23**), which has also been isolated from *Dicranostigma* plants. Berberine **(23)** has been identified as a strong AChE inhibitor and an inhibitor of other targets that occur in AD

(Table. 3). The biological activities of these compounds in relation to AD have recently been summarised in various articles [35, 68-77], therefore, only the results of the latest studies are summarised in the next paragraph.

For example, intragastric administration of 50 mg/kg of BBR (**23**) once daily for 14 days demonstrated a pronounced improvement in spatial memory deficits in a rat AD model [77], which was also proved in a study with streptozocin-diabetic rats at a dose of 100 mg/kg. In another study, a daily dose of BBR (**23**) (50 mg/kg) for three weeks in nonalcoholic steatohepatitis rats had neuroprotective effects on increased $A\beta_{42}$ production, AChE activity, and inflammation [78]. Another study using rats with diabetes also demonstrated that BBR (**23**) given orally (100 mg/kg) improved learning and memory deficits due to the prevention of oxidative stress and ChE activity [79]. Due to its neuroprotective capabilities, BBR (**23**) has also been shown to improve doxorubicin-induced cognitive decline in rats, with the underlying mechanisms studied comprising attenuating the expression of inflammatory proteins and genes, the apoptotic factors BAX and Bcl2, up-regulating the expression of peroxisome proliferator-activated receptor-γ 1α and manganese superoxide dismutase, and overall improving synaptic plasticity through cyclic adenosine monophosphate response element-binding protein and brain-derived neurotrophic factor [80]. In a rabbit model of AD simulated by injection of aluminium into the intraventricular fissure, oral administration of BBR (**23**) chloride (50 mg/kg) protected the rabbit hippocampus from degeneration and prevented increased BACE-1 activity by 40% [81]; however, the IC_{50} for BACE-1 was determined in another study to be higher than 100 μM [82]. BBR (**23**) has also been shown to reduce a formation of Aβ and decrease BACE-1 expression by activating AMP-activated protein kinase in N2a mouse neuroblastoma cells [83]. The decrease in $A\beta_{40/42}$ production by BBR (**23**) was also confirmed by a study in HEK293 cells, which can be explained by inhibition of BACE expression through activation of the extracellular signal-regulated kinase 1/2 pathway [84]. The study by Brunhofer et al. reported an IC_{50} for the inhibition of $A\beta_{1–40}$ of 43.84 μM, as well as an IC_{50} for the induction of $A\beta_{1–40}$ disaggregation (104.90 μM) [85]. Furthermore, BBR (**23**) is capable of mitigating tau protein hyperphosphorylation by inhibiting the nuclear factor-κB pathway [86] and by inhibiting GSK-3β [87], further reducing the cognitive deficit in AD, which was also verified in a mouse model [87]. It should be noted that BBR (**23**) has significant cholinesterase inhibitory activity, as shown in Table 1. For *h*AChE, its IC_{50} ranges from 0.52 μM to 0.7 μM with K_i = 0.54 μM [88, 89]. Compared to BuChE inhibition, BBR (**23**) appears to be selectively active towards AChE, as its IC_{50} values are several times higher, up to 30.7 μM for *h*BuChE inhibition [89]. BBR (**23**) can also inhibit the MAO-A enzyme with an IC_{50} of 126 μM [90]. BBR (**23**), according to

in vitro PAMPA studies, appears to be unable to cross the BBB [89, 91]; however, Wang et al. detected that BBR (**23**) can accumulate in the hippocampus of rats [92].

From the roots and aerial parts of *Chelidonium majus* (Papaveraceae) were isolated two benzophenanthridine alkaloids, previously identified in *Dicranostigma* plants, namely chelerythrine (**17**) and sanguinarine (**19**). Both alkaloids have been tested against AD targets in various studies. Chelerythrine (**17**) demonstrated dual cholinesterase activities. Interestingly, it showed slightly higher activity towards the *h*AChE (1.54 ± 0.07 μM) than towards the *Ee*AChE (3.78 ± 0.15 μM). A reverse situation was obtained for BuChE, as chelerythrine (**17**) was slightly more active toward the horse *eq*BuChE (6.33 ± 0.95 μM) when compared to the human enzyme (10.34 ± 0.24 μM; Table 3). Chelerythrine (**17**) inhibited AChE-induced Aβ aggregation at 5, 10, and 100 μM with 48.5%, 65.0%, and 88.4%, which indicates that chelerythrine (**17**) can be recognised as a potent inhibitor of AChE-induced $A\beta_{1–40}$ aggregation [85]. Chelerythrine (**17**) demonstrated a 67% inhibition of $A\beta_{1–40}$ aggregation at a concentration of 10 μM; thus, the value of IC_{50} was subsequently determined (4.2 ± 0.43 μM), which indicated that chelerythrine (**17**) is a highly active inhibitor of $A\beta_{1–40}$ aggregation. Additionally, chelerythrine (**17**) was also tested for its ability to disaggregate the already preformed $A\beta_{1–40}$ aggregates. This ability could be more relevant from a clinical perspective, when disaggregation of already existing Aβ fibrils in the AD brain could be indicated, especially at the beginning of the treatment to reduce the neurotoxic effects of Aβ fibrils and thus prevent neurodegeneration. Chelerythrine (**17**) showed high activity in disaggregating the preformed $A\beta_{1–40}$ aggregates, with an IC_{50} of 13.03 ± 2.89 μM after 45 min of incubation [85]. Chelerythrine (**17**) also selectively inhibited an isoform of recombinant human MAO-A with an IC_{50} value of 0.55 ± 0.042 μM [93] and was recognised as a reversible competitive MAO-A inhibitor (K_i = 0.22 ± 0.033 μM) [93].

The next benzophenathridine alkaloid sanguinarine (19) also showed promising inhibitory activity against *h*AChE with an IC_{50} value of 1.93 ± 0.01 μM, but it was inactive against *h*BuChE (IC_{50} > 200 μM) [13]. Consistent with this result, sanguinarine (**19**) demonstrated high inhibition activity against *h*AChE in another study, which was proved with IC_{50} 1.85 μg/ml as equal to 5.57 μM determined using the HPLC-DAD method [94]. Sanguinarine (**19**) also inhibited MAO activity in the mouse brain using kynuramine as substrate with a value of 24.5 μM and was recognised as a reversible non-competitive MAO-A inhibitor (*Ki* = 22.1 μM) [95]. Otherwise, an *in vitro* study through an artificial membrane showed that sanguinarine (**19**) was found to be highly permeable to cross the BBB with a value of 4.25×10^{-6} cm/s [91]. Furthermore, the study of the *in silico* design of the anticholinesterase

dual binding site indicated that sanguinarine was the most potent anti-AChE ligand with an affinity of -10.4 kcal/mol which was higher than galanthamine (-7.7 kcal/mol). Sanguinarine (**19**) is prone to bind to the peripheral anionic site (PAS) of AChE. It can be assumed that sanguinarine (**19**) acts the same mechanism as galanthamine and may reduce the aggregation of amyloid-beta (Aβ) in the brain of AD [96]. Finally, sanguinarine (**19**) inhibited aggregation of $A\beta_{1\text{-}42}$ and was able to modulate amyloid aggregation [97].

From the roots and aerial parts of *Chelidonium majus* (Papaveraceae) were also isolated two derivatives of previously mentioned alkaloids 6-ethoxydihydrosanguinarine and 6-ethoxydihydrochelerythrine and inhibitory activity of *h*AChE/*h*BuChE was evaluated. Both compounds should be recognised as isolation artefacts, as in the presence of common solvents such as MeOH, EtOH, and $CHCl_3$, the free benzophenanthridine alkaloids (sanguinarine (**19**) and chelerythrine (**17**)) easily produce adducts. On the other hand, these artefacts showed balanced inhibition activity of cholinesterase, with IC_{50} values lower than 5 μM; 6-ethoxydihydrochelerythrine was the most potent (Table 3). These compounds can be used as templates for further development of antidementia drugs with a benzophenanthridine scaffold in the structure [98].

Table 3. Biological activities of selected IAs identified in plants of genus *Dicranostigma*, in connection with the potential treatment of Alzheimer's disease

Compound	AChE IC_{50} (μM)	BuChE IC_{50} (μM)	$A\beta_{1\text{-}42}$ IC_{50} (μM)	MAO-A IC_{50} (μM)	PAMPA BBB Permeation Pe ($\times 10^{-6}$ cm/s)	Ref.
Berberine (**23**)	0.520 ± 0.042[a]; 0.61 ± 0.04[a]; 0.7 ± 0.1 [a] ;	30.7 ± 3.5 [c] ;	43.84 ± 6.09	126	0.1 ± 0.1 (CNS−); 0.02 (CNS−)	[82, 85, 88-91]
Chelerythrine (**17**)	1.54 ± 0.07[a]; 1.03 ± 0.11[b]	10.34 ± 0.24 [c] 3.55 ± 0.18 [d]	4.20 ± 0.43	0.55 ± 0.042	3.25 (CNS+/−)	[85, 93]
Sanguinarine (**19**)	1.93 ± 0.01[a]	> 200 [b]	n.d.	24.5	4.23 (CNS+/-)	[13, 91, 94, 95]
6-Ethoxydihydrosanguinarine	3.25 ± 0.24[a]	4.51 ± 0.31 [c]	n.d.	n.d.	n.d.	[98]
6-Ethoxydihydrochelerythrine	0.83 ± 0.04[a]	4.20 ± 0.19 [c]	n.d.	n.d.	n.d.	[98]

[a] *h*AChE, [b] EeAChE, [c] *h*BuChE, [d] eqBuChE, n.d. = not determined.

3.5.3.2 Antimycobacterial activity of selected isoquinoline alkaloids

Tuberculosis (TB) is a kind of widespread infectious disease, caused by *Mycobacterium tuberculosis* (Mtb). The World Health Organisation (WHO) has issued the Global Tuberculosis Report in 2021, mentioning that *Mtb* has infected about a quarter of the world's population, but only a small portion (5-10%) will develop this bacterial disease. TB was the leading cause of death from a single infectious agent and ranked above HIV/AIDS (13th leading cause worldwide in 2019) until the COVID-19 pandemic [99, 100].

Only a limited number of alkaloids identified in *Dicranostigma* plants have been screened for their antimycobacterial potential. Only a few alkaloids active against some *Mycobacterium* species, especially benzophenanthridine alkaloids, were reported to occur in *Dicranostigma* and other genera of plants. Chelerythrine (**17**) and sanguinarine (**19**) isolated from Sanguinaria canadensis were screened for their antimycobacterial potential against three species of Mycobacteria, namely *M. aurum*, *M. smegmatis* and *M. bovis* which is commonly used as a slowly growing screening model for *M. tuberculosis* [101, 102]. Chelerythrine (**17**) was more active than sanguinarine (**19**) against all tested species (Table 4). Benzophenanthridine alkaloids, unlike other alkaloids, are unique in their reactivity, as they undergo a dynamic equilibrium between the alkanolamine (base form) and iminium ion form in any protic solvent due to the sensitivity of the polar bond (N C) to the attack of nucleophiles (Fig. 7a and b) [103]. The equilibrium is pH dependent [103-105]. The conversion of alkanolamine from the iminium ion improves the lipophilicity of the benzophenanthridine alkaloid and the higher hydrophilicity of alkanolamine can result in an increase in the bioavailability of the alkaloid to the organism. Experiments to determine the effect of medium pH on antimycobacterial activity were carried out in sanguinarine (**19**), but no significant differences in antimycobacterial activity were observed.

Table 4. Antimycobacterial activities of isolated compounds against *M. aurum*, *M. smegmatis*, and *M. bovis* BCG

Compound	IC_{50} value ± SD (n) µg/ml			Ref.
	M. aurum	***M. smegmatis***	***M. bovis* BCG (n=1)**	
Sanguinarine (**19**)	9.61 ± 4.52 (7) [25.04 µM)	41.18 ± 16.85 (5) [112.2 µM]	24.5 [66.8 µM]	[102]
Chelerythrine (**17**)	7.30 ± 1.91 (3) [19.02 µM]	29.00 ± 17.60 (5) [75.56 µM]	14.3 [37.3 µM]	[102]
Streptomycin	1.14 ± 0.02 (3) [0.78 µM]	0.17 ± 0.04 (3) [0.12 µM]	n.d.	[102]

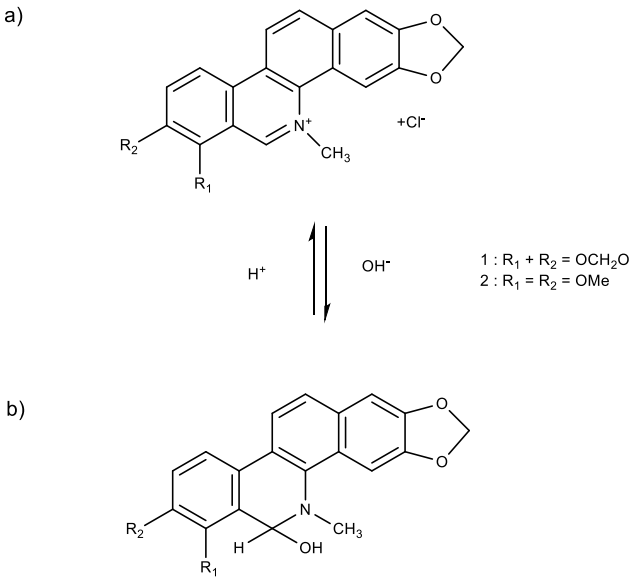

Fig. 7. Iminium ion (a) and alkanolamine (b) forms of the alkaloids sanguinarine (**19**) and chelerythrine (**17**)

Berberine (**23**) has been tested for its antimycobacterial activity within the study in which 13-n-octylberberine derivatives were synthesised and evaluated for their activities against drug-susceptible *M. tuberculosis* [106]. The results obtained for berberine (**23**) are summarised in the following table (Table 5).

Table 5. *In vitro* anti-tubercular activities of the key compounds against MDR strains of *M. tuberculosis*[a] (MIC: μg/ml[b])

Compound	Rifampisin and isoniazid-resistant strain types					Drug-susceptible strain type
	44	83	164	431	926	$H_{37}RV$
Berberine	4	4	4	4	n.d	2.0
Rifampisin	64	>64	>64	>64	>32	0.0625
Isoniazid	4	4	4	64	32	0.0625

[a] MDR strains were isolated from patients with tuberculosis in China.
[b] MIC: minimum inhibitory concentration.

3.5.3.3 Cytotoxic activity

Six aporphine alkaloids along with one benzophenanthridine alkaloid and two protopine alkaloids: corydine (**1**), isocorydine (**6**), 10-*O*-methylhernovine (**9**), corytuberine (**10**), nantenine (**12**), lagesianine A (**13**), dihydrosanguinarine (**15**), dihydrocryptopine (**30**), and protopine (**31**) were isolated and characterised from the crude extract of *D. leptopodum* [19]. To obtain their potential pharmacological activities, compounds **1**–**9** were evaluated for their cytotoxicities against H1299, MCF-7, and SMMC-7721 tumour cell lines using the CCK-8 assay. The results of this study are summarised in the following table (Table 6). Compounds **12**, **10**, and **15** showed cytotoxicity against SMMC-7721 cells with IC_{50} values of 70.08 ± 4.63, 73.22 ± 2.35, and 27.77 ± 2.29 μM, respectively. Compound **15** showed balanced cytotoxicity against all three tested cell lines (Table 6).

Table 6. Cytotoxicities of compounds from *Dicranostigma leptopodum* (Maxim.) Fedde

Compound	IC_{50} (μM)[a,b]		
	H1299	MCF-7	SMMC-7721
Corydine (**1**)	>100	>100	>100
Isocorydine (**6**)	>100	>100	>100
10-*O*-methylhernovine (**9**)	>100	>100	>100
Corytuberine (**10**)	53.58 ± 5.47	72.30 ± 1.72	73.22 ± 2.35
Nantenine (**12**)	>100	>100	70.08 ± 4.63
Lagesianine A (**13**)	>100	>100	>100
Dihydrosanguinarine (**15**)	28.22 ± 1.03	28.34 ± 2.00	27.77 ± 2.29
Dihydrocryptopine (**30**)	>100	>100	>100
Protopine (**31**)	>100	>100	>100
Doxorubicin[c]	11.70 ± 1.53	7.82 ± 0.89	2.74 ± 0.34

[a]IC_{50} value was the 50 % inhibition concentration and was calculated from regression lines using five different concentrations in replicate experiments for six times. [b]Solvent used in the cytotoxicity test was DMSO, and the purity of compounds under the test is greater than 90 %. [c]Doxorubicin was used as a positive control.

The treatment of human hepatocellular carcinoma (HCC) cell lines with (+)-isocorydine (**6**), which was isolated from *Dicranostigma leptopodum*, resulted in a growth inhibitory effect caused by the induction of G2/M phase cell cycle arrest and apoptosis. Furthermore, isocorydine (**6**) induced phase arrest of G2/M by increasing the expression levels of cyclin B1 and p-CDK1,

which was caused by decreasing the expression and inhibiting the activation of Cdc25C. The phosphorylation levels of Chk1 and Chk2 were increased after ICD (**6**) treatment. Furthermore, G2/M arrest induced by ICD (**6**) can be disrupted by Chk1 siRNA but not by Chk2 siRNA. In addition, isocorydine treatment led to a decrease in the percentage of $CD133^+$ PLC/PRF/5 cells. Interestingly, isocorydine (**6**) treatment dramatically decreased tumorigenicity of SMMC-7721 and Huh7 cells. These findings indicate that isocorydine (**6**) could be a potential therapeutic drug for the chemotherapeutic treatment of HCC [107].

Chelerythrine (**17**) showed a wide range of cytotoxic activity against nine human tumour cell lines, including MCF7, MCF7ADR, HT29, DaOY, LnCaP, SQ-20B, JSQ-3, SCC-35, and SCC61 *in vitro*. Furthermore, chelerythrine (**17**) significantly inhibited tumour growth in mice bearing SQ-20B xenografts *in vivo* [108]. Chelerythrine (**17**), chelirubine (**18**), and sanguinarine (**19**) from *D. lactucoides* induced apoptosis at a concentration of 1 µg/ml with a strong antiproliferative effect *in vitro* [109]. In another study, chelerythrine (**17**) and sanguinarine (**19**) slightly decreased dioxin-induced 7-ethoxyresorufin-O-deethylase (EROD) activity, but not affected aryl hydrocarbon receptor (AhR) transcriptional activity in human hepatoma cells (HepG2). This study informed that chelerythrine (**17**) and sanguinarine (**19**) did not affect CYP1A1 expression, indicating that their biological effects were pleiotropic and did not have a specific cellular target [110]. In addition, sanguinarine (**19**), induced apoptosis of human pancreatic carcinoma cells (AsPC-1 and BxPC-3) cells through modulations of the Bcl-2 family proteins and KB cancer cells related to increased production of reactive oxygen species and depolarisation of the mitochondrial membrane potential [111, 112].

From evidence and perspectives for the development of new anticancer drugs, sanguinarine (**19**) showed many antitumor activities, including inducing apoptosis in tumour cells through activation of NF-κB, the mitochondrial damage and cell cycle arrest, inhibition of tumour progression associated with chronic inflammation through inhibition of NF-κB, inhibition of tumour angiogenesis through inhibition of VEGF secretion and transduction of VEGF signal (Akt, p38 and VE-cadherin), inhibition of tumour cell migration by inhibition of MMP-9 and STAT3 activation, and enhancement of chemosensitivity of Caco2 and CEM/ADR5000 adriamycin resistant leukaemia cells [113].

Berberine (**23**) induced AMP-activated protein kinase (AMPK) by decreasing integrin β1 protein levels and the phosphorylation of integrin β1 signalling targets that led to inhibits human colon cancer (SW 480 and HCT116) cell migration [114]. In addition, it reduced the metastatic potential of breast cancer cells due to mediated suppression of matrix

metalloproteinases (MMP2 and MMP9) including inhibition of the nuclear factor kappa B (NF-κB) and activator protein-1 (AP-1) pathways [115].

Protopine (**31**) significantly increased CYP1A1 mRNA levels in human liver cells and HepG2 hepatoma cells, as well as inhibited mitosis and induces apoptosis in prostate cancer cells [116, 117].

3.5.3.4 Antiinflammatory activity

As mentioned above, the most attractive secondary metabolites of *Dicranostigma* plants are quaternary [109, 118]. In recent studies, the anti-inflammatory potential of the major and minor quaternary benzophenanthridine alkaloids (sanguinarine (**19**), chelerythrine (**17**), sanguilutine, sanguirubine, chelirubine (**18**), chelilutine, and macarpine) has been evaluated *in vitro*. The anti-inflammatory potential of selected alkaloids was evaluated as for their ability to modulate the lipopolysaccharide-induced secretion of tumour factor α (TNF-α) in the macrophage-like cell line THP-1. The results of the anti-inflammatory assays indicate that the presence of methylenedioxy ring attached at carbon (C)7-C8 is important to reduce TNF-α secretion at a concentration of 100 nM [119]. Interestingly, this effect did not show a simple dependence on concentration. Cyclooxygenase-1 (COX-1)and COX-2 inhibitory activities have also been studied [119]. Macarpine showed considerable activity to inhibit COX-2 with an IC_{50} value of 148 μM. The results demonstrated that macarpine preferentially inhibited COX-2 rather than COX-1. Other compounds were inactive or showed a non-significant inhibitory potential at a concentration of 150 μM.

In other studies, both sanguinarine (**19**) and chelerythrine (**17**) have indicated a promising anti-inflammatory effect *in vitro* and *in vivo* [120-122]. Sanguinarine (**19**) inhibited the expression of inflammatory mediators. Furthermore, sanguinarine (**19**) inhibited mitogen-activated protein kinase (MAPK) activation, modulating inflammatory mediators of peritoneal macrophage synthesis and release *in vitro* [120]. However, chelerythrine (**17**) significantly inhibited the production of exudates and prostaglandin E2 through the regulation of cyclooxygenase-2 (COX-2) [121]. Chelerythrine (**17**) reduced the IL-6 mRNA level. Sanguinarine reduced gene expression of CCL-2 and IL-6. The effect of sanguinarine (**19**) was comparable to prednisone [122].

Other alkaloids present in plants of the genus *Dicranostigma* are worth including the anti-inflammatory activity of protopine (**31**). Protopine (**31**) strongly inhibited platelet aggregation induced by different types of platelet agonists such as Arachidonic Acid (AA), Adenosine Diphosphate (ADP), collagen, and Platelet Activating Factor (PAF) in a

concentration-related manner. Furthermore, it selectively inhibited the synthesis of thromboxane A_2 (TXA_2) through the COX pathway in platelet. Subsequently, pre-treatment with protopine (**31**) (50-100 mg/kg) in rabbits caused protection against AA or PAF that induced sudden death. It also inhibited paw oedema in rats induced by carrageenan with a potency of three-fold greater than aspirin [123]. In another study, protopine (**31**) reduced the release of inflammatory mediators (NO and PGE_2) and downregulated their parallel genes (iNOS and COX-2), both in LPS-induced BV2 cells *in vitro* and in a CA-induced inflammation model in mice *in vivo*. In this study, protopine has been found to inhibit the level of IL-1β, IL-6, MCP-1, and TNF-α production but also suppressed its expression of mRNA and increased IL-10 cytokine mRNA levels in LPS-induced BV2 microglial cells. Furthermore, MAPK phosphorylation is significantly attenuated when pre-treatment of BV2 cells with protopine [124].

3.5.3.5 Antibacterial activity

An alkaloidal extract of *D. leptopodum* was studied for its antibacterial activity. This extract showed promising activity against *Klebsiella pneumoniae* with an IC_{50} value of 1.389 mg/ml. In addition, the extract has been able to destruct the cell wall, increase membrane permeability, and inhibit bacterial growth [21]. Essential oil prepared by supercritical extraction from the same plant showed bactericidal effects with minimum inhibitory concentration (MIC) against *Escherichia coli*, *Staphylococcus aureus*, and *Pseudomonas aeruginosa* with values of 0.25 g/ml, 0.30 g/ml, and 0.26 g/ml, respectively [58].

In addition, the alkaloidal extract of *D. franchetianum* showed inhibition activity against Gram-positive bacteria, such as *Enterococcus faecalis*, *Staphylococcus aureus*, and *Staphylococcus hycius* with MIC values of 512 µg/ml, 64 µg/ml, and 256 µg/ml, respectively, and Gram-negative bacteria (*Escherichia coli*) with a MIC value of 512 µg/ml. The GC/MS analysis of the tested alkaloidal extract showed high concentrations of isocorydine (70% of TIC) and protopine (21% of TIC) in the mixture [125].

3.5.3.6 Hepatoprotective activity

The administration of carbon tetrachloride (CCl_4) can cause acute or chronic liver damage in rodents and is used as an experimental model of liver damage for the evaluation of the therapeutic effect of many hepatoprotective drugs [126, 127]. The extract of *D. leptopodum* protected liver damage caused by CCl_4 in mice by improving antioxidant enzyme activities such as superoxide dismutase (SOD), catalase (CAT), and glutathione peroxidase (GPx) and

reducing MDA levels. In addition, mitochondrial function improved by preventing respiratory chain disruption and suppressing mitochondrial Na^+K^+-ATPase and Ca^{2+}-ATPase activity [128]. Extract of *D. leptopodum* significantly reduced the elevation of serum GPT and LDH levels, as well as the content of MDA in liver plasma. The extract of *D. leptopodum* also protected against liver injury caused by BCG and LPS in mice [129]. Therefore, extracts of *D. leptopodum* could be potential hepatoprotective agents against liver toxicity [128]. HPLC analysis of the tested extract showed that corydine (**1**), isocorydine (**6**), and protopine (**31**) were the compounds present in the highest concentrations. The continuation of this study is necessary to test pure alkaloids.

3.5.3.7 Further biological activities

The extract of *D. leptopodum* showed an effect on the oxidative hemolysis of mouse erythrocytes *in vitro*. *D. leptopodum* extract was found to be effective in suppressing the hemolysis induced by hydrogen peroxide (H_2O_2) or acetyl phenyl hydrazine (APH), which might be related to the enhancement activity of glucose-6-phosphate dehydrogenase (G-6-PD) [20].

The dried root extract of *D. lactucoides* showed high toxicity against algae (*Pseudokirchneriella subcapitata*, *Scenedesmus quadricauda*), with EC_{50} values of 21.27 mg/l and 20.61 mg/l, respectively. Furthermore, the toxicity of the extract against cyanobacteria (*Microcystis aeruginosa*, *Synechococcus leopoliensis*) has also been evaluated, and the EC_{50} values of each phytoplankton were 55.81 mg/l and 45.60 mg/l, respectively. Since the major components of the extract were identified as sanguinarine (**19**) and chelerythrine (**17**), there is a high probability that quaternary benzophenanthridine alkaloids are responsible for these effects [130].

4 EXPERIMENTAL PART

4.1 General Experimental Procedures

All solvents were treated using standard techniques before use. All reagents and catalysts were purchased from Sigma Aldrich, Czech Republic, and used without purification. NMR spectra were recorded in either $CDCl_3$ or CD_3OD on a VNMR S500 spectrometer (Varian, Palo Alto, CA, USA) operating at 500 MHz for proton nuclei and 125.7 MHz for carbon nuclei at ambient temperature. ESI-HRMS was obtained with a Waters Synapt G2-Si hybrid mass analyser of a quadrupole-time-of-flight type (Q-TOF), coupled to a Waters Acquity I-Class UHPLC system (Waters, Millford, MA, USA). The EI-MS data were obtained on an Agilent 7890A GC 5975 inert MSD operating in EI mode at 70 eV (Agilent Technologies, Santa Clara, CA, USA). A DB-5 column (30 m × 0.25 mm × 0.25 μm, Agilent Technologies, USA) was used with a temperature program: 100–180 °C at 15 °C/min, 1 min hold at 180 °C, and 180–300 °C at 5 °C/min and 5 min hold at 300 °C; and detection range m/z 40–600. The injector temperature was 280 °C. The flow rate of carrier gas (helium) was 0.8 ml/min. A split ratio of 1:15 was used. Fractionations of fractions II and V were performed with a BÜCHI Sepacore flash system ×10 equipped with a BÜCHI control unit C-620, BÜCHI fraction collector C-660, UV photometer C-640, and BÜCHI pump modules C-605 (BÜCHI, Flawil, CH). TLC was carried out on Merck precoated silica gel 60 F254 and Merck precoated silica gel 60 RP-18 F254 plates. The compounds in the plate were observed under UV light (254 and 366 nm) and visualised by spraying with Dragendorff's reagent.

4.2 Plant Material

The plant material used from *Dicranostigma franchetianum* came from a monoculture introduced to the Garden of Medicinal Plants at the Faculty of Pharmacy, Charles University in Hr. Králové in 2014 (seeds from the Centre of Medicinal Plants of Masaryk University in Brno). Botanical identification was performed by Prof. L. Opletal. A voucher specimen is deposited in the Herbarium of the Faculty of Pharmacy in Hradec Králové under number: CUFPH-16130/AL-540.

4.3 Extraction and isolation of alkaloids

Finely cut and dried aerial parts of *D. franchetianum* (11.87 kg) were minced and sequentially extracted with 95% EtOH (500 g of material boiled with 3 L of EtOH) for 30 min. The combined extracts were evaporated to the consistency of a thin syrup, to which 6 L of distilled water was added at 80 ° C and the pH was adjusted to 1–1.5 by adding 2% H_2SO_4. The suspension was

filtered through Celite 545. The filtrate was alkalised with 10% Na_2CO_3 (pH 9–10) and extracted with $CHCl_3$ (3 × 5 L). The organic layer was evaporated to give 120 g of dark brown syrup. This alkaloid summary extract was again dissolved in 2% H_2SO_4 (3 L), defatted with Et_2O (3 × 2 L), and alkalised to pH 9–10 with 10% Na_2CO_3. The water layer was extracted with EtOAc (4 × 2 L) to give 47 g of concentrated alkaloidal extract in the form of brown syrup marked as extract A.

The extract A (47 g), adsorbed on silica gel (ratio of media to sample 2:1) and loaded onto a PP pre-column (cartridge 40 × 150 mm, Büchi), was separated by flash chromatography (Sepacore® Flash Chromatography System ×10, Büchi) on silica gel (silica gel 60, 40–63 µm, glass column 49 × 460 mm, Büchi) using a mobile phase containing light petroleum (solvent A), EtOAC (solvent B) and MeOH (solvent C). The extract separation was carried out for 360 min, starting with isocratic elution with solvents A and B (20% B, 15 min), followed by linear gradient elution (20% B <100% B, 150 min) and isocratic solvent elution (100% B, 15 min). The extract chromatography was continued by linear gradient elution with solvents B and C (100% B -> 100% C, 165 min), and the separation was completed by isocratic elution with solvent C (15 min). The separation flow rate was set at 110 ml/min, and UV detection was performed at 254 nm, 290 nm, 315 nm, and 365 nm. A total of 208 fractions (190 ml) were collected and, according to analytical TLC, combined into 12 fractions (A/1-A/12). The separation of fractions into individual alkaloids was carried out by preparative TLC on silica gel (silica gel 60 GF_{254}). The conditions for preparative TLC, additional separation processes (e.g., crystallisation) for each fraction, and the isolated amount of each alkaloid were as follows:
Fraction **A/1** (250 mg, cHx:Et_2NH, 97:3, 2×) gave compound **DF-01** (140 mg).
Fraction **A/2** (190 mg, cHx:Et_2NH, 95:5, 2×) gave compound **DF-02** (77 mg).
Fraction **A/3** (434 mg, To:Et_2NH, 99:1, 2×) gave compounds **DF-04** (120 mg) and **DF-05** (20 mg).
Fraction **A/4** (807 mg, To:cHx:EtOAc:MeOH, 45:30:35:1) gave compound **DF-03** (149 mg) and compound **DF-06** (30 mg).
Fraction **A/5** was crystallised from EtOH/$CHCl_3$ (2.2 g, To:cHx:Et_2NH, 45:45:10) to give white crystals of **DF-08** (458 mg). The mother liqueur was separated by preparative TLC to give alkaloids **DF-07** (15 mg), additional amounts of **DF-07** (135 mg) and **DF-09** (452 mg).
The fraction **A/6** (8.9 g) was partially separated by preparative TLC (2.0 g, To:Et_2NH, 96:4, 3×) into 2 zones **A/6/F1** (23 mg) and **A/6/F2** (1.5 g). Subsequently, the subfraction **A/6/F1** was separated by additional preparative TLC (EtOAc:MeOH:H_2O 100:13:10, 2×) to give **DF-10** (8

mg). Subfraction **A/7**(28 mg) gave compound **DF-11** (6 mg) after recrystallization from the mixture EtOH:$CHCl_3$.

The fraction **A/8** (890 mg, To:cHx:Et_2NH, 6:3:1) gave the subfractions **A/8/F1**–**F3**. Subfraction **A/8/F1** (115 mg) was recrystallised from the mixture EtOH:$CHCl_3$ (1:1) to give compound **DF-12** (56 mg). Additional preparative TLC of subfraction **A/8/F2** (78 mg, To:cHx:Et_2NH, 5:4:1, 2×) gave compounds **DF-13** (15 mg) and **DF-14** (13 mg).

Fraction **A/9** (730 mg, EtOAc:MeOH:H_2O:TFAA, 100:40:5:0.1, 2×) gave four subfractions **A/9/F1–F4**. Crystallisation of subfraction **A/9/F1** (97 mg) yielded compound **DF-15** (34 mg). Additional preparative TLC of subfraction **A/9/F3** (40 mg, EtOAc:MeOH:H_2O:TFAA 100:40:5:0.1, 2×) gave compound **DF-16** (10 mg).

The fraction **A/10** (184 mg, To:cHx:EtOAc:MeOH 45:30:35:1, 1×) gave three subfractions **A/10/F1-F3**. Subfraction **A/10/F1** (53 mg) yielded compound **DF-17** (17 mg), after additional preparative TLC (To:Et_2NH, 95:5,2×).

Other fractions and subfractions obtained within the separation process of part A (A/11: 48 mg; A/12: 29 mg) have not been used to isolate alkaloids due to the low amount or complex mixture of compounds.

The aqueous phase after obtaining the alkaloid fraction A was alkalised with 40% NaOH (pH 12-12.5) and extracted 5x with 2 L of Et_2O. The Et_2O extract was concentrated, dissolved in 200 ml in a mixture of $CHCl_3$/EtOH 9:1, and the solution was filtered through a basic alumina column (60 g; 22 x 155 mm) and washed with $CHCl_3$/EtOH 9:1. The yellow phase was collected. The residue (4.2 g, yellow-brown) was dissolved in 110 ml of Et_2O at boiling, 11 g of anhydrous citric acid was added, and the Et_2O was distilled off. The crystalline powder was dispersed in cold MeOH, and the suspension was filtered and washed.

The crystalline matter was dissolved in 150 ml of water, alkalised with 40% NaOH (pH 12-12.5) and extracted 4 times with 200 ml of Et_2O. After evaporation, crystallisation was carried out twice from dilute HCl to yield **DF-18** (1.1 g).

The methanolic filtrate after separation of the citrate crystal fraction was evaporated, dissolved in water, alkalised with 40% NaOH (pH 12-12.5) and shaken 6 times with 150 ml of Et_2O. The dried Et_2O extract (1.45 g, yellow, solid) was dissolved in 14 ml of MeOH and separated using TLC (40 plates, 200 x 120 mm, $CHCl_3$:EtOAc:Et_2NH, 70:20:10, 2x) to give **DF-19** (42 mg) and **DF-20** (25 mg).

The remaining aqueous extract was neutralised after the removal of the bases of quaternary protoberberine (pH 12-12.5) neutralized with 40% sulfuric acid (pH 3-4), then 40 g of potassium iodide was added and the solution was shaken 7 times with 700 ml of $CHCl_3$/EtOH

8:2. The organic phase was evaporated (viscous brown evaporate, 5.2 g), dissolved in water with the addition of HCl, the solution was filtered through a layer of diatomaceous earth, alkalised with 10% Na_2CO_3 (pH 9-10) and shaken 5 times with 100 ml of Et_2O. The aqueous phase was neutralised with sulfuric acid (pH 3-4), 10 g of potassium iodide was added, and the solution was shaken 6 times with 100 ml of a mixture of $CHCl_3$/EtOH 8:2. The light brown precipitate (1.8 g) was dissolved in 100 ml of hot MeOH, a small amount of activated carbon was added and after shaking a rapid filtration was carried out through a layer of diatomaceous earth. The pellet (1.2 g, faintly brownish) was dissolved in a mixture of $CHCl_3$/MeOH 9:1, filtered through a small column of silica gel deactivated with 10% water (7.2 g; 15 x 90 mm), the column was washed with the same solvents and only the Dragendorff positive eluate was collected (monitoring after 5 ml). A brownish precipitate (320 mg) was crystallised from MeOH to give **DF-21** (43 mg).

4.4 *In vitro* acetylcholinesterase and butyrylcholinesterase assay

The inhibitory activities of prepared compounds and standards against human recombinant AChE (E.C. 3.1.1.7) and human plasma BChE (E.C. 3.1.1.8) were determined using a modified method of Ellman, as recently described by our group, and expressed as IC_{50} (the concentration of the compound that is required to reduce 50% of the cholinesterase activity). [39, 40] Human recombinant AchE, phosphate buffer (PB, pH = 7.4), 5,5'-dithio-bis(2-nitrobenzoic) acid (Ellman's reagent, DTNB), acetylthiocholine (ATCh), butyrylthiocholine (BTCh), and other used compounds were purchased from Sigma-Aldrich (Prague, Czech Republic). Human plasma was used as a source of BuChE and prepared from heparinised human blood. Blood was centrifuged for 20 minutes (4 °C, 2300 × g) by Hettich Universal 320R centrifuge. The plasma was separated and stored at −80 °C. During measurement, 96-well polystyrene microplates (ThermoFisher Scientific, Waltham, MA, USA) were used.

The solutions of the corresponding cholinesterase in PB were prepared up to the final activity 0.002 U/µl. The assay medium (100 µl) consisted of cholinesterase (10 µl), DTNB (20 µl of 0.01 M solution), and PB (40 µl of 0.1 M solution). The solutions of the tested compounds (10 µl of different concentrations) were pre-incubated for 5 minutes in the assay medium and then a solution of the substrate (20 µl of 0.01 M ATCh or BTCh iodide solution) was added to initiate the reaction. The increase in absorbance was measured at 412 nm using the Multimode microplate reader Synergy 2 (BioTek Inc., Winooski, VT, USA). For the calculation of the resulting measured activity (the percentage of inhibition I) following formula was used:

$$I = \left(1 - \frac{\Delta A_i}{\Delta A_0}\right) \times 100$$

where ΔA_i indicates the change of absorbance provided by adequate enzyme exposed to the corresponding inhibitor and ΔA_0 indicates absorbance change when a solution of PB was added instead of a solution of inhibitor. Software Microsoft Excel (Redmont, WA, USA) and GraphPad Prism version 6.07 for Windows (GraphPad Software, San Diego, CA, USA) were used for the statistical data evaluation.

4.5 *In vitro* prolyloligopeptidase assay

Prolyl oligopeptidase (POP; EC 3.4.21.26) was dissolved in phosphate buffered saline (PBS; 0.01M Na/K phosphate buffer, pH 7.4, containing 137 mM NaCl and 2.7 mM KCl); the specific activity of the enzyme was 0.2 U/ml. The assay was performed on standard 96-well polystyrene microplates with a flat and clear bottom. Stock solutions of tested compounds were prepared in dimethyl sulfoxide (DMSO; 10 mM). Dilutions (10^{-3}–10^{-7} M) were prepared from the stock solution with deionised H_2O; the control was carried out with the same concentration of DMSO. POP substrate, (*Z*)-Gly-Pro-*p*-nitroanilide, was dissolved in 50% 1,4-dioxane (5 mM). For each reaction, PBS (170 µL), tested compound (5 µL), and POP (5 µL) were incubated for 5 min at 37 °C. The substrate (20 µL) was then added, and the microplate was incubated for 30 min at 37 ° C. The formation of *p*-nitroanilide, directly proportional to the POP activity, was measured spectrophotometrically at 405 nm using a microplate ELISA reader (Multi-mode microplate reader Synergy 2, BioTek Instruments Inc., Vermont, USA). The inhibition potency of tested compounds was calculated by non-linear regression analysis and was expressed as an IC_{50} value (concentration of inhibitor which causes 50% POP inhibition). All calculations were performed using GraphPad Prism software version 6.07 for Windows (GraphPad Software, San Diego, CA, USA).

4.6 Docking study of active alkaloids in the active site of *h*AChE and *h*BuChE

The crystalline structure of *h*AChE complexed with a co-crystallized inhibitor was sourced from the Protein Data Bank (PDB) at www.rcsb.org under the ID code: 4M0E [131]. Similarly, the crystalline structure of *h*BuChE was obtained from the same database under the ID: 1P0P [132]. Prior to molecular docking, all ions, co-crystallized ligands, and residual solvents were removed from the protein structure. The cleaned protein was subsequently prepared with the DockPrep function of Chimera software v. 1.15 [133] and the AutoDockTools program v. 1.5.7 [134]. The ligand molecules (**DF-02**,**-03**,**-05**) were prepared employing ChemDraw Professional v 20.0

(PerkinElmer Informatics, Inc.) and their geometry was optimized using the general AMBER force field in Avogadro software v. 1.2.0 [135]. Subsequently, they were converted for docking using OpenBabel v. 2.3.1 [136]. The actual molecular docking at the enzymes' active sites was performed with the AutoDock Vina tool v. 1.1.2 [137]. This tool applies a semi-flexible method (flexible ligand, rigid protein) and was set to the following parameters: exhaustiveness = 8, num_modes = 9, grid box size = 22×22×22 Å. In order to improve the likelihood of obtaining optimal results, the experiment was run twenty times. Based on the docking score of the resultant positions and a visual inspection of the resultant locations with The PyMOL Molecular Graphics System v. 2.5.0 (Schrödinger, LLC.) and Discovery Studio Visualiser v. 4.5 (BIOVIA, San Diego), the most probable binding positions of the ligands (**DF-02**,-**03**,-**05**) in the active sites of *h*AChE and *h*BuChE were selected and compared. The method's validity was confirmed by redocking the original co-crystallized ligands to their parent proteins (RMSD < 1 Å).

4.7 Antimycobacterial screening

Antimycobacterial screening has been conducted in cooperation with the Department of Biological and Medical Sciences, Faculty of Pharmacy, Charles University, Heyrovskeho 1203, 500 05 Hradec Kralove, Czech Republic.

The antimycobacterial assay was performed with rapidly growing *Mycolicibacterium smegmatis* DSM 43465 (ATCC 607), *Mycolicibacterium aurum* DSM 43999 (ATCC 23366), and non-tuberculous mycobacteria, namely *Mycobacterium avium* DSM 44156 (ATCC 25291), and *Mycobacterium kansasii* DSM 44162 (ATCC 12478) from German Collection of Microorganisms and Cell Cultures (Braunschweig, Germany), and with an avirulent strain of *Mtb* H37Ra ITM-M006710 (ATCC 9431) from Belgian Co-ordinated Collections of Micro-organisms (Antwerp, Belgium). The technique used for activity determination was the microdilution broth panel method using 96-well microtitration plates. The culture medium was Middlebrook 7H9 broth (Sigma-Aldrich, Steinheim, Germany) enriched with 0.4% glycerol (Sigma-Aldrich, Steinheim, Germany) and 10% Middlebrook OADC growth supplement (Himedia, Mumbai, India) [138, 139].

The mycobacterial strains were cultured on Middlebrook 7H9 agar and suspensions were prepared in Middlebrook 7H9 broth. The final density was adjusted to 1.0 on the McFarland scale and diluted in the ratio of either 1:20 (for rapidly growing mycobacteria) or 1:10 (for slow-growing mycobacteria) with broth.

The tested compounds were dissolved in DMSO (Sigma-Aldrich, Steinheim, Germany), and then Middlebrook broth was added to obtain a concentration of 2000 µg/ml. The standards

used for activity determination were INH, RIF, and CPX (Sigma-Aldrich, Steinheim, Germany). The final concentrations were reached by binary dilution and addition of mycobacterial suspension and were set at 500, 250, 125, 62.5, 31.25, 15.625, 7.81, and 3.91 µg/ml. INH was diluted in the range 500–3.91 µg/ml for screening against rapidly growing mycobacteria, 2000–15.625 µg/ml for *M. avium*, 50–0.39 µg/ml for *M. kansasii*, and 1–0.0078 µg/ml for *Mtb*. RIF final concentrations ranged from 50 to 0.39 µg/ml for rapidly growing mycobacteria, from 1 to 0.0078 µg/ml for *M. avium*, and from 0.1 to 0.00078 µg/ml for *Mtb* and *M. kansasii*. CPX was used for screening antimycobacterial activity with final concentrations of 1, 0.5, 0.25, 0.125, 0.0625, 0.0313, 0.0156, and 0.0078 µg/ml. The final concentration of DMSO did not exceed 2.5% (*v/v*) and did not affect the growth of any of the strains. Positive (broth, DMSO, bacteria) and negative (broth, DMSO) growth controls were included.

Plates containing slow-growing mycobacteria were sealed with polyester adhesive film and incubated in the dark at 37 °C without agitation. The addition of a 0.01% solution of resazurin sodium salt followed after 48 h of incubation for *M. smegmatis*, 72 h for *M. aurum*, 96 h for *M. avium* and *M. kansasii*, and after 120 h for *Mtb*. The microtitration panels were then incubated for a further 2.5 h to determine the activity against *M. smegmatis*, 4 h for *M. aurum*, 6 h for *M. avium* and *M. kansasii* and 18 h for *Mtb*.

The antimycobacterial activity was expressed as minimal inhibition concentration (MIC) and the value was read based on stain colour change (blue colour–active compound; pink colour–inactive compound). MIC values for standards were in the range 15.625–31.25 µg/ml for INH, 12.5–25 µg/ml for RIF and 0.0625–0.125 µg/ml for CPX against *M. smegmatis*, 1.95–3.91 µg/ml for INH, 0.39–0.78 µg/ml for RIF, and 0.0078–0.0156 µg/ml for CPX against *M. aurum*, 500–1000 µg/ml for INH, 0.0625–0.125 µg/ml for RIF and 0.5 µg/ml for CPX against *M. avium*, 3.125–6.25 µg/ml for INH, 0.025–0.05 µg/ml for RIF and 0.25 µg/ml for CPX against *M. kansasii*, and 0.125–0.25 µg/ml for INH, 0.00156–0.0031 µg/ml for RIF and 0.125–0.25 for CPX against *Mtb*. All experiments were conducted in duplicate.

5 RESULTS

5.1 The overview of the isolated alkaloids and their structural analysis

DF-01: Dihydrosanguinarine

Summary formula: $C_{20}H_{15}NO_4$

Based on the performed experiments (MS, NMR, optical rotation) and the comparison of the acquired data with that in the literature, the compound was identified as the benzophenanthridine-type alkaloid (+)-dihydrosanguinarine [19].

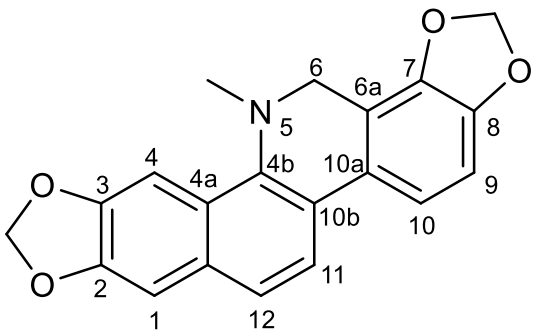

Molecular weight: 333.34

MS analysis

EI-MS *m/z* $[M]^+$ 333 (100), 332 (70), 318 (9), 317 (8), 304 (4), 290 (13), 274 (4), 260 (4)

NMR analysis

^{1}H NMR (500 MHz, $CDCl_3$)

7.71 (1H, d, *J* = 8.5 Hz, H-11), 7.69 (1H, s, H-4), 7.50 (1H, d, *J* = 8.5 Hz, H-12), 7.32 (1H, d, *J* = 8.0 Hz, H-10), 7.13 (1H, s, H-1), 6.87 (1H, d, *J* = 8.0 Hz, H-9), 6.30 (2H, s, 7, 8-OCH_2O–), 6.08 (2H, s, 2, 3-OCH_2O–), 4.22 (2H, s, H-6), 2.64 (3H, s, N-CH_3).

^{13}C NMR (125 MHz, $CDCl_3$)

104.3, 148.1, 147.5, 100.7, 126.5, 142.5, 48.5, 113.6, 144.6, 147.1, 107.2, 116.2, 127.3, 124.4, 120.4, 123.9, 130.8, 101.0, 101.3, 41.6

Optical rotatory

$[\alpha]_D^{21.8}$= +20º (c=0.1 g/100 ml, $CHCl_3$)

DF-02: Dihydrochelerythrine

Summary formula: $C_{21}H_{19}NO_4$

Based on the performed experiments (MS, NMR, optical rotation) and the comparison of the acquired data with that in the literature, the compound was identified as the benzophenanthridine-type alkaloid (+)-dihydrochelerythrine [140].

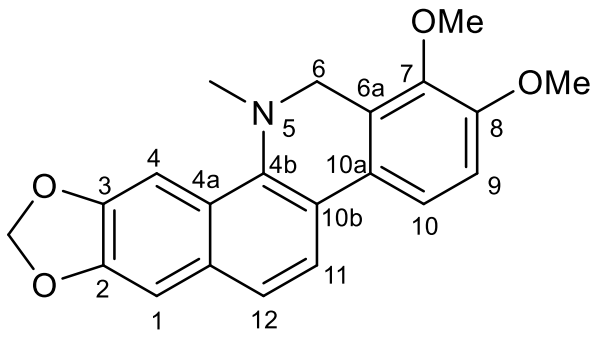

Molecular weight: 349.38

MS Analysis

EI-MS *m/z* $[M]^+$ 349 (100), 348 (85), 334 (17), 333 (14), 332 (12), 319 (15), 318 (15), 304 (11), 290 (19), 276 (9), 174 (8)

NMR Analysis

^{1}H NMR ($CDOD_3$, TMS)

7.70 (1H, d, J = 8.4 Hz, H-11), 7.67 (1H, s, H-4), 7.50(1H, d, J = 8.4 Hz, H-10), 7.48(1H, d, J = 8.4 Hz, H-12), 7.11 (1H, s, H-1), 6.93 (1H, d, J = 8.4 Hz, H-9), 6.05 (2H, s, OCH_2O), 3.94 (3H, s, 8-OCH_3), 3.87 (3H, s, 7-OCH_3), 4.30 (2H, s, H-6) and 2.59 (3H, s, NCH_3)

^{13}C NMR (125 MHz, CD_3OD)

152.2, 148.0, 147.4, 146.0, 142.6, 130.7, 126.3, 126.2, 126.2, 124.2, 123.7, 120.1, 118.6, 110.8, 104.3, 101.0, 100.6, 61.1, 55.7, 48.7, 40.7

Optical rotatory

$[\alpha]_D^{22.3}$= +64º (c=0.1 g/100 ml, $CHCl_3$)

DF-03: 6-Ethoxydihydrochelerythrine

Summary formula: $C_{23}H_{23}NO_5$

Based on the performed experiments (MS, NMR, optical rotation) and the comparison of the acquired data with that in the literature, the compound was identified as the benzophenanthridine-type alkaloid (-)-6-ethoxydihydrochelerythrine [140].

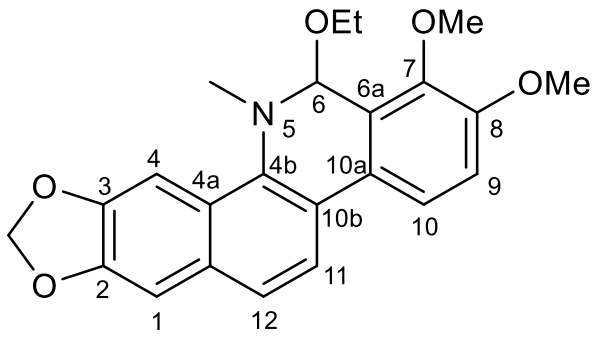

Molecular weight: 393.44

MS Analysis

EI-MS *m/z*: $[M]^+$ 393 (12), 348 (80), 333 (6), 318 (6), 290 (12)

NMR Analysis

^{1}H NMR ($CDOD_3$, TMS)

7.76 (1H, d, J = 8.5 Hz, H-11), 7.66 (1H, s, H-4), 7.62 (1H, d, J = 8.6 Hz, H-10), 7.45 (1H, d, J = 8.5 Hz, H-12), 7.12(1H, s, H-1), 7.02 (1H, d, J = 8.6 Hz, H-9), 6.04 (2H, s, OCH_2O), 5.67 (1H, s, H-6), 3.96 (3H, s, 8-OCH_3), 3.92 (3H, s, 7-OCH_3), 3.72(2H, q, J = 7.0 Hz, -OCH_2CH_3), 2.74(3H, s, -NCH_3), 1.09 (3H, t, J = 7.0 Hz, -OCH_2CH_3)

^{13}C NMR (125MHz, CD_3OD)

152.2, 147.8, 147.3, 146.6, 138.7, 131.0, 126.8, 126.0, 124.9, 123.3, 122.7, 120.1, 119.0, 112.9, 104.6, 101.0, 100.7, 84.5, 61.7, 61.6, 56.0, 40.7, 15.2

Optical rotatory

$[\alpha]_D^{25}$= -8º (c=0.1 g/100 ml, $CHCl_3$)

DF-04: Stylopine

Summary formula: $C_{19}H_{17}NO_4$

Based on the performed experiments (MS, NMR, optical rotation) and the comparison of the acquired data with that in the literature, the compound was identified as the protoberberine-type alkaloid (+)-stylopine [141].

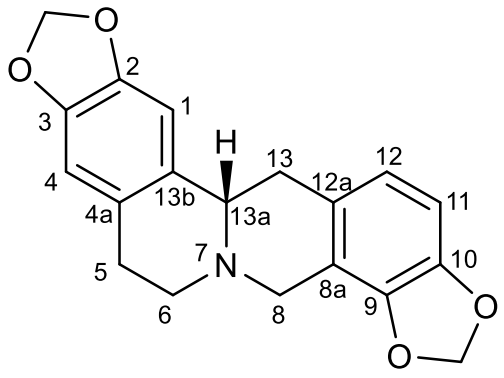

Molecular weight: 323.34

MS Analysis

EI-MS *m/z* $[M]^+$ 323 (25), 174 (15), 148 (100), 91 (10), 77 (5)

NMR Analysis

^{1}H NMR (400 MHz, $CDCl_3$)

7.57 (1H, s, H-4), 6.76 (1H, d, J=8.0 Hz, H-12), 6.70 (1H, s, H-1), 6.60 (1H, d, J=8.0 Hz, H-11), 5.93 (1H, d, J=1.6 Hz, -O-CH2-O-), 5.90 (1H, d, J=1.6 Hz, -O-CH2-O-), 5.89 (2H, s, -O-CH2- O-), 4.07 (1H, d, J=15.2 Hz, H-8a), 3.54 (1H, dd, J=3.2, 11.0 Hz, H-14), 3.51 (1H, d, J=15.2 Hz, H-8b), 3.20 (1H, dd, J=3.2, 15.8 Hz, H-13a), 3.13 (1H, m, H-6a), 3.07 (1H, m, H-5a), 2.78 (1H, dd, J=11.0, 15.8 Hz, H-13b), 2.63 (1H, m, H-5b), 2.58 (1H, m, H-6a)

^{13}C NMR (100MHz, $CDCl_3$)

146.02, 145.82, 144.82, 143.11, 130.53, 128.39, 127.61, 127.61, 120.93, 108.33, 106.67, 105.43, 100.95, 100.70, 59.73, 52.89, 51.83, 36.45, 29.56

Optical rotatory

$[\alpha]_D^{16}$= +297º (c=0.18 g/100 ml, $CHCl_3$)

DF-05: 6-Methoxydihydrochelerythrine

Summary formula: $C_{22}H_{21}NO_5$

Based on the performed experiments (MS, NMR, optical rotation) and the comparison of the acquired data with that in the literature, the compound was identified as the benzophenanthridine-type alkaloid (-)-6-methoxydihydrochelerythrine [142].

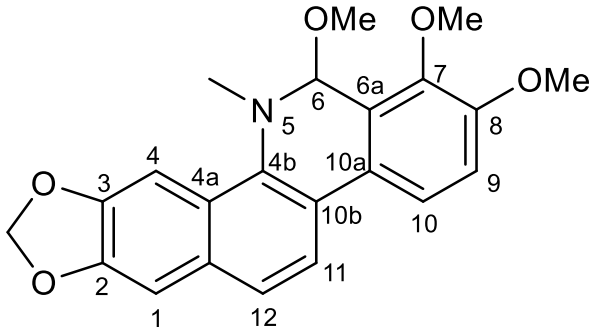

Molecular weight: 379.41

MS Analysis

EI-MS *m/z* (%): 379 (85), 349 (15), 348 (70), 318 (75), 290 (100)

NMR Analysis

^{1}H NMR (400 MHz, $CDCl_3$)

7.78 (1H, d, J = 8.6 Hz, H-11), 7.71 (1H, s, H-4), 7.63 (1H, d, J = 8.6 Hz, H-10), 7.48 (1H, d, J = 8.6 Hz, H-12), 7.13 (1H, s, H-1), 7.05 (1H, d, J = 8.6 Hz, H-9), 6.06, 6.05 (2H, each d, J = 1.1 Hz, –OCH_2O-2,3), 5.55 (1H, s, H-6), 3.97 (3H, s, 7-OCH_3), 3.93 (3H, s, 8-OCH_3), 3.47 (3H, s, 6-OCH_3), 2.77 (3H, s, N–CH_3)

^{13}C NMR (100 MHz, $CDCl_3$)

152.2, 148.1, 147.5, 146.8, 138.5, 131.2, 126.9, 125.9, 125.0, 123.6, 122.7, 120.1, 119.1, 113.1, 104.8, 101.2, 100.8, 86.2, 61.8, 56.1, 54.1, 40.8

Optical Rotatory

$[\alpha]_D^{25.9}$= -16º (c=0.1 g/100 ml, $CHCl_3$)

DF-06: *Bis*-[6-(5,6-dihydrochelerythrinyl)]ether

Summary formula: $C_{42}H_{36}N_2O_9$

Based on the performed experiments (MS, NMR, optical rotation) and the comparison of the acquired data with that in the literature, the compound was identified as the benzophenanthridine-type alkaloid (-)-*bis*-[6-(5,6-dihydrochelerythrinil)]ether [143].

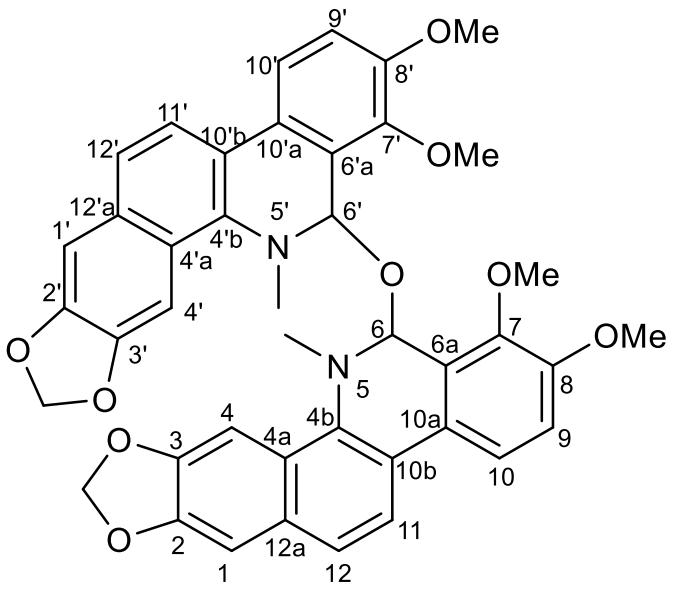

Molecular weight: 712.76

MS Analysis

EI-MS *m/z* (%): [M $^+$] 713 (0.9), 433 (0.7), 378 (6), 362 (9), 350 (64), 348 (100), 333 (25)

NMR Analysis

^{1}H NMR (300 MHz, $CDCl_3$)

7.93 (2H, s, H-4, H-4‘), 7.68 (2H, d, J=8.5 Hz, H-11, H-11‘), 7.48 (2H, d, J = 8.7 Hz, H-10, H-10‘), 7.44 (2H, d, J = 8.5 Hz, H-12, H-12‘), 7.16 (2H, s, H-1, H-1‘), 6.84 (2H, d, J = 8.7 Hz, H-9, H-9‘), 6.61 (2H, s, H-6, H-6‘), 6.11 (4H, s, 2 x-OCH_2O-), 3.72 (6H, s, OMe-8, OMe-8‘), 3.05 (6H, s, 5-NMe, 5‘-NMe), 2.41 (6H, s, OMe-7, OMe-7‘),

^{13}C NMR (75 MHz, $CDCl_3$)

152.07, 148.03, 147.47, 146.27, 138.37, 131.16, 126.89, 126.11, 125.47, 123.22, 123.22, 119.79, 118.66, 112.25, 104.46, 101.09, 100.81, 77.42, 60.37, 55.62, 40.83

Optical rotatory

$[\alpha]_D^{25}$= -12º (c= 0.1 g/100 ml, $CHCl_3$)

DF-07: Sanguinarine

Summary formula: $C_{20}H_{14}NO_4^+$

Based on the performed experiments (MS, NMR, optical rotation) and the comparison of the acquired data with that in the literature, the compound was identified as the benzophenanthridine-type alkaloid (±)-sanguinarine [140].

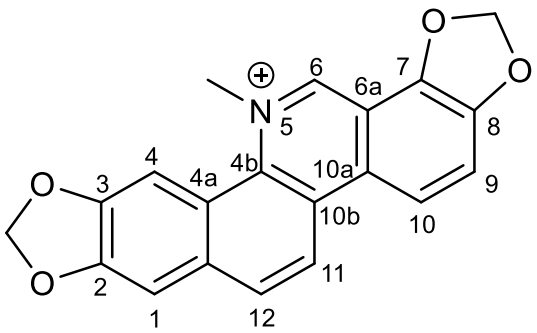

Molecular weight: 332.09

MS analysis

EI-MS *m/z*: $[M]^+$ 317 (74.23), 316 (3.98), 315 (2.40), 289.2 (47.08), 287 (7), 275.1 (4.41), 273 (4.14), 261 (4.74), 259.9 (17.39), 258.9 (4.99), 232.1 (11.25), 204 (6.15), 203.1 (9.15)

NMR analysis

^{1}H NMR ($CDOD_3$, TMS)

9.95(1H, s, H-6), 8.57(1H, d, J = 8.9 Hz, H-11), 8.48(1H, d, J = 8.8 Hz, H-10), 8.19 (1H, d, J = 8.9 Hz, H-12), 8.13(1H, s, H-4), 7.95(1H, d, J = 8.8 Hz, H-9), 7.55(1H, s, H-1), 6.54 (2H, s, 1,2-OCH_2O), 6.30(2H, s, 7,8-OCH_2O), 4.49 (3H, s, NCH_3)

^{13}C NMR (125MHz, CD_3OD)

107.2, 150.6, 150.6, 105.2, 121.8, 133.0, 150.7, 111.1, 148.1, 149.3, 121.4, 118.4, 128.9, 127.4, 119.8, 133.0, 133.9, 104.3, 106.5, 53.2

Optical rotatory

In virtue of the absence of any chiral centre, the optical rotation was not measured.

DF-08: Protopine

Summary formula: $C_{20}H_{19}NO_5$

Based on the performed experiments (MS, NMR, optical rotation) and the comparison of the acquired data with that in the literature, the compound was identified as the protopine-type alkaloid (±)-protopine [19].

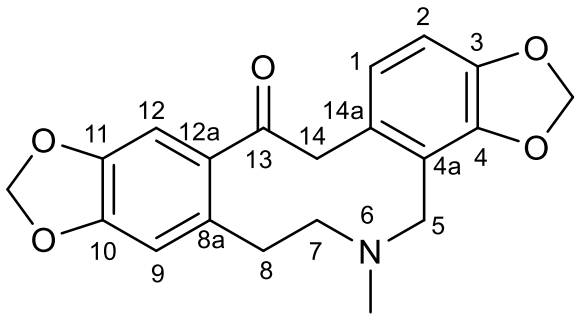

Molecular weight: 353.37

MS Analysis

EI-MS *m/z* (%): [M^+] 354 (70), 336 (10), 305 (5), 275 (20), 265 (7), 247 (14), 206 (19), 189 (88), 188 (100), 165 (14), 149 (44)

NMR Analysis

^{1}H NMR (500 MHz, $CDCl_3$)

6.93 (1H, s, H-4), 6.66 (1H, s, H-1), 6.71 (1H, d, *J* = 7.7 Hz, H-11), 6.68 (1H, d, *J* = 7.7 Hz, H-12), 5.97 (2H, s, 2, 3-OCH_2O–), 5.95 (2H, s, 9, 10-OCH_2O–), 2.00 (3H, s, N-CH_3)

^{13}C NMR (125 MHz, $CDCl_3$)

110.3, 148.0, 146.2, 108.0, 135.6, 31.4, 57.7, 51.1, 117.5, 146.0, 145.9, 106.8, 124.9, 128.6, 46.1, 197.5, 132.3, 101.2, 100.9, 41.6

Optical Rotatory

In virtue of the absence of any chiral centre, the optical rotation was not measured.

DF-09: Allocryptopine

Summary formula: $C_{21}H_{23}NO_5$

Based on the performed experiments (MS, NMR, optical rotation) and the comparison of the acquired data with those in the literature, the compound was identified as the protopine-type alkaloid (±)-allocryptopine [141].

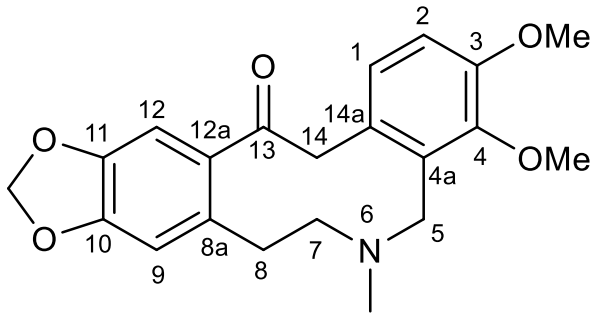

Molecular weight: 369.41

MS Analysis

EI-MS *m/z* (%): [M^+] 352.1 (100), 339.1 (14), 321.0 (33), 290.2 (20), 188.2 (60).

NMR Analysis

^{1}H NMR (400 MHz, $CDCl_3$)

6.88 (1H, s, H-1), 6.84 (1H, d, J=8.4 Hz, H-11), 6.73 (1H, d, J=8.4 Hz, H-12), 6.56 (1H, s, H-4), 5.85 (2H, s, -O-CH2-O-), 3.93 (2H, br. s, H-8), 3.78, 3.71 (both 3H, each s, 9-OMe, 10-OMe), 3.68 (2H, br. s, H-13), 2.68 (2H, br. s, H-5), 2.54 (2H, br. s, H-6), 1.79 (3H, s, N-Me)

^{13}C NMR (100 MHz, $CDCl_3$)

190.98, 151.22, 147.73, 146.94, 145.74, 135.4, 132.4, 129.04, 128.09, 127.37, 110.34, 110.1, 108.9, 100.96, 60.57, 57.22, 55.44, 50.06, 45.87, 41.03, 32.01.

Optical Rotatory

In virtue of the absence of any chiral centre, the optical rotation was not measured.

DF-10: Cryptopine

Summary formula: $C_{21}H_{23}NO_5$

Based on the performed experiments (MS, NMR, optical rotation) and the comparison of the acquired data with the literature, the compound was identified as the protopine-type alkaloid (±)-cryptopine [144].

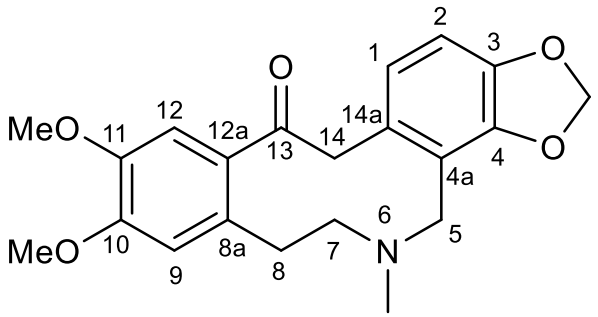

Molecular weight: 369.41

MS Analysis

ESI-MS *m/z* (%): [M^+] 369 (10), 190 (20), 179 (40), 148 (100), 91 (5), 77 (5)

NMR Analysis

^{1}H NMR (500 MHz, DMSO-d6)

6.93 (1H, s, H-1), 6.82 (1H, s, H-4), 6.71 (2H, m, H-11), 5.96 (2H, s, -OCH_2O-), 3.89 (2H, br, H-13), 3.75 (6H, s, -OCH_3 x 2), 3.59 (2H, m, H-8), 2.89 (2H, m, H-5), 2.49 (2H, m, H-6), 1.79 (3H, s, N-CH_3)

^{13}C NMR (125 MHz, DMSO-d6)

194.8, 148.8, 146.4, 146.4, 146.4, 145.7, 134.3, 131.2, 130.0, 125.0, 118.0, 113.9, 111.7, 106.3, 100.7, 57.3, 55.6, 55.5, 50.4, 45.8, 41.0, 22.8

Optical Rotatory

In virtue of the absence of any chiral centre, the optical rotation was not measured.

DF-11: Chelidonine

Summary formula: $C_{20}H_{19}NO_5$

Based on the performed experiments (MS, NMR, optical rotation) and the comparison of the acquired data with the literature, the compound was identified as the benzophenanthridine-type alkaloid (+)-chelidonine [145].

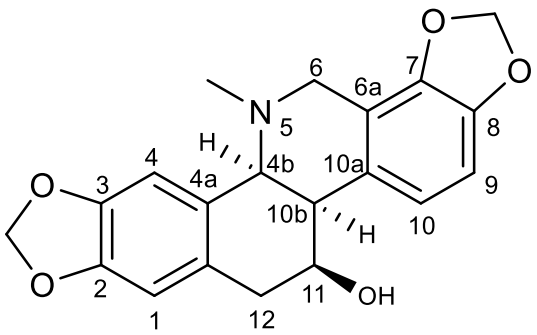

Molecular weight: 353.37

MS Analysis

ESI-MS *m/z* (%): [M^+] 353 (9.7), 336 (12), 335 (48), 334 (34.2), 332 (99.99), 303 (38), 176 (40)

NMR Analysis

^{1}H NMR (250 MHz, $CDCl_3$)

6.76 (2H, s, H-9 and H-10), 6.67 (1H, s, H-2), 6.65 (1H, s, H-1), 5.97 (4H, m, 2 x –OCH_2O-), 4.23 (1H, br, s, H-11), 3.21 (1H, d, J = 17.5 Hz, H-12), 3.08 (1H, dd, J = 17.5 and 4.5 Hz, H-12), 2.99 (1H, t, J = 2.6 Hz, H-13), 2.28 (3H, s, NMe)

^{13}C NMR (62.83 MHz, $CDCl_3$)

148.2, 145.6, 145.3, 143.1, 131.4, 128.9, 125.8, 120.4, 117.1, 111.9, 109.2, 107.4, 101.4, 101.1, 72.4, 62.9, 53.9, 42.4, 42.1, 39.7

Optical Rotatory

$[\alpha]_D^{20}$= +117º (c = 0.3 g/100 ml, $CHCl_3$)

DF-12: Isocorydine

Summary formula: $C_{20}H_{23}NO_4$

Based on the performed experiments (MS, NMR, optical rotation) and the comparison of the acquired data with the literature, the compound was identified as the aporphine-type alkaloid (+)-isocorydine [141].

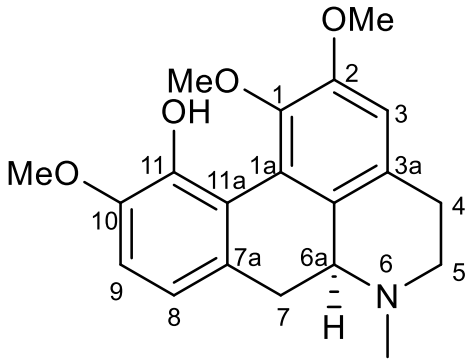

Molecular weight: 341.40

MS Analysis

ESI-MS *m/z* (%): [M^+] 341 (20), 340 (68), 326 (100), 310 (10), 298 (7)

NMR Analysis

^{1}H NMR (400 MHz, $CDCl_3$)

6.71 (1H, d, J=8.2 Hz, H-8), 6.67 (1H, d, J=8.2 Hz, H-9), 6.56 (1H, s, H-3), 3.79 (1H, dd, J=12.8, 4.4 Hz, H-6a), 3.77 (3H, s, 2-OMe), 3.74 (3H, s, 10-OMe), 3.57 (3H, s, 1-OMe), 3.03 (1H, m, H-5a), 2.92 (1H, m, H-4a), 2.85 (1H, dd, J=11.0, 5.5 Hz, H-5b), 2.70 (1H, m, H-7a), 2.53 (1H, m, H-4b), 2.41 (1H, m, H-7b), 2.38 (3H, s, N-Me)

^{13}C NMR (100 MHz, $CDCl_3$)

150.67, 148.86, 143.36, 141.51, 129.58, 129.53, 128.52, 125.32, 119.64, 118.62, 110.47, 110.23, 62.43, 61.63, 55.67, 55.40, 43.49, 35.44, 28.87

Optical Rotatory

$[\alpha]_D^{23.5}$= +264º (c=0.1 g/100 ml, $CHCl_3$)

DF-13: Glaucine

Summary formula: $C_{21}H_{25}NO_4$

Based on the performed experiments (MS, NMR, optical rotation) and the comparison of the acquired data with the literature, the compound was identified as the aporphine-type alkaloid (+)-glaucine [146].

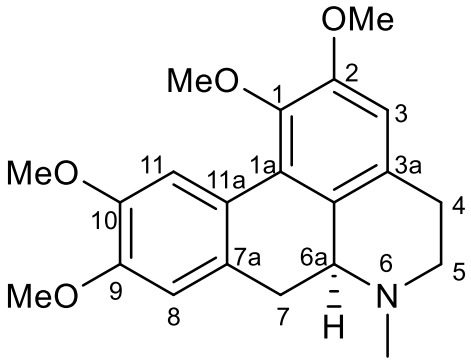

Molecular weight: 355.43

MS Analysis

EI-MS *m/z* (%): [M^+] 355 (100), 341 (43.9), 339 (5), 324 (21.4), 298 (17.9), 282 (29.2), 265 (8.77), 251 (7.6), 238 (5.7), 223 (8), 210 (9.6), 195 (9.3), 180 (14.5), 165 (18.7), 152 (33.6), 139 (29.5), 127 (8.3), 111 (14), 97 (15.5), 83 (12.7), 71 (19.8), 54 (68.8)

NMR Analysis

^{1}H NMR (600 MHz, CD_3OD)

7.87 (1H, s, H-11), 6.99 (1H, s, H-8), 6.88 (1H, s, H-3), 3.83 (3H, s, 9-OMe), 3.80 (3H, s, 2-OMe), 3.77 (3H, s, 10-OMe), 3.62 (3H, s, 1-OMe), 3.40 (2H, dd, J = 13.5 and 3.6 Hz, H-5), 3.19-3.13 (2H, m), 3.07 (3H, s, N-Me), 2.98 (2H, dd, J = 17.4 and 3.0 Hz, H-4), 2.70 (1H, t, J= 13.8, H-6a).

^{13}C NMR (150 MHz, CD_3OD)

152.99, 148.41, 147.60, 144.42, 126.31, 126.25, 126.10, 123.07, 120.80, 111.73, 111.53, 111.01, 61.15, 59.72, 55.83, 55.54, 55.43, 51.45, 40.94, 30.31, 25.65

Optical Rotatory

$[\alpha]_D^{27}$ = +127.4º (c=0.13 g/100 ml, MeOH)

DF-14: Corydine

Summary formula: $C_{20}H_{23}NO_4$

Based on the performed experiments (MS, NMR, optical rotation) and the comparison of the acquired data with those in the literature, the compound was identified as the aporphine-type alkaloid (+)-corydine [147].

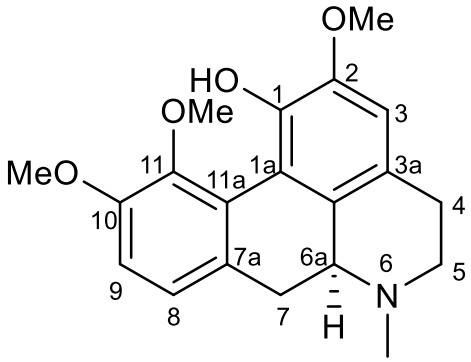

Molecular weight: 341.40

MS Analysis

EI-MS *m/z* (%): [M^+] 341 (85), 326 (55), 324 (35), 310 (100), 295 (10), 268 (10)

NMR Analysis

^{1}H NMR (500 MHz, $CDCl_3$)

2.33 (1H, ddd, J = 13.7, 12.8, 1.0 Hz, H-7b), 2.43 (1H, ddd, J = 12.0, 11.2, 3.9 Hz, H-5b), 2.46 (3H, s, NCH_3), 2.59 (1H, dd, J = 16.0, 3.9 Hz, H-4b), 2.85 (1H, ddd, J = 13.7, 3.5, 1.3 Hz, H-6a), 2.93 (1H, ddd, J = 11.2, 6.0, 1.3 Hz, H-5a), 2.96 (1H, dd, J = 12.8, 3.5 Hz, H-7a), 3.08 (1H, br ddd, J = 16.0, 12.0, 6.0 Hz, H-4a), 3.66 (3H, s, OCH_3-11), 3.83 (3H, s, OCH_3-10), 3.84 (3H, s, OCH_3-2), 6.61 (1H, s, H-3), 6.80 (1H, d, J = 8.0 Hz, H-9), 7.01 (1H, dd, J = 8.0, 1.0 Hz, H-8), 8.61 (1H, s, OH)

^{13}C NMR (126 MHz, $CDCl_3$)

151.8, 149.1, 143.8, 142.3, 130.9, 128.2, 126.5, 124.3, 124.0, 119.3, 111.3, 110.8, 62.8, 62.0, 56.0, 56.0, 52.8, 44.0, 35.6, 29.1

Optical rotatory

$[\alpha]_D^{17.8}$= +172º (c=0.1 g/100 ml, $CHCl_3$)

DF-15: Isocorypalmine

Summary formula: $C_{20}H_{23}NO_4$

Based on the performed experiments (MS, NMR, optical rotation) and the comparison of the acquired data with that in the literature, the compound was identified as the protoberberine-type alkaloid (-)-isocorypalmine [148].

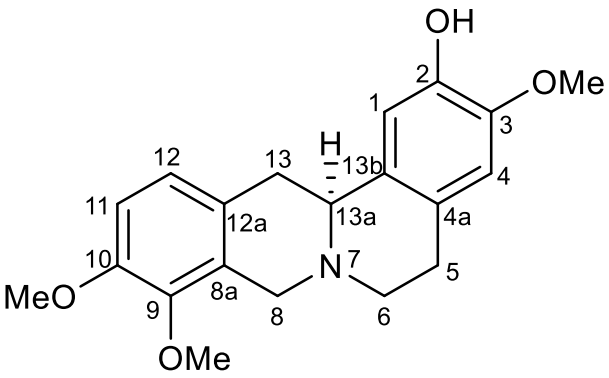

Molecular weight: 341.40

MS Analysis

EI-MS *m/z* (%): [M^+] 342 (15), 325 (8), 293 (5), 192 (15), 178 (100), 151 (10).

NMR Analysis

^{1}H NMR (500 MHz, $CDCl_3$)

6.86 (1H, d, J = 8.3 Hz, H-12), 6.82 (1H, s, H-1), 6.78 (1H, d, J = 8.3 Hz, H-11), 6.59 (1H, s, H-4), 4.23 (1H, d, J = 15.5 Hz, H-8), 3.87 (3H, s, 9-OMe), 3.84 (3H, s, 3-OMe), 3.84 (3H, s, 10-OMe), 3.52 (1H, br, d, J= 15.5 Hz, H-8), 3.51 (1H, m, H-13a), 3.25 (1H, dd, J= 15.8 and 3.6 Hz, H-13), 3.19 (1H, m, H-6), 3.13 (1H, m, H-5), 2.80 (1H, dd, J= 15.8 and 11.2 Hz, H-13), 2.66 (1H, m, H-5), 2.63 (1H, m, H-6)

^{13}C NMR (125 MHz, $CDCl_3$)

150.0, 145.0, 144.7, 144.1, 130.4, 128.5, 127.6, 125.9, 123.8, 111.2, 110.9, 110.5, 60.0, 59.1, 55.8, 55.8, 53.9, 51.5, 36.1, 29.1

Optical rotatory

$[\alpha]_D^{25}$= -173º (c=0.2 g/100 ml, $CHCl_3$)

DF-16: Laudanosine

Summary formula: $C_{21}H_{27}NO_4$

Based on the performed experiments (MS, NMR, optical rotation) and the comparison of the acquired data with the literature, the compound was identified as the benzyltetrahydroisoquinoline-type alkaloid (±)-laudanosine [149].

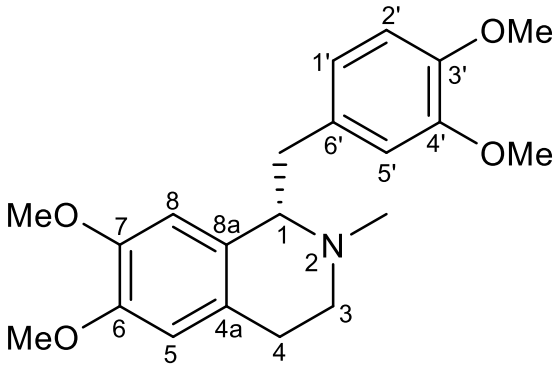

Molecular weight: 357.44

MS Analysis

EI-MS *m/z* (%): [M^+] 327 (35), 295 (5), 206 (100), 189 (10), 165 (8)

NMR Analysis

^{1}H NMR (400 MHz, $CDCl_3$)

6.74 (d, J = 8.1 Hz, 1H, H-5′), 6.61 (dd, J = 8.1, 1.9 Hz, 1H, H-6′), 6.58 (d, J = 1.9 Hz, 1H, H-2′), 6.54 (s, 1H, H-5), 6.03 (s, 1H, H-8), 3.82, 3.81 (2s, 2 × 3H, C6 -OCH_3, C4′-OCH_3), 3.76 (s, 3H, C3′-OCH_3), 3.68 (dd, J = 7.7, 4.9 Hz, 1H, H-1), 3.55 (s, 3H, C7 -OCH_3), 3.19 − 3.13 (m, 1H, Ha-3), 3.13 (dd, J = 13.7, 4.9 Hz, 1H, Ar-CHa), 2.87− 2.69 (m, 2H, Ha-4, Hb-3), 2.75 (dd, J = 13.7, 7.7 Hz, 1H, Ar-CHb), 2.57 (dt, J = 14.9, 4.0 Hz, 1H, Hb-4), 2.52 (s, 3H, N-CH_3)

^{13}C NMR (100.6 MHz, $CDCl_3$)

148.5, 147.3, 147.2, 146.3, 132.4, 129.1, 125.9, 121.8, 112.9, 111.1, 111.0, 110.9, 64.8, 55.9, 55.8, 55.7, 55.5, 46.9, 42.6, 40.8, 25.5

Optical rotatory

In virtue of the absence of any chiral centre, the optical rotation was not measured.

DF-17: Scoulerine

Summary formula: $C_{19}H_{21}NO_4$

Based on the performed experiments (MS, NMR, optical rotation) and the comparison of the acquired data with that in the literature, the compound was identified as the protoberberine-type alkaloid (-)-scoulerine [150].

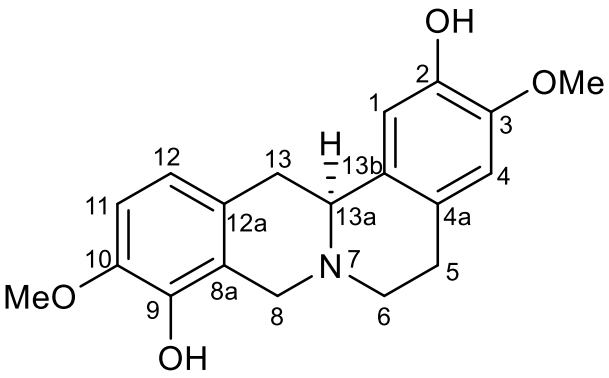

Molecular weight: 327.38

MS Analysis

EI-MS *m/z* %: [M^+] 327 (55), 310 (8), 178 (100), 176 (32), 163 (13), 150 (48), 135 (27), 107 (16)

NMR Analysis

^{1}H NMR (300 MHz, $CDCl_3$)

6.84 (1H, s, Ar), 6.75 (1H, d, J = 8.3 Hz, Ar), 6.68 (1H, d, J = 8.3 Hz, Ar), 6.61 (1H, s, Ar), 4.25 (1H, d, J = 15.6 Hz, N-CH_2-Ar), 3.88 (3H, s, OCH_3), 3.87 (3H, s, OCH_3), 3.49-3.57 (2H, m, N-CH2-Ar + CH), 3.11-3.28 (3H, m, CH_2), 2.83 (1H, dd, J1 = 15.9 Hz, J2 = 11.4 Hz, CH_2), 2.63-2.70 (2H, m, CH_2)

^{13}C NMR (75 MHz, $CHCl_3$)

145.1, 144.0, 143.9, 141.5, 130.6, 128.2, 126.1, 121.2, 119.3, 111.4, 110.6, 109.0, 59.2, 56.2, 55.9, 53.5, 51.6, 36.3, 29.2

Optical rotatory

$[\alpha]_D^{25.9}$= -280º (c=0.1 g/100 ml, $CHCl_3$)

DF-18: Berberine

Summary formula: $C_{20}H_{18}NO_4^+$

Based on the performed experiments (MS, NMR, optical rotation) and the comparison of the acquired data with those in the literature, the compound was identified as the protoberberine-type alkaloid (±)-berberine [141].

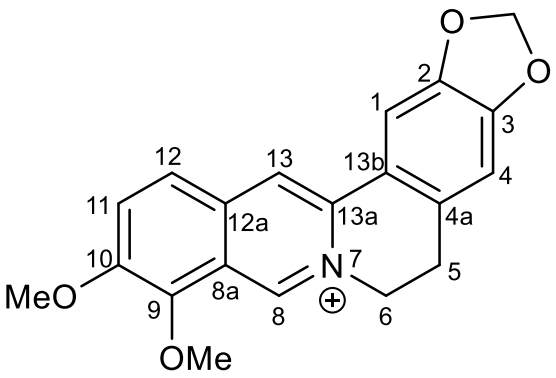

Molecular weight: 336.36

MS Analysis

EI-MS *m/z* (%): [M^+] 336 (97), 321 (100), 320 (67), 306 (27), 292 (54)

NMR Analysis

^{1}H NMR (400 MHz, CD_3OD)

9.75 (1H, s, H-8), 8.67 (1H, s, H-13), 8.09 (1H, d, J=9.2 Hz, H-11), 7.97 (1H, d, J=9.2 Hz, H-12), 7.63 (1H, s, H-1), 6.94 (1H, s, H-4), 6.09 (2H, s, -O-CH_2-O-), 4.92 (2H, t-like, J=6.4 Hz, H-6), 4.19 (3H, s, O-Me), 4.09 (3H, s, O-Me), 3.24 (2H, t-like, J=6.4 Hz, H-5)

^{13}C NMR (100 MHz, CD_3OD)

151.99, 151.84, 149.73, 146.24, 145.56, 139.47, 134.97, 131.74, 127.88, 124.40, 123.17, 121.72, 121.35, 109.29, 106.44, 103.58, 62.53, 57.61, 57.17, 28.21

Optical rotatory

In virtue of the absence of any chiral centre, the optical rotation was not measured.

DF-19: Coptisine

Summary formula: $C_{19}H_{14}NO_4^+$

Based on the performed experiments (MS, NMR, optical rotation) and the comparison of the acquired data with those in the literature, the compound was identified as the protoberberine-type alkaloid (±)-coptisine [151].

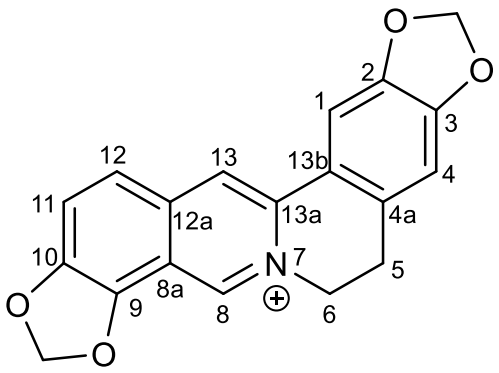

Molecular weight: 320.32

MS Analysis

EI-MS *m/z*: $[M]^+$ 320 (100), 318 (4), 293 (3), 292 (14), 291 (5), 290 (6), 277 (5), 263 (3), 249 (3)

NMR Analysis

^{1}H NMR (400 MHz, DMSO-d6)

9.95 (1H, s, H-8), 8.94 (1H, s, H-13), 8.04 (1H, d, J = 8.5 Hz, H-11), 7.81 (1H, d, J = 8.8 Hz, H-12), 7.78 (1H, s, H-1), 7.04 (1H, s, H-4), 6.53 (2H, s, -OCH_2O-), 6.17 (2H, s, -OCH_2O-), 4.87 (2H, t, J = 6.3 Hz, H-6), 3.19 (2H, t, J = 6.3 Hz, H-5)

^{13}C NMR (100 MHz, DMSO-d6):

150.3, 148.2, 147.6, 145.1, 144.4, 137.4, 132.9, 131.1, 122.3, 121.6, 121.5, 120.7, 112.2, 109.0, 105.8, 105.0, 102.6, 55.6, 26.8

Optical rotatory

In virtue of the absence of any chiral centre, the optical rotation was not measured.

DF-20: Palmatine

Summary formula: $C_{21}H_{22}NO_4^+$

Based on the performed experiments (MS, NMR, optical rotation) and the comparison of the acquired data with those in the literature, the compound was identified as the protoberberine-type alkaloid (±)-palmatine [151].

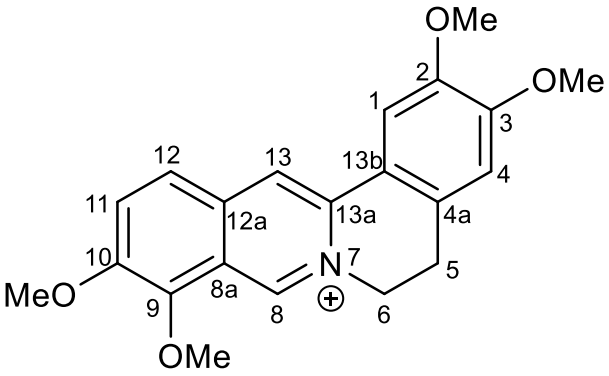

Molecular weight: 352.40

MS Analysis

EI-MS *m/z*: $[M]^+$ 352 (5), 337 (26), 323 (22), 321 (6), 115 (26), 55 (53), 43 (100)

NMR Analysis

^{1}H NMR (400 MHz, MeOD-d_4)

9.75 (s, 1H, H-8), 8.79 (s, 1H, H-13), 8.10 (d, *J* = 9.1 Hz, 1H, H-11), 8.00 (d, *J* = 9.1 Hz, 1H, H-12), 7.65 (s, 1H, H-1), 7.03 (s, 1H, H-4), 4.92 (m, 1H, H-6), 4.19 (s, 3H, 9-OMe), 4.09 (s, 3H, 10-OMe), 3.97 (s, 3H, 2-OMe), 3.92 (s, 3H, 3-OMe), 3.32 (m, 1H, H-5)

^{13}C NMR (100MHz, CD_3OD)

151.5, 150.2, 148.7, 145.4, 143.6, 137.7, 133.1, 128.6, 126.8, 123.4, 121.3, 119.8, 118.9, 111.29, 108.72, 61.87, 61.87, 57.0, 56.1, 55.8, 26.0

Optical rotatory

In virtue of the absence of any chiral centre, the optical rotation was not measured.

DF-21: Magnoflorine

Summary formula: $C_{20}H_{24}NO_4^+$

Based on the performed experiments (MS, NMR, optical rotation) and the comparison of the acquired data with that in the literature, the compound was identified as the aporphine-type alkaloid (+)-magnoflorine [152].

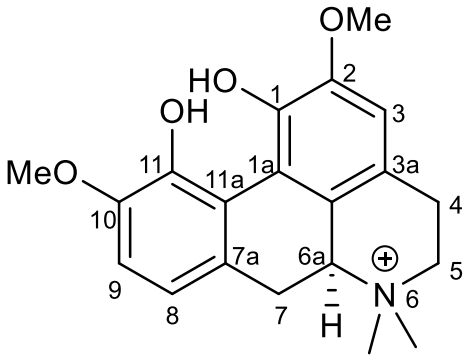

Molecular weight: 342.41

MS Analysis

EI-MS *m/z*: $[M]^+$ 342 (100), 341 (88), 327 (45), 301 (62), 273(25), 253 (30), 227 (25), 163 (31), 58 (42)

NMR Analysis

^{1}H NMR (500 MHz, DMSO-d6)

6.66 (1H, d, J = 8.0 Hz, H-9), 6.47 (1H, d, J = 7.9 Hz, H-8), 6.45 (1H, s, H-3), 3.82 (3H, s, 10-OCH_3), 3.80 (1H, m, H-6a), 3.75 (3H, s, 2-OCH_3), 3.40 (1H, m, H-5b), 3.30 (1H, m, H-5a), 3.21 (3H, s, N-CH_3b), 2.75 (3H, s, N-CH_3a), 3.10 (1H, m, H-4a), 2.56 (1H, br-d, J = 15.6, H-4b), 2.91 (1H, br-d, H-7b), 2.37 (1H, br-t, J = 12.8, H-7a)

^{13}C NMR (125 MHz, DMSO-d6)

152.7, 151.4, 149.8, 149.0, 126.1, 123.1, 123.0, 121.1, 117.5, 116.5, 110.7, 109.7, 70.7, 62.1, 56.3, 56.0, 53.9, 43.6, 31.5, 24.6

Optical rotatory

$[\alpha]_D^{26}$= +240º (c=0.1 g/100 ml, MeOH)

5.2 Screening of biological activities of isolated alkaloids from *Dicranostigma franchetianum*

5.2.1 Biological activity in connection with Alzheimer´s disease

Alkaloids were tested for their inhibitory activity against *h*AChE, *h*BuChE, and POP. The inhibitory activity values are summarised in the table (Table 7). The most interesting values have a yellow label.

Table 7. *In vitro, h*AChE/*h*BuChE and POP inhibition activity of isoquinoline alkaloids isolated from *D. franchetianum* and calculated BBB score.

Alkaloid	IC_{50}, *h*AChE ± SEM (μM)[b]	SI for *h*AChE[c]	IC_{50}, *h*BuChE ± SEM (μM)[b]	SI for *h*BuChE[d]	IC_{50}, POP ± SEM (μM)[b]	BBB score[e]
dihydrosanguinarine (**DF-01**)	>100	n.c.	>100	n.c.	>50	n.c.
dihydrochelerythrine (**DF-02**)	3.3 ± 0.7	4.27	14.1 ± 1.6	0.23	22 ± 3	4.50
6-ethoxydihydrochelerythrine (**DF-03**)	1.2 ± 0.2	2.91	3.2 ± 0.2	0.34	10 ± 1	4.07
stylopine (**DF-04**)	>100	n.c.	>100	n.c.	21 ± 3	n.c.
6-methoxy-dihydrochelerythrine (**DF-05**)	5.7 ± 1.2	1.5	8.7 ± 1.7	0.65	42 ± 2	4.08
bis-[6-(5,6-dihydro-chelerythrinyl)]ether (**DF-06**)	43 ± 5	2.14	92 ± 12	0.46	>50	1.39
sanguinarine (**DF-07**)	7.2 ± 0.4	0.53	3.8 ± 0.6	1.89	1.5 ± 0.1	4.56
protopine (**DF-08**)	>100	n.c.	>100	n.c.	>50	n.c.
allocryptopine (**DF-09**)	>100	n.c.	>100	n.c.	>50	n.c.
cryptopine (**DF-10**)	>100	n.c.	>100	n.c.	32 ± 3	n.c.
chelidonine (**DF-11**)	17 ± 1	n.c.	12 ± 2	n.c.	>50	3.83
isocorydine (**DF-12**)	>100	n.c.	>100	n.c.	19 ± 2	n.c.
glaucine (**DF-13**)	>100	n.c.	>100	n.c.	>50	n.c.
corydine (**DF-14**)	>100	n.c.	>100	n.c.	>50	n.c.
isocoryplamine (**DF-15**)	>100	n.c.	>100	n.c.	>50	n.c.
laudanosine (**DF-16**)	>100	n.c.	>100	n.c.	>50	n.c.
scoulerine (**DF-17**)	60 ± 10	> 1.66	>100	< 0.60	>50	n.c.
berberine (**DF-18**)	0.71 ± 0.10	42.25	30 ± 4	0.02	>50	4.54
palmatine (**DF-19**)	1.1 ± 0.1	> 58.82	> 100	< 0.02	>50	4.51
coptisine (**DF-20**)	9.4 ± 0.5	0.94	8.9 ± 1.2	1.05	50 ± 3	4.48
magnoflorine (**DF-21**)	> 100	n.c.	> 100	n.c.	70 ± 7	n.c.
galanthamine[f]	2.0 ± 0.1	17.00	34 ± 2	0.06	n.t.	5.0
eserine[f]	0.20 ± 0.01	1.50	0.30 ± 0.01	0.67	n.t.	5.0
baicalein	n.t	-	n.t	-	14 ± 1	n.c.

[a] Compounds were tested at the concentration of 100 μM; [b] Concentration required to decrease enzyme activity by 50%, the values are reported as mean ± SEM of three independent measurements, each performed in triplicate; [c] Calculated SI for *h*AChE

as *h*BuChE IC_{50}/*h*AChE IC_{50}; [d] Calculated SI for *h*BuChE as *h*AChE IC_{50}/hBuChE IC_{50}; [e] Calculated *in silico* using BBB score; [f] Reference compound; n.c. means not calculated, n. t means not tested.

5.2.2 Antimycobacterial activity of isoquinoline alkaloids isolated from *Dicranostigma franchetianum*

Considering the anti-TB potency of alkaloids containing an isoquinoline heterocycle in their structure [153], the compounds isolated in sufficient amounts have been screened for their antimycobacterial potential against five *Mycobacterium* or *Mycolicibacterium* strains (Table 8).

Table 8. *In vitro* antimycobacterial activity against *Mtb* H37Ra, *Mycolicibacterium aurum, Mycobacterium avium, Mycobacterium kansasii,* and *Mycolicibacterium smegmatis* (MIC), and calculated lipophilicity (ClogP) of isoquinoline alkaloids isolated from *D. franchetianum*.

Alkaloid	*Mtb* H37Ra (µg/ml)	*Mtb* H37Ra (µM)[a]	*M. aurum* (µg/ml)	*M. avium* (µg/ml)	*M. kansasii* (µg/ml)	*M. smegmatis* (µg/ml)	ClogP[b]
dihydrosanguinarine (**DF-01**)	≥500	≥1501	≥500	≥500	125	≥500	5.23
dihydrochelerythrine (**DF-02**)	250	716	250	62.5	250	≥500	4.92
6-ethoxydihydrochelerythrine (**DF-03**)	31.25	79	15.625	31.25	31.25	31.25	5.47
stylopine (**DF-04**)	≥125	≥387	≥125	≥125	≥125	≥125	3.81
bis-[6-(5,6-dihydro-chelerythrinyl)]ether (**DF-06**)	31.25	44	31.25	31.25	31.25	31.25	8.89
protopine (**DF-08**)	≥500	≥1416	≥500	250	120	≥500	3.57
allocryptopine (**DF-09**)	≥250	≥678	≥250	≥250	250	≥250	3.48
cryptopine (**DF-10**)	≥125	≥339	≥125	≥125	≥125	≥125	3.48
isocorydine (**DF-12**)	≥500	≥1432	≥500	≥500	125	≥500	2.60
glaucine (**DF-13**)	125	≥352	125	125	62.5	≥250	3.07
corydine (**DF-14**)	≥500	≥1466	250	62.5	250	≥500	2.82
isocoryplamine (**DF-15**)	≥250	≥733	≥250	≥250	≥250	≥250	2.72
scoulerine (**DF-17**)	250	764	125	250	15.625	125	2.25
berberine (**DF-18**)	125	336	62.5	31.25	31.25	62.5	-0.77
isoniazid[c]	0.25	1.82	3.91	500	6.25	31.25	-0.67
rifampicin[c]	0.00625	0.0075	0.39	0.125	0.025	12.5	3.71
ciprofloxacin[c]	0.25	0.75	0.015625	0.5	0.25	0.0625	-0.62

[a]Calculated from MIC (µg/ml) and MW, [b]CLogP calculated in ChemDraw v18.1.; [c]standard

6 DISCUSSION

Twenty-one previously described IAs (**DF-01**–**21**, Fig. 8, Fig. 9) have been isolated from the whole plant of *D. franchetianum* by standard chromatographic methods, as described in the Experimental section. By a combination of MS, ESI-HRMS, 1D and 2D NMR experiments, optical rotation, and by comparison of the obtained data with the literature, the compounds were identified as dihydrosanguinarine (**DF-01**), dihydrochelerythrine (**DF-02**), 6-ethoxydihydrochelerythrine (**DF-03**), stylopine (**DF-04**), 6-methoxydihydrochelerythrine (**DF-05**), *bis*-[6-(5,6-dihydrochelerythrinyl)]ether (**DF-06**), sanguinarine (**DF-07**), protopine (**DF-08**), allocryptopine (**DF-09**), cryptopine (**DF-10**), chelidonine (**DF-11**), isocorydine (**DF-12**), glaucine (**DF-13**), corydine (**DF-14**), isocorypalmine (**DF-15**), laudanosine (**DF-16**), scoulerine (**DF-17**), berberine (**DF-18**), palmatine (**DF-19**), coptisine (**DF-20**), and magnoflorine (**DF-21**). The isolated IAs belong to the benzophenanthridine (**DF-01–03**, **-05, -07, -11**), protoberberine (**DF-04**, **-15**, **-17**, **-18-20**), bisbenzylphenanthridine (**DF-06**), protopine (**DF-08**–**10**), aporphine (**DF-12**–**14, -21**), and simple benzylisoquinoline (**DF-16**) structural types. Alkaloids dihydrosanguinarine (**DF-01**), dihydrochelerythrine (**DF-02**), 6-ethoxydihydrochelerythrine (**DF-03**), 6-methoxydihydrochelerythrine (**DF-05**), bis-[6-(5,6-dihydrochelerythrinyl)]ether (**DF-06**), cryptopine (**DF-10**), glaucine (**DF-13**), isocorypalmine (**DF-15**), laudanosine (**DF-16**), scoulerine (**DF-17**), and palmatine (**DF-19**) have been isolated for the first time from *D. franchetianum* and alkaloids dihydrosanguinarine (**DF-01**), dihydrochelerythrine (**DF-02**), 6-ethoxydihydrochelerythrine (**DF-03**), 6-methoxydihydrochelerythrine (**DF-05**), bis-[6-(5,6-dihydrochelerythrinyl)]ether (**DF-06**), laudanosine (**DF-16**), scoulerine (**DF-17**), and palmatine (**DF-19**) have been isolated for the first time from the genus *Dicranostigma*.

However, alkaloid **DF-03** should be recognised only as an isolated artefact. According to the isolation conditions, chelerythrine was unintentionally introduced to ethanol in an acidic environment at the very beginning of phytochemical work, where the iminium electrophile was readily trapped by a nucleophile. Thus, this nucleophilic addition furnished a hemiaminal ether **DF-03**. Compound **DF-05** is a dimer of two molecules of dihydrochelerythrine (**DF-02**) connected at position C-6 by an ether bridge and has been previously isolated from *Zanthoxylum paracanthum* and *Z. monophylum* [154, 155]. Dostál et al. have previously reported chelerythrine-like compounds in a thorough description of the dimerisation. We assume that the action of the basic aqueous conditions of the phytochemical process produced this dimer **DF-05** [156]. As a result of the induced dimerisation, chelerythrine has never appeared in our final steps of isolation.

As the main alkaloids have been isolated dihydrosanguinarine (**DF-01**), dihydrochelerythrine (**DF-02**), 6-ethoxydihydrochelerythrine (**DF-03**), stylopine (**DF-04**), sanguinarine (**DF-07**), protopine (**DF-08**), allocryptopine (**DF-09**), isocorydine (**DF-12**), and berberine (**DF-18**). In previous phytochemical studies, 14 IAs have been isolated in total from *D. franchetianum* (Table 2) [22-25, 52], most of them were members of the aporphine and benzophenathridine type.

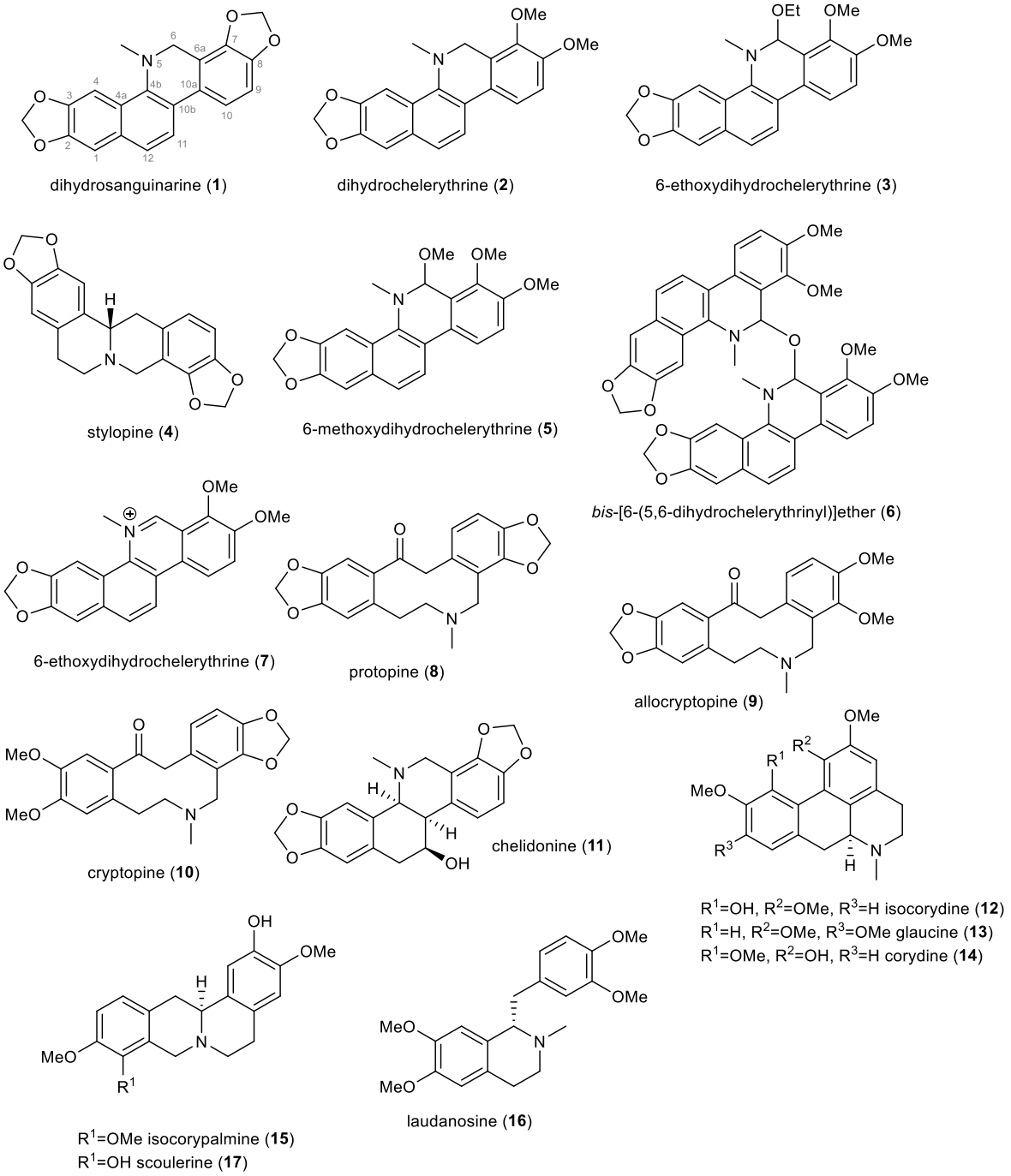

Fig. 8. Overview of tertiary isoquinoline alkaloids isolated from *Dicranostigma franchetianum*

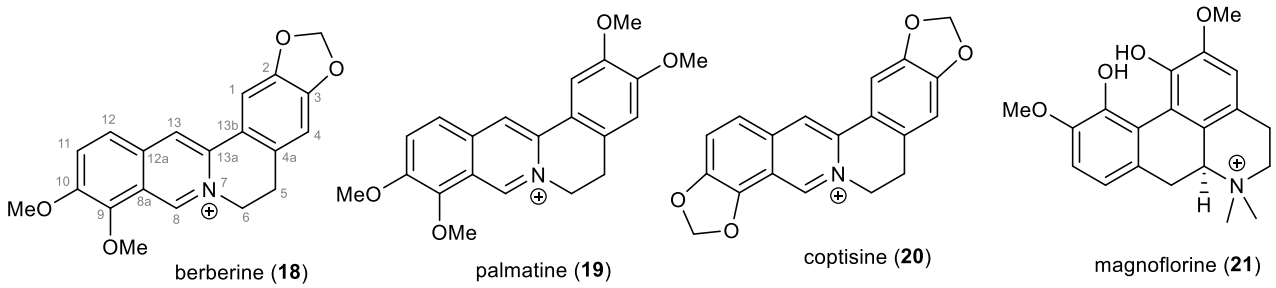

Fig. 9. Overview of quaternary isoquinoline alkaloids isolated within dissertation thesis from *Dicranostigma franchetianum*

All IAs isolated in sufficient amounts have been screened for various biological activities (inhibition of AChE/BuChE, POP, and antimycobacterial activity) to identify promising compounds for more detailed biological studies.

Within the AChE/BuChE assay, several promising results have been obtained. In the *h*AChE assay, the quaternary alkaloids berberine (**DF-18**) and palmatine (**DF-19**) had the strongest inhibition potency, with values of IC_{50} 0.71 ± 0.10 μM and 1.1 ± 0.1 μM, respectively. Quaternary nitrogen in these compounds plays an important role in binding to the enzyme [157]. However, these compounds might have limited permeation through the blood-brain barrier (BBB) [158]. On the basis of this fact, more promising results are obtained for derivatives or isolation artefacts of the quaternary benzophenathridine alkaloid chelerythrine. Dihydrochelerythrine (**DF-02**), 6-ethoxydihydrochelerytrine (**DF-03**) and 6-methoxydihydrochelerythrine (**DF-05**) showed *h*AChE inhibition potency at a low micromolar value (IC_{50} for (**DF-02**) 3.3 ± 0.7 μM, (**DF-03**) 1.2 ± 0.2 μM, and (**DF-05**) 5.7 ± 1.2 μM).

BuChE has emerged as a valid substitute capable of cleaving ACh. In later stages of AD, AChE activity is downregulated by up to 33-45% of normal values, while the activity of BuChE is improved to 40-90% in certain brain regions [159]. This dramatic switch between the AChE/BuChE ratio highlighted the supportive role of BuChE in hydrolysing the excess of ACh. Thus, all isolated compounds have also been tested for their inhibition activity of *h*BuChE. The strongest *h*BuChE activity has been obtained for 6-ethoxydihydrochelerytrine (**3**) and sanguinarine (**7**) with values of IC_{50} 3.2 ± 0.2 μM and 3.8 ± 0.6 μM, respectively. Both compounds demonstrated balanced inhibition activity against both cholinesterases (Table 7).
A molecular dynamic simulation was performer to determine the structural aspects crucial for the AChE/BuChE inhibition activity of **DF-02**, **-03**, and **-05**. The docking results of ligands **DF-02**, **-03**, and **-05** in the active site of *h*AChE revealed a largely similar binding position for these compounds (Fig. 10). Given the sole difference of a substituent at C6 amongst these compounds, this finding is not entirely surprising.

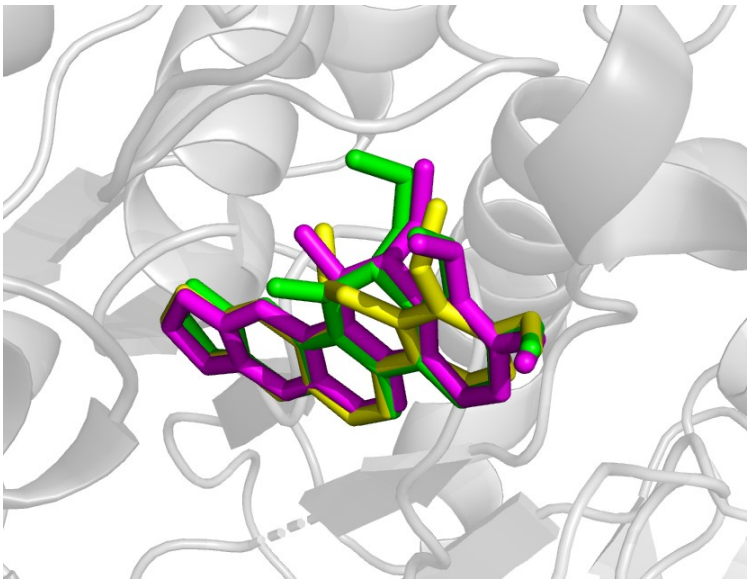

Fig. 10. The binding pose of DF-02 (yellow), -03 (green), and -05 (magenta) in the active site of *h*AChE. The image was generated by The PyMOL Molecular Graphics System v. 2.5.0, Schrödinger, LLC.

However, the length of the substituent's alkyl chain demonstrated a slight impact on the alteration of activity in AChE inhibition. The most pronounced inhibition activity was displayed by compound **DF-03**, which carries a 6-ethoxy substituent. This heightened activity can probably be attributed to the additional hydrophobic alkyl interaction that this substituent forms with Leu289 and a carbon-hydrogen bond with the hydroxyl group of Trp286 in the P-site of the binding cavity. Further critical interactions anchoring **DF-03** in the binding pocket include: π-π sandwich stacking with Trp286, parallel displaced π-π interaction with Tyr341 in the P-site, T-shaped π-π stacking with Phe297, and a weaker hydrogen bond between the methylenedioxy part of the ligand and the free amine group of Phe295 in the acyl-binding pocket. Additionally, two carbon-hydrogen bonds with hydroxyl groups of Ser293 and Tyr341 were observed (Fig. 11, Fig. 12).

Previous docking research on structurally similar compounds, chelerythrine and sanguinarine, in the active site of *h*AChE yielded significantly different binding positions despite comparable activity levels. Chelerythrine formed five hydrophobic interactions with Pro235, Pro410, Trp532, and one hydrogen bond with Asn233. Meanwhile, sanguinarine formed four hydrophobic bonds with Pro235, Val370, Pro410, Trp532, and one hydrogen bond with Asn233 [160]. These divergent positions are likely due to the presence of a positively charged aromatic nitrogen, absent in our dihydro-saturated ligands. The electrostatic influence of such an element within the ligand can significantly modify the ligand's binding affinity towards its target molecule. Nonetheless, in our case, the activity of **DF-02**, **-03**, and **-05** was

maintained, even in the absence of this charged nitrogen. Interestingly, dihydrosanguinarine (**DF-01**) demonstrated no activity against *h*AChE in our study.

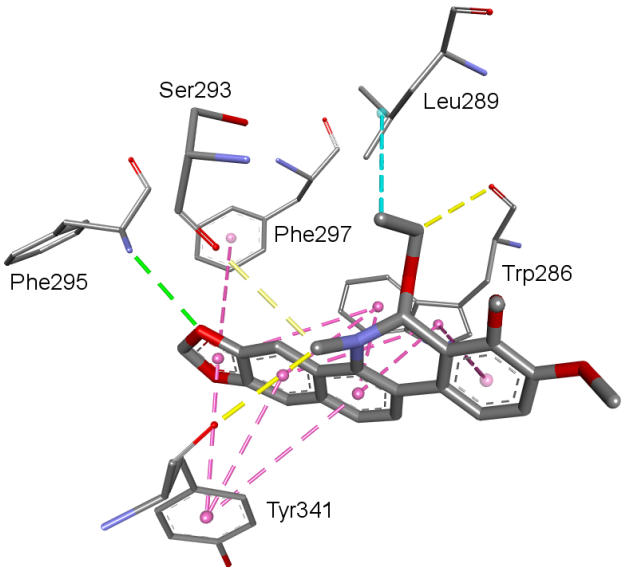

Fig. 11. The most probable binding position of DF-03 in the active site of *h*AChE. The π-π interactions are depictured in pink dashed lines, carbon hydrogen bonds in yellow dashed lines, hydrogen bond in a green dashed line, and alkyl hydrophobic interaction in the cyan dashed line. The image was prepared in Discovery Studio Visualiser v. 4.5, BIOVIA, San Diego.

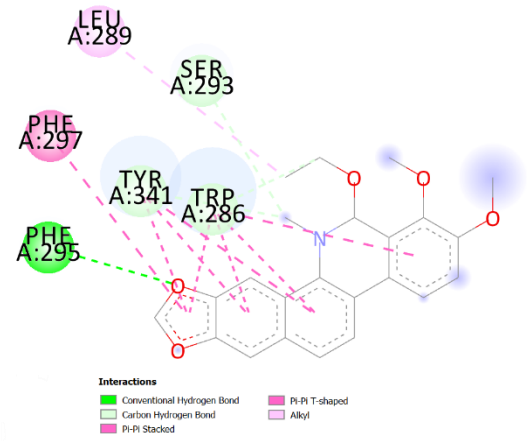

Fig. 12. 2D representation of the interactions of ligand DF-03 in the active site of *h*AChE. The diagram was generated by Discovery Studio Visualiser v. 4.5, BIOVIA, San Diego.

Examining the docking results of ligands **DF-02**, **-03**, and **-05** in the active site of *h*BuChE reveals a similar phenomenon to that observed with *h*AChE. The ligands exhibit similar binding poses, and the activity is slightly modified by the C6 substituent (Fig. 13).

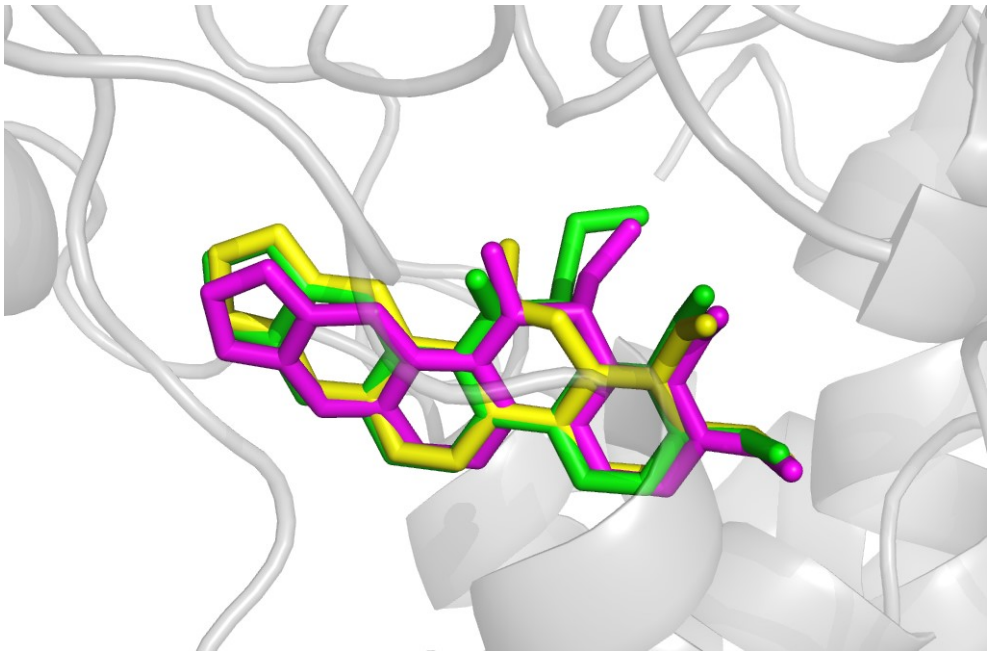

Fig. 13. The binding pose of DF-02 (yellow), -03 (green), and -05 (magenta) in the active site of *h*BuChE. The image was generated by The PyMOL Molecular Graphics System v. 2.5.0, Schrödinger, LLC.

The most active ligand was the 6-ethoxy derivative **DF-03**. Its ethyl appendage forms an additional hydrophobic interaction with Leu286 and Phe329, located between the acyl pocket and the anionic site of the *h*BuChE binding cavity. Other important interactions anchoring DF-**03**'s skeleton include three carbon-hydrogen bonds with Thr120, Ala328, and His438 – the latter being one of the amino acid residues in the catalytic triad. The ligand's aromatic naphthalene core interacts with a hydroxyl group of Ser287 through a π-donor hydrogen bond. Additionally, the doubly substituted benzene ring interacts with Phe329 through parallel displaced π-π stacking and with Tyr332 through π-π T-shaped stacking (Fig. 14, Fig. 15).

Comparison with previous docking research on chelerythrine and sanguinarine (**DF-07**) reveals significantly different binding positions for our ligands in the active site of *h*BuChE [160], similar to the observations made for *h*AChE. Once more, this discrepancy can be attributed to the electrostatic influence of the charged nitrogen. However, its absence exerted little effect on the activity against *h*BuChE.

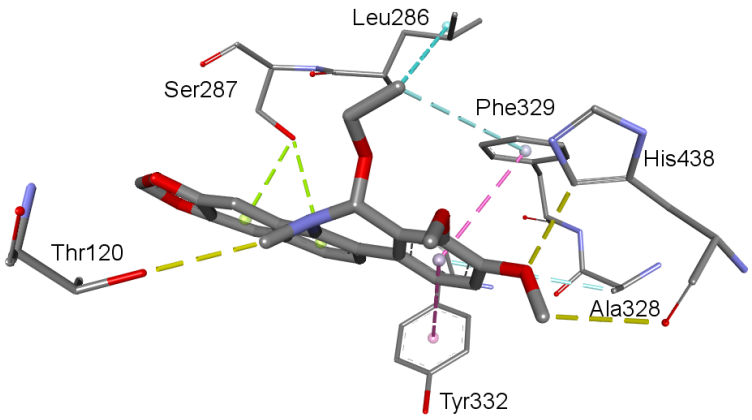

Fig. 14. The most probable binding position of DF-03 in the active site of *h*BuChE. The π-π interactions are depictured in pink dashed lines, carbon hydrogen bonds in yellow dashed lines, π-donor hydrogen bond in a green dashed lines, and alkyl and π-alkyl hydrophobic interaction in the cyan dashed line. The image was prepared in Discovery Studio Visualiser v. 4.5, BIOVIA, San Diego.

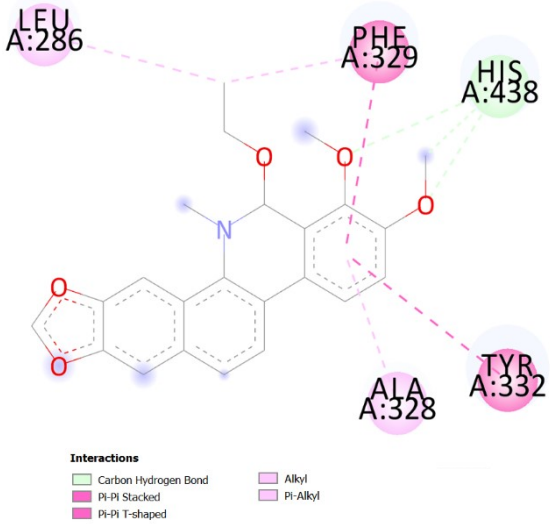

Fig. 15. 2D representation of interactions of ligand DF-03 in the active site of *h*BuChE. The diagram was generated by Discovery Studio Visualiser v. 4.5, BIOVIA, San Diego.

In recent studies, POP inhibitors have shown a great potential to become effective antidementia drugs [161]. POP inhibition can represent an additional supporting approach in AD treatment; hence the POP inhibitory ability of isolated compounds was tested. The most pronounced inhibitory activity was shown by sanguinarine (**DF-07**), with an IC_{50} value of 1.5 ± 0.1 μM, with this being a ten-fold better POP inhibitor than the standard baicalein used (IC_{50} = 14 ± 1 μM), which is recognised as a POP inhibitor [162].

Since one of the basic features of anti-AD drugs is their ability to reach the CNS, it is important to evaluate this parameter at the earliest stage of drug discovery. Based on this assumption, we applied the so-called BBB score algorithm [163]. It is a well-proven predictive tool that was developed to distinguish between CNS and non-CNS drugs. The BBB score for a

molecule can be calculated by inputting several physicochemical parameters, including the molecular weight, topological polar surface area, pKa, number of heavy atoms, number of aromatic rings, and number of hydrogen-bond donors and acceptors. All compounds with BBB score values greater than 4.0 are assumed to enter the CNS. Interestingly, quaternary alkaloids berberine (**DF-18**), as well as palmatine (**DF-19**), showed BBB scores that indicate their potential to reach the CNS area (Table 7). However, previous experiments using the parallel artificial membrane permeability assay (PAMPA), which is a useful technique to predict passive diffusion through biological membranes [164], classified berberine (**DF-18**) as a drug with no potency to cross the BBB by passive diffusion [89]. The BBB score indicated that both compounds showing the most promising profile of biological activity related to AD 6-ethoxydihydrochelerytrine (**DF-03**) and sanguinarine (**DF-07**) should be able to cross the BBB. Given the fact that different results were obtained for berberine, further studies are needed to confirm this assumption.

Considering the anti-TB potency of alkaloids containing an isoquinoline heterocycle in their structure [153], the compounds isolated in sufficient amounts have been screened for their antimycobacterial potential against five *Mycobacterium* or *Mycolicibacterium* strains (Table 8). Most of the tested alkaloids showed either weak or no antimycobacterial potency (MIC ≥ 125 µg/ml, Table 8). Alkaloids **DF-03** and **DF-06**, which contain a benzophenanthridine skeleton in their structure, showed moderate activity against all mycobacterial strains (MICs 15.625–31.25 µg/ml, Table 8). As mentioned above, both alkaloids should be recognised as isolation artefacts. However, compound **DF-06** exhibited strong activity against *Aspergillus fumigatus* (IC_{50} = 0.9 µM) and methicillin-resistant *Staphylococcus aureus* (IC_{50} = 1 µM) [155]. The improved antimycobacterial activity of **DF-03** and **DF-06**, compared to dihydrochelerythrine itself (**DF-02**), can be an inspiration for the preparation of more potent antimycobacterial compounds derived from the benzophenanthridine skeleton.

In previous studies, berberine (**DF-18**) exerted potent antimycobacterial activity against *M. intracellulare* with a MIC value of 1.56 µg/ml [165], and moderate activity against *Mycolicibacterium smegmatis* (MIC 25 µg/ml) [166]. On the contrary, the study of Gentry et al. 1998 revealed a weak activity of **DF-18** against *M. intracellulare* (MIC 200 µg/ml). For this reason, we revised the data for berberine (**DF-18**) when challenged with other *Mycobacterium* strains; the compound demonstrated moderate activity against *M. avium* and *M. kansasii* with MIC values of 31.25 µg/ml against both strains (Table 8). The semisynthetic derivatives of **DF-18** are reported as compounds with a strong antimycobacterial potential, for example 2,3,9-triethoxy-3,9-dibenzyloxy-10-methoxy-13-*n*-octylprotoberberine chloride that exhibits activity

against the drug-susceptible *Mtb* strain H37Rv with a MIC value of 0.125 μg/ml. Furthermore, this berberine derivative showed an intriguing effect against RIF- and INH-resistant *Mtb*, implying a new mechanism of action [106].

Because berberine (**DF-18**) was isolated in quantity allowing preparation of its semisynthetic derivatives, the study continued in cooperation with Biomedical Research Centre, University Hospital Hradec Kralove with the design and synthesis of C-9 substituted berberine analogues to inspect their antimycobacterial activity [167] (Fig. 9).

For this reason, structural modifications of berberine (**DF-18**) that increase its lipophilicity, mainly in the C-9 position, have been pursued to address these drawbacks [168, 169]. Based on our previous report on the antimycobacterial activity of semisynthetic derivatives of Amaryllidaceae alkaloids, which showed promising activity against three *Mycobacterium* strains [170], berberine (**DF-18**) was selected for the preparation of a small library of its semisynthetic derivatives, which have been screened for antimycobacterial activity against five and *Mycobacterium* and *Mycolicibacterium* strains (*Mycobacterium tuberculosis* H37Ra, *Mycobacterium avium, Mycobacterium kansasii, Mycolicibacterium smegmatis* and *Mycolicibacterium aurum,*). Given the need for long-term administration of anti-TB drugs, their potential hepatotoxicity *in vitro* using a hepatocellular HepG2 cell line has also been determined.

Derivatives (**18a**–**18k**; Figure 16) of berberine (**DF-18**) were synthesised using the same method as reported by Sobolová et al. 2020 [168].

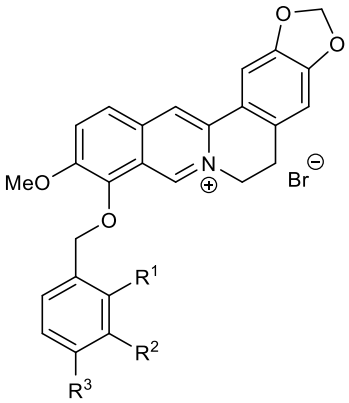

18a R^1=H, R^2=H, R^3=H
18b R^1=Me, R^2=H, R^3=H
18c R^1=H, R^2=Me, R^3=H
18d R^1=H, R^2=H, R^3=Me
18e R^1=Br, R^2=H, R^3=H
18f R^1=H, R^2=Br, R^3=H
18g R^1=H, R^2=H, R^3=Br
18h R^1=H, R^2=Cl, R^3=H
18i R^1=H, R^2=H, R^3=Cl
18k R^1=H, R^2=Cl, R^3=Cl

Fig. 16. Berberine derivatives from our library were investigated as antitubercular agents as a continuation of the phytochemical study of *D. franchetianum* in cooperation with the Biomedical Research Centre, University Hospital Hradec Kralove.

In all cases, the replacement of the methoxy group at position C-9 with differently substituted benzyl appendages was associated with a significant increase in antimycobacterial activity against all studied *Mycobacterium* strains (MIC 0.39–7.81 μg/ml). For all the tested

compounds, *Mycolicibacterium smegmatis* was the most sensitive strain. Among the methyl substituted benzylberberine derivatives (**DF-18b**–**18d**), a *para* position of the methyl group on the aromatic ring produced the most active compound. Bromine substitution within the benzyl moiety resulted in better activity against all strains, generating the most active compound within the study 9-*O*-(2-brombenzyl)berberine (**DF-18e**) (MIC 0.390–3.125 μg/ml). For this halogen substituent, the *ortho* position at the aromatic ring was connected with the highest activity.

Among berberine derivatives, compound **DF-18h** exhibited the highest cytotoxicity with an IC_{50} value of 9.44 ± 0.29 μM. The most active derivatives in terms of the highest antimycobacterial potency, i.e., **DF-18e** and **DF-18k**, showed cytotoxicity, with IC_{50} values of 11.61 ± 0.29 μM, and 12.66 ± 2.51 μM, respectively, reaching SI values of 3.92 for **DF-18e**, and 4.55 for **DF-18k**. These values indicate a potential risk of hepatotoxicity. Therefore, further research to find a balance between antimycobacterial efficacy and hepatotoxicity will be necessary to optimise the berberine scaffold.

In conclusion, it is possible to state that isoquinoline alkaloids are still attractive from the point of view of their biological activity and possible use in the therapy of various diseases. As demonstrated in the follow-up study, the preparation of semi-synthetic derivatives of natural alkaloids is also an interesting topic. In addition to berberine, bulbocapnine derivatives are currently being prepared, which will be subjected to a biological activity screening in the near future.

7 ABSTRACT

Charles University, Faculty of Pharmacy in Hradec Králové
Department of Pharmacognosy and Pharmaceutical Botany
Candidate: Viriyanata Wijaya, M.Sc.
Supervisor: Prof. RNDr. Lubomír Opletal, CSc.
Title of Doctoral Thesis: Alkaloids of *Dicranostigma franchetianum* (Prain) Fedde and their selected biological activity

Dicranostigma franchetianum (Prain) Fedde (Papaveraceae) is one of the representatives of the small genus *Dicranostigma* Hook. f. & Thomson. *D. franchetianum* (Prain) Fedde has been selected for the phytochemical investigation according to the screening study. In the primary screening of the alkaloid extract for cholinesterases inhibition, the inhibitory value was high (*h*AChE/*h*BChE, IC_{50} μg/ml; 1.67 ± 0.11 and 3.85 ± 0.31) and together at least 15 alkaloids were found in the extract. The primary ethanol extract was prepared from 11.8 kg of dry herb (Garden of Medicinal Plants, Faculty of Pharmacy in Hradec Kralove). Using common chromatographic methods, 21 isoquinoline alkaloids of various structural types were isolated. All compounds have been identified using various spectrometric techniques (GC-MS, HPLC-MS, and 1D- and 2D-NMR, optical rotatory. The alkaloids obtained in sufficient amounts were determined for human acetylcholinesterase (*h*AChE), human butyrylcholinesterase (*h*BChE), and prolyloligopeptidase (POP). In the *h*AChE assay, the quaternary alkaloids berberine (**DF-18**) and palmatine (**DF-19**) demonstrated the strongest inhibition potency, with values of IC_{50} 0.71 ± 0.10 μM and 1.1 ± 0.1 μM, respectively. Whereas in the *h*BuChE assay, benzophenanthridine alkaloids 6-ethoxydihydrochelerythrine (**DF-03**) and sanguinarine (**DF-07**) showed the strongest inhibition potency, with values of IC_{50} 3.2 ± 0.2 μM and 3.8 ± 0.6 μM, respectively. Furthermore, sanguinarine (**DF-07**) was the most effective in inhibiting POP with IC_{50} values of 1.5 ± 0.1 μM higher than baicalein as standard (IC_{50} = 14 ± 1 μM). However, CNS availability was calculated by applying the blood-brain barrier (BBB) score. Based on the score, compound **DF-02, -03, -05, -07, -11, 18-20** was assumed that compounds can pass through the BBB.

Furthermore, the compounds isolated in sufficient amounts have been tested for their antimycobacterial potential against five *Mycobacterium* or *Mycolicibacterium* strains. Alkaloids 6-ethoxydihydrochelerythrine and bis-[6-(5,6-dihydro-chelerythrinyl)]ether, which

contain a benzophenanthridine skeleton in their structure, showed moderate activity against all the tested mycobacterial strains (MICs 15.625–31.25 μg/ml).

Keywords: *Dicranostigma franchetianum* (Prain) Fedde, Papaveraceae, alkaloids, biological activity, acetylcholinesterase, butyrylcholinesterase, prolyloligopeptidase, antimycobacterial activity

8 ABSTRAKT

Univerzita Karlova, Farmaceutická fakulta v Hradci Králové
Katedra farmakognozie a farmaceutické botaniky
Kandidát: Viriyanata Wijaya, M.Sc.
Školitel: Prof. RnDr. Lubomír Opletal, CSc.
Název práce: Alkaloidy *Dicranostigma franchetianum* (Prain) Fedde a jejich vybraná biologická aktivita

Dicranostigma franchetianum (Prain) Fedde (Papaveraceae) je jedním ze zástupců malého rodu *Dicranostigma* Hook. f. & Thomson. Tato rostlina byla vybrána pro podrobnou fytochemickou studii na základě výsledků screeningové studie. Při screeningu alkaloidního extraktu vykázal tento alkaloidní extract zajímavou inhibiční aktivitu vůči cholinesterasám (*h*AChE/*h*BChE, IC_{50} μg/ml; 1,67 ± 0,11 a 3,85 ± 0,31), navíc se podařilo v extraktu identifikovat minimálně 15 alkaloidů. Primární ethanolový extrakt byl připraven z 11,8 kg suché byliny (původ: Zahrada léčivých rostlin, Farmaceutická fakulta v Hradci Králové). Zsa využití běžných chromatografických metod bylo izolováno celkem 21 isochinolinových alkaloidů různých strukturních typů. Všechny sloučeniny byly identifikovány pomocí různých spektrometrických technik (GC-MS, HPLC-MS a 1D- a 2D-NMR, optická aktivita). Všechny alkaloidy byly podrobeny studiu na jejich inhibiční potenciál vůči lidské rekombinantní acetylcholinesterase (*h*AChE), lidské rekombinantní butyrylcholinesterase (*h*BChE) a prolyloligopeptidase (POP). Ve studii na inhibiční aktivitu vůči *h*AChE vykázaly nejzajímavější aktivitu alkaloidy berberin (**DF-18**) a palmatin (**DF-19**) s hodnotami IC_{50} 0,71 ± 0,10 μM a 1,1 ± 0,1 μM, v daném pořadí. Zatímco v testu *h*BuChE vykazovaly benzofenantridinové alkaloidy 6-ethoxydihydro-chelerythrin (**DF-03**) a sanguinarin (**DF-07**) nejsilnější inhibiční účinnost, s hodnotami IC_{50} 3,2 ± 0,2 μM a 3,8 ± 0,6 μM. Sanguinarin (**DF-07**) navíc vykazoval i velmi zajímavou inhibiční aktivitu vůči POP (IC_{50} = 1,5 ± 0,1 μM). Vzhledem k tomu, že testované látky by měly působit v CNS, byla hodocena i jejich schopnost přestupu přes HEB za využití BBB skóre. Na základě výsledků existuje předpoklad, že látky **DF-02, -03, -05, -07, -11, -18-20** jsou schopné přestupu přes HEB do CNS. Sloučeniny izolované v dostatečném množství byly také testovány na jejich antimykobakteriální potenciál proti pěti kmenům *Mycobacterium* a *Mycolicibacterium*. Alkaloidy 6-ethoxydihydrochelerythrin a bis-[6-(5,6-dihydro-chelerythrinyl)]ether, které ve své struktuře obsahují benzofenantridinový skelet, vykazovaly mírnou aktivitu proti všem testovaným mykobakteriálním kmenům (MIC 15,625–31,25 μg/ml).

Klíčová slova: *Dicranostigma franchetianum* (Prain) Fedde, Papaveraceae, alkaloidy, biologická aktivita, acetylcholinesterasa, butyrylcholinesterasa, prolyloligopeptidasa, antimykobakteriální aktivita

9 LIST OF PUBLICATIONS

9.1 Publications related to the dissertation

P1. **Wijaya, V.**, Janďourek, O., Křoustková, J., Hradiská-Breiterová, K., Korábečný, J., Sobolová, K., Kohelová, E., Hošťálková, A., Konečná, K., Šafratová, M., Vrabec, R., Kuneš, J., Opletal, L., Chlebek, J., Cahlíková, L. Alkaloids of *Dicranostigma franchetianum* (Papaveraceae) and Berberine Derivatives as A New Class of Antimycobacterial Agents. *Biomolecules*, 2022, 12(6), 844. $IF_{2022} = 5.5$

Full-text: https://doi.org/10.3390/biom12060844

Author's contribution: Preparation of the crude extract from the plant. Complete flash chromatography, and isolation of all alkaloids. Preparation of alkaloids for biological study and writing of the isolation process. Reading of the final manuscript.

P2. Cahlíková, L., Vrabec, R., Pidaný, F., Peřinová, R., Maafi, N., Mamun, A.A., Ritomská, A, **Wijaya, V.**, Blunden, G. Recent Progress on Biological Activity of Amaryllidaceae and Further Isoquinoline Alkaloids in Connection with Alzheimer's Disease. *Molecules*, 2021, 26, 5240. $IF_{2021} = 4.411$

Full-text: https://doi.org/10.3390/molecules26175240

Author's contribution: Participation in the literature search of the selected topics. Data collection and evaluation of the draft manuscript. Reading of the final manuscript.

9.2 Publications not included in the dissertation

P1. Shidiq, N., Rahmadani, A., **Wijaya, V.,** Rijai, L. Sintesis senyawa turunan flavanon dan uji Bioaktivitas Senyawa Kalkon sebagai Senyawa Antara dalam Sintesis Senyawa Flavanon. Synthesis of flavanone derivatives and Bioactivity Test of Chalcone Compounds as Intermediates in the Synthesis of Flavanone Compounds [translation title]. *Proceeding of Mulawarman Pharmaceutical Conferences*, 2018, 8, 68-74.

Full-text: https://doi.org/10.25026/mpc.v8i1.305

Author's contribution: Participation in the literature search of the selected topics. Data collection and evaluation of the draft manuscript. Reading of the final manuscript.

P2. **Wijaya, V.,** Supriyatna, S., & Milanda, T. Uji Aktivitas Antibakteri dari Isolat Daun Tendani (*Goniothalamus macrophyllus* Hook. f. & Thomson.). Antibacterial Activity Test of Tendani Leaf Isolate (*Goniothalamus macrophyllus* Hook. f. & Thomson.) [translation title]. *Journal of Tropical Pharmacy and Chemistry*, 2016, 3(4), 322–324.

Full-text: https://doi.org/10.25026/jtpc.v3i4.121

Author's contribution: Preparation of isolate for the antibacterial activity. Data collection, evaluation, and writing of result of the draft manuscript. Reading of the final manuscript.

P3. Wijaya, V., Supriyatna, S., & Milanda, T. Isolasi Senyawa Aktif Dari Fraksi Etil Asetat Daun *Goniothalamus macrophyllus*. Isolation of the Active Compound from the Ethyl Acetate Fraction of *Goniothalamus macrophyllus* Leaves [translation title]. *Proceeding of Mulawarman Pharmaceuticals Conferences*, 2015, 2(1), 113–125.
Full-text: https://doi.org/10.25026/mpc.v2i1.49
Author's contribution: Preparation of the crude extract from the plant. Complete column chromatography, and isolation of one flavonoid. Writing of isolation process and result from identification and characterization by UV-Vis, IR, and MS. Reading of the final manuscript.

9.3 Conferences

9.3.1 Lectures

L1. Wijaya, V., Kohelová, E., Opletal, L., Jenčo, J., Šafratová, M. Alkaloids of the *Dicranostigma franchetianum* Hook f. et Thomson (Papaveraceae) Herb Above-Ground and Their Inhibition of Acetyl- and Butyryl-cholinesterase. 12th Postgraduate and 10th Postdoc Conference, Charles University, Faculty of Pharmacy in Hradec Králové, Czech Republic, 1st and 2nd February 2022.

L2. Wijaya, V., Kohelová, E., Opletal, L., Jenčo, J., Šafratová, M. Phytochemical investigation of the *Dicranostigma franchetianum* Hook f. et Thomson (Papaveraceae) herb: preliminary study. 11th Postgraduate and 9th Postdoctoral Conference, Charles University, Faculty of Pharmacy in Hradec Králové, Czech Republic, 27th and 28th January 2021.

L3. Wijaya V., Opletal, L., Hulcová, D., Kuneš, J., Maříková, J., Chlebek, J.: *Nuphar lutea* L. alkaloids and their neuroprotective activity. 10th Postgraduate and 8th Postdoctoral Conference, Charles University, Faculty of Pharmacy in Hradec Kralove, Czech Republic, 22nd and 23rd January 2020.

9.3.2 Posters

P. Wijaya V., Opletal L., Hulcová D., Kuneš J., Maříková J., Chlebek J.: *Nuphar lutea* L. alkaloids and their neuroprotective activity. Conferences of the Slovak Pharmaceutical Society (Drug Synthesis and Analysis), Faculty of Pharmacy in Bratislava, 5th and 6th September 2019.

10 REFERENCES

1. Farnsworth, N.R.; Akerele, O.; Bingel, A. S.; Soejarto, D. D.; Guo, Z. Medicinal plants in therapy. *Bull. World. Health. Organ.* **1985**, *63* (6), 965-981. https://www.ncbi.nlm.nih.gov/pmc/articles/PMC2536466/
2. Fabricant, D.S.; Farnsworth N.R. The value of plants used in traditional medicine for drug discovery. *Environmental health perspectives* **2001**, *109* (Suppl 1), 69-75. https://doi.org/10.1289/ehp.01109s169
3. Dias, D.A.; Urban S.; Roessner U. A historical overview of natural products in drug discovery. *Metabolites* **2012**, *2* (2), 303-336. https://doi.org/10.3390/metabo2020303
4. Edeoga H.O; Okwu D.E.; Mbaebie, B.O. Phytochemical constituents of some Nigerian Medicinal Plants. *African Journal of Biotechnology* **2005**, *4* (7), 685-688. https://doi.org/10.5897/AJB2005.000-3127
5. Schläger, S.; Dräger, B. Exploiting plant alkaloids. *Current Opinion in Biotechnology* **2016**, *37*, 155-164. https://doi.org/10.1016/j.copbio.2015.12.003
6. Bribi, N. Pharmacological activity of Alkaloids: A Review. *Asian Journal of Botany* **2018**, *1*, 1-6. https://doi.org/10.63019/ajb.v1i2.467
7. Heywood, V.H. *Flowering plants of the world*. Oxford University Press: Oxford, UK, 2009.
8. Feng, R. Z.; Lian, W. Y.; Fu, G. X; Xiao, P.G. Chemotaxonomy and Resource Utilization of the Tribe Chelidonieae (Papaveraceae). *J. Syst. Evol.* **1985**, *23* (1), 36-42. https://www.jse.ac.cn/EN/Y1985/V23/I1/36
9. Yu, X.; Gao, X.; Zhu, Z.; Cao, Y.; Zhang, Q.; Tu, P.; Chai., X. Alkaloids from the Tribe Bocconieae (Papaveraceae): A Chemical and Biological Review. *Molecules* **2014**, *19*, 13042-13060. https://doi.org/10.3390/molecules190913042
10. Kukula-Koch, W.; Widelski, J. *Pharmacognosy. Fundamentals, Applications and Strategies*. Academic Press: Cambridge, UK, 2017.
11. Ingkaninan, K.; Phengpa, P. Acetylcholinesterase inhibitors from *Stephania venosa* tuber. *J. Pharm. Pharmacol.* **2006**, *58* (5), 695-700. https://doi.org/10.1211/jpp.58.5.0015
12. Hung, T.M.; Nguyen, H.D.; Kim, J. C.; Jang, H. S; Ryoo, S. W; Lee, J. H.; Choi, J. S.; Bae, K. H.; Min, B. S. Alkaloids from roots of *Stephania rotunda* and their cholinesterase inhibitory activity. *Planta Med.* **2010**, *76* (15), 1762-1764. https://doi.org/10.1055/s-0030-1249814
13. Huang, Q.Q.; Bi, J. L.; Sun, Q. Y.; Yang, F. M.; Wang, Y. H.; Tang, G. H.; Zhao, F. W.; Wang, H.; Xu, J. J.; Kennelly, E. J.; Long, C. L.; Yin, G. F. Bioactive isoquinoline alkaloids from *Corydalis saxicola. Planta Med*. **2012**, *78* (1), 65-70. https://doi.org/10.1055/s-0031-1280126
14. Dang, Y.; Gong, H. F.; Liu, J. X.; Yu, S. J. Alkaloid from *Dicranostigma leptopodum* (Maxim) Fedde. Chinese Chem. Lett. **2009**, *20* (10), 1218-1220. https://doi.org/10.1016/j.cclet.2009.05.020
15. Liu, D.H.; Zhang, T.C.; Liu, J. X.; Di, D. L.; Dang, Y. Chemical Constituents of Alkaloids from *Dicranostigma leptopodum.* Chin. Trad. Herb. Drugs. **2011**, *42* (8), 1505-1509. https://jglobal.jst.go.jp/en/detail?JGLOBAL_ID=201402285923258724
16. Chen, Y.; Li, R.; Gao, R.; Yan, Q.; Zhong, M.; Liu, J.; Zhao, Q; Di, D. Total content determination for the effective fraction of the alkaloids in *Dicranostigma leptopodum* (Maxim.) Fedde by HPLC and ultraviolet-visible spectrophotometry. *Anal. Methods.* **2016**, *8* (12), 2645-2652. https://doi.org/10.1039/C5AY03054D
17. Chen, Y.; Liu, J.; Yan, Q.; Zhong, M.; Liu, J.; Di, D.; Liu, J. Simultaneous determination of the content of isoquinoline alkaloids in *Dicranostigma leptopodum* (Maxim) Fedde and the effective fractionation of the alkaloids by high-performance liquid chromatography with diode array detection. *J. Sep. Sci.* **2015**, *38*, 9-17. https://doi.org/10.1002/jssc.201400905

18. Liu, Y.; Chen, X.; Liu, J.; Di, D. Three-phase solvent systems for the comprehensive separation of a wide variety of compounds from *Dicranostigma leptopodum* by high-speed counter-current chromatography: Liquid Chromatography. *J. Sep. Sci.* **2015**, *38*, 2038-2045. https://doi.org/10.1002/jssc.201401466

19. Sun, R. Q.; Jiang, H. Y.; Zhang, W. J.; Yang, K.; Wang, C. F.; Fan, L.; He, Q.; Feng, J. B.; Du, S. S.; Deng, Z. W.; Geng, Z. F. Cytotoxicity of Aporphine, Protoberberine, and Protopine Alkaloids from *Dicranostigma leptopodum* (Maxim.) Fedde. *Evid-based Compl. Alt.* **2014**, 1-6. https://doi.org/10.1155/2014/580483

20. Zhao, Q.; Han, Y.; Du, Y. P.; Wang, T.P.; Wang, Q. The effect of *Dicranostigma leptopodum* (Maxim) fedde (DLF) extraction on suppressing oxidative hemolysis of erythrocytes and its mechanism. *J. Lanzhou Univ. Med. Sci.* **2006**, *32* (3), 40-45.

21. Tingpu, W.; Yixia, G; Qiang, Z; Yijun, Y.; Weichao, M.; Li, X.; Chenghui, L. Antibacterial activity and mechanism of alkaloids from *Dicranostigma leptopodum* (Maxim) Fedde on *Klebsiella pneumoniae. J. Tianshui Norm. Uni.* **2018**, *38* (2), 24-28.

22. Chelombit'ko, V.A. *Dicranostigma franchetianum* (Prain) Fedde: A plant promising as a source of the alkaloid isocorydine. *Pharm. Chem. J.* **1979**, *13* (8), 844-845. https://doi.org/10.1007/BF00772226

23. Táborská, E.; Věžník, F.; Slavíková, L.; Slavík, J. Quaternary alkaloids of three species of *Dicranostigma* Hook. f. et Thoms. *Collect. Czech. Chem. Commun.* **1978**, *43*, 1108-1112. https://doi.org/10.1135/cccc19781108

24. Slavíková, L.; Slavik, J. Alkaloide der mohngewächse (Papaveraceae) IX. *Dicranostigma Franchetianum* (Prain) Fedde. *Collect. Czech. Chem. Commun.* **1959**, *24*, 559-563. https://doi.org/10.1135/cccc19590559

25. Manske, R.H.F. The Alkaloids of papaveraceous plants: XXXII. *Stylophorum diphyllum* (Michx.) Nutt., *Dicranostigma franchetianum* (Prain) Fedde and *Glaucium serpieri* Heldr. *Can. J. Res. B.* **1942**. *20* (4), 53-56. https://doi.org/10.1139/cjr42b-009

26. Meyer, A.; Imming, P. Benzylisoquinoline Alkaloids from the Papaveraceae: The Heritage of Johannes Gadamer (1867–1928). *Journal of Natural Products* **2011**, *74* (11), 2482-2487. https://doi.org/10.1021/np2005049

27. DeBono, A.; Capuano, B.; Scammells, P. Progress Toward the Development of Noscapine and Derivatives as Anticancer Agents. *Journal of medicinal chemistry* **2015**, *58* (15), 5699-5727. https://doi.org/10.1021/jm501180v

28. Obiang-Obounou, B.W.; Kang, O. H.; Choi, J. G.; Keum, J. H.; Kim, S. B.; Mun, S. H.; Shin, D. W.; Kim, K. W.; Park, C. B.; Kim, Y. G.; Han, S. H.; Kwon, D. Y. The mechanism of action of sanguinarine against methicillin-resistant *Staphylococcus aureus. J. Toxicol. Sci.* **2011**, *36* (3), 277-283. https://doi.org/10.2131/jts.36.277

29. Ustünes, L.; Laekeman, G.; Gözler, B.; Vlietinck, A.; Ozer, A., Herman, A. *In Vitro* Study of the Anticholinergic and Antihistaminic Activities of Protopine and Some Derivatives. *Journal of natural products* **2004**, *51*, 1021-1022. https://doi.org/10.1021/np50059a043

30. Diogo, C.; Machado, N.; Barbosa, I.; Serafim, T.; Burgeiro, A.; Oliveira, P. Berberine as a Promising Safe Anti-Cancer Agent- Is there a Role for Mitochondria? *Current drug targets* **2011**, *12*, 850-859. https://doi.org/10.2174/138945011795528930

31. Efferth, T., Chen, Z. P.; Kaina, B.; Wang, G. Molecular Determinants of Response of Tumor Cells to Berberine. *Cancer genomics & proteomics* **2005**, *2* (2), 115-123. https://cgp.iiarjournals.org/content/2/2/115

32. Mazzini, S.; Bellucci, M.C.; Mondelli, R. Mode of binding of the cytotoxic alkaloid berberine with the double helix oligonucleotide d(AAGAATTCTT)2. *Bioorganic & Medicinal Chemistry* **2003**, *11* (4), 505-514. https://doi.org/10.1016/S0968-0896(02)00466-2

33. Gilca, M.; Gaman, L.; Panait, E.; Stoian, I.; Atanasiu, V. *Chelidonium majus*--an integrative review: traditional knowledge versus modern findings. *Forsch Komplementmed* **2010**, *17* (5), 241-248. https://doi.org/10.1159/000321397

34. O'Keefe, B.R.; Beecher, C. Isolation and Characterization of S-Adenosyl-L-Methionine:Tetrahydroberberine-cis-N-Methyltransferase from Suspension Cultures of *Sanguinaria canadensis* L. *Plant Physiol.* **1994**, *105* (1), 395-403. https://doi.org/10.1104/pp.105.1.395

35. Shang, X. F.; Yang, C. J.; Morris-Natschke, S. L.; Li, J. C.; Yin, X., D.; Liu, Y. Q.; Guo, X.; Peng, J. W.; Goto, M.; Zhang, J. Y.; Lee, K. H. Biologically active isoquinoline alkaloids covering 2014–2018. *Medicinal Research Reviews* **2020**, *40* (6), 2212-2289. https://doi.org/10.1002/med.21703

36. Deng, X.; Zhao, L; Fang, T.; Xiong, Y.; Ogutu, C.; Yang, D.; Vimolmangkang, S.; Liu, Y.; Han, Y. Investigation of benzylisoquinoline alkaloid biosynthetic pathway and its transcriptional regulation in lotus. *Hortic Res.*, **2018**, *5*, 29-44. https://doi.org/10.1038/s41438-018-0035-0

37. Desgagné-Penix, I.; Facchini, P.J., *Benzylisoquinoline alkaloid biosynthesis*. John Wiley and Sons Ltd.: Chichester, UK, 2011.

38. Sato, F. *2.26 - Plant Alkaloid Engineering*, in *Comprehensive Natural Products III*. Elsevier: Oxford, 2020, 700-755. https://doi.org/10.1016/B978-0-12-409547-2.14696-7

39. Grey-Wilson, C. *835. Dicranostigma leptopodum* Papaveraceae. *Curtis's Botanical Magazine* **2016**, *33* (2), 159-168. https://doi.org/10.2307/48505701

40. Chengyih, W.; Hsuan, C. Two New Species of *Dicranostigma*. *Acta Botanica Yunnanica* **1985**. *7* (1), 87-89. https://archive.org/details/plantdiversity-0253-2700-31553/mode/2up

41. Mingli, Z.; Grey-Wilson, C. *Dicranostigma J. D. Hooker & Thomson*, in *Flora of China*. Science Press: Beijing. 2008, 281-282.

42. Qiang, Z. Insights into Chemical Constituents of Alkaloids from Wild Medicinal Plant *Dicranostigma leptodum* (Maxim.) Fedde. *J. Phys. Conf. Ser.* **2019**, 1176, 1-6. https://doi.org/10.1088/1742-6596/1176/4/042056

43. Zhang, W.-H.; Lv, M.-H.; Jun, H.; Wang, Q.-P.; Wang, Q. *Dicranostigma leptopodum* (Maxim) Fedde induced apoptosis in SMMC-7721 human hepatoma cells and inhibited tumor growth in mice. *Nat. Sci.* **2010**, *2* (5), 457-463. http://dx.doi.org/10.4236/ns.2010.25056

44. Zhong, M.; Ma, Y.-X.; Liu, J.-X.; Di, D.-L. A new quaternary protoberberine alkaloid isolated from *Dicranostigma leptopodum (Maxim) Fedde. Nat. Prod. Res.* **2014**, *28*, 507-510. https://doi.org/10.1080/14786419.2013.879586

45. Seeds, C. 2022. *Dicranostigma franchetianum*. Crowmarsh Battle Barns, 114 Preston Crowmarsh, Wallingford, OX10 6SL England. Available online: www.chilternseeds.co.uk/item_459a_dicranostigma_franchetianum_seeds (accessed on 1 November 2022)

46. Society, A.G. 2018. *Dicranostigma lactucoides.* Alpine Garden Society, AGS Centre, Avon Bank, Pershore, Worcestershire, WR10 3JP. Available online: encyclopaedia.alpinegardensociety.net/plants/Dicranostigma/lactucoides (accessed on 1 November 2022)

47. Chang, X. R.; Wang, H. X.; Ma, G. E. Study on the chemical constituents of *Dicranostigma leptopodum.* Chin. Pharm. Bull. **1981**, *2* (16), 52-54.

48. Suchomelová, J., Bochořáková, H.; Paulová, H.; Musil, P.; Táborská, E. HPLC quantification of seven quaternary benzo[c]phenanthridine alkaloids in six species of the family Papaveraceae. *Journal of Pharmaceutical and Biomedical Analysis* **2007**, *44* (1), 283-287. https://doi.org/10.1016/j.jpba.2007.02.005

49. Chang, X. R.; Wang, H. X.; Zhou G. Z.; Ma G. E. Study on the Chemical Constituents and Morphology of *Dicranostigma leptopodum.* Chin. J. Pharm. Anal. **1982**, *5*, 273-278.

50. Zhao, Q., Wang, T. P., Sun, G. L., Yang, M., The research progress of the component analysis and pharmacological effects about *Dicranostigma leptopodum* (Maxim) Fedde's alkaloid. *J. Longdong Univ*. **2010**, *21* (2), 53-59.
51. Manske, R. The alkaloids of papaveraceous plants: L. *Dicranostigma lactucoides* Hook. f. et Thoms. *and Bocconia pearcei* Hutchinson. *Canadian Journal of Chemistry* **1954**, *32*, 83-85. https://doi.org/10.1139/v54-014
52. Henry, T.A. *The plant alkaloids. 4th ed.* J. & A. Churchill Ltd.: London, 1949.
53. Gregorová, J.; Babica, J.; Marek, R.; Paulová, H.; Táborská, E.; Dostál, J. Extractions of isoquinoline alkaloids with butanol and octanol. *Fitoterapia* **2010**, *81* (6), 565-568. https://doi.org/10.1016/j.fitote.2010.01.020
54. Ševčík, J.; Vičar, J.; Ulrichova, J.; Válka, I.; Lemr, K.; Simánek, V. Capillary electrophoretic determination of sanguinarine and chelerythrine in plant extracts and pharmaceutical preparations. *Journal of Chromatography A* **2000**, *866*, 293-298. https://doi.org/10.1016/S0021-9673(99)01126-7
55. Zhou, R.H. *Medicinal Plant Chemical Taxonomy in Shanghai.* Shanghai Science and Technology Press: Shanghai, China, 1988.
56. Wang, F.; Li, Y.-M. New hopane triterpene from *Dicranostigma leptopodum (Maxim) Fedde.* Journal of Asian Natural Products Research **2010**, *12*, 94-97. https://doi.org/10.1080/10286020903443028
57. Lei, Q.-F.; Zhao, X.-L.; Xu, L.-J.; Peng, Y.; Xiao, P.-G. Chemical Constituents of Plants from Tribe Chelidonieae and their Bioactivities. Chinese Herbal Medicines, **2014**, *6*, 1–21. https://doi.org/10.1016/S1674-6384(14)60001-0
58. Xie, Z. X.; Li, S. W.; Zhou, D. S.; Song, X. D.; Jia N.; Liang J. P. Study on Essential Oil Composition Analysis and Antibacterial Activity from *Dicranostigma leptopodum* (Maxim.) Fedde. China Animal Husbandry and Veterinary Medicine, **2020**, *47* (5), 1611-1617. https://doi.org/10.16431/j.cnki.1671-7236.2020.05.036
59. Dostal J.; Potacek, M. Quaternary benzo[c]phenanthridine alkaloids. *Collect. Czech. Chem. Commun.* **1990**, *55*, 2840-2873. https://doi.org/10.1135/cccc19902840
60. Walterová, D.; Ulrichová, J.; Válka, I.; Vicar, J.; Vavrecková, C; Taborská, E; Harjrader R.J., Meyer D.L., Cerná H, Simánek V. Benzo[c]phenanthridine alkaloids sanguinarine and chelerythrine: biological activities and dental care applications. Acta. Univ. Palacki. Olomouc. Fac. Med. **1995**, *139*, 7-16. https://europepmc.org/article/med/8686560
61. Cummings, J.; Lee, G.; Zhong, K.; Fonseca, J.; Taghva, K. Alzheimer's disease drug development pipeline: 2021. *Alzheimer's & Dementia: Translational Research & Clinical Interventions* **2021**, *7* (1), e12179. https://doi.org/10.1002/trc2.12179
62. Abdelnour, C.; Agosta, F.; Bozzali, M.; Fougère, B.; Iwata, A.; Nilforooshan, R., Takada, L. T., Viñuela, F.; Traber, M. Perspectives and challenges in patient stratification in Alzheimer's disease. *Alzheimer's Res. Ther.* **2022**, *14* (1), 112-123. https://doi.org/10.1186/s13195-022-01055-y
63. Lu, K., Wang, Y., Zhang, H., Tian, C., Wang, W., Yang, T., Qi, B., Wu, S. Rational design of a theranostic agent triggered by endogenous nitric oxide in a cellular model of Alzheimer's disease. *J. Med. Chem.* **2022**, *65* (13), 9193–9205. https://doi.org/10.1021/acs.jmedchem.2c00399
64. Guo, J.; Cheng, M.; Liu, P.; Cao, D.; Luo, J.; Wan, Y.; Fang, Y.; Jin, Y.; Xie, S. S., Liu, J. A multi-target directed ligands strategy for the treatment of Alzheimer's disease: Dimethyl fumarate plus Tranilast modified Dithiocarbate as AChE inhibitor and Nrf2 activator. *Eur. J. Med. Chem.* **2022**, *242*, 114630. https://doi.org/10.1016/j.ejmech.2022.114630
65. Košak, U.; Brus, B.; Knez, D.; Žakelj, S.; Trontelj, J.; Pišlar, A.; Šink, R.; Jukič, M.; Živin, M.; Podkowa, A.; Nachon, F.; Brazzolotto, X.; Stojan, J.; Kos, J.; Coquelle, N.; Sałat, K.; Colletier, J.-P.; Gobec, S. The magic of crystal structure-based inhibitor optimization: Development of a

butyrylcholinesterase inhibitor with picomolar affinity and in vivo activity. *J. Med. Chem*. **2018**, *61* (1), 119–139. https://doi.org/10.1021/acs.jmedchem.7b01086

66. Padhi, D.; Govindaraju, T. Mechanistic insights for drug repurposing and the design of hybrid drugs for Alzheimer's disease. *J. Med. Chem*. **2022**, *65* (10), 7088–7105. https://doi.org/10.1021/acs.jmedchem.2c00335
67. Daley, S.-k.; Cordell, G.A. Alkaloids in Contemporary Drug Discovery to Meet Global Disease Needs. *Molecules* **2021**, *26* (13), 3800. https://doi.org/10.3390/molecules26133800
68. Imenshahidi, M.; H. Hosseinzadeh. *Berberis Vulgaris* and berberine: An update review. Phytotherapy Research **2016**, *30* (11), 1745-1764. https://doi.org/10.1002/ptr.5693
69. Imenshahidi, M.; H. Hosseinzadeh. Berberine and barberry *(Berberis vulgaris)*: A clinical review. Phytotherapy Research **2019**, *33* (3), 504-523. https://doi.org/10.1002/ptr.6252
70. Cheng, Z.; Kang, C.; Che, S.; Su, J.; Sun, Q.; Ge, T.; Guo, Y.; Lv, J.; Sun, Z.; Yang, W.; Li, B.; Li, X.; Cui, R. Berberine: A Promising Treatment for Neurodegenerative Diseases. *Frontiers in Pharmacology* **2022**, *13,* 845591. https://doi.org/10.3389/fphar.2022.845591
71. Akbar, M.; Shabbir, A.; Rehman, K.; Akash, M.; Sajid Hamid Shah, M. A. Neuroprotective potential of berberine in modulating Alzheimer's disease via multiple signaling pathways. *Journal of Food Biochemistry* **2021**, *45* (10), e13936. https://doi.org/10.1111/jfbc.13936
72. Cai, Z.; Wang, C.; Yang, W. Role of berberine in Alzheimer's disease. *Neuropsychiatr. Dis. Treat.* **2016**, *12*, 2509-2520. https://doi.org/10.2147/ndt.S114846
73. Yuan, N.-N.; Cai, C.-Z.; Wu, M.-Y., Su, H.-X.; Li, M.; Lu, J.-H. Neuroprotective effects of berberine in animal models of Alzheimer's disease: a systematic review of pre-clinical studies. *BMC Complementary and Alternative Medicine* **2019**, *19* (1), 109-118. https://doi.org/10.1186/s12906-019-2510-z
74. Ji, H.-F.; Shen L. Berberine: A Potential Multipotent Natural Product to Combat Alzheimer's Disease. *Molecules* **2011**, *16*, 6732-6740. https://doi.org/10.3390/molecules16086732
75. Singh, A.K.; Singh, S. K.; Nandi, M. K.; Mishra, G.; Maurya, A.; Rai, A.; Rai, G. K.; Awasthi, R.; Sharma, B.; Kulkarni, G. T. Berberine: A Plant-derived Alkaloid with Therapeutic Potential to Combat Alzheimer's disease. Cent. Nerv. Syst. Agents. Med. Chem. **2019**, *19* (3), 154-170. https://doi.org/10.2174/1871524919666190820160053
76. Durairajan, S.S.K.; liu, L.-F; Lu, J.-H; Chen, L.-L; Yuan, Q.; Chung, S. K., Huang, L.; Li, X.-S.; Huang, J.-D.; Li, M. Berberine ameliorates β-amyloid pathology, gliosis, and cognitive impairment in an Alzheimer's disease transgenic mouse model. *Neurobiology of Aging* **2012**, *33* (12), 2903-2919. https://doi.org/10.1016/j.neurobiolaging.2012.02.016
77. Zhu, F.; Qian, C. Berberine chloride can ameliorate the spatial memory impairment and increase the expression of interleukin-1beta and inducible nitric oxide synthase in the rat model of Alzheimer's disease. *BMC Neuroscience* **2006**, *7*(1), 78-86. https://doi.org/10.1186/1471-2202-7-78
78. Ghareeb, D.A.; Khalil, S.; Hafez, H. S.; Bajorath, J.; Ahmed, H. E. A.; Sarhan, E.; Elwakeel, E.; El-Demellawy, M. A. Berberine Reduces Neurotoxicity Related to Nonalcoholic Steatohepatitis in Rats. *Evidence-Based Complementary and Alternative Medicine* **2015**, 361847. https://doi.org/10.1155/2015/361847
79. Bhutada, P.; Mundhada, Y.; Bansod, K.; Tawari, S.; Patil, S.; Dixit, P.; Umathe, S.; Mundhada, D. Protection of cholinergic and antioxidant system contributes to the effect of berberine ameliorating memory dysfunction in rat model of streptozotocin-induced diabetes. *Behavioural Brain Research* **2011**, *220* (1), 30-41. https://doi.org/10.1016/j.bbr.2011.01.022
80. Shaker, F. H.; El-Derany, M. O.; Wahdan, S. A.; El-Demerdash, E.; El-Mesallamy, H. O. Berberine ameliorates doxorubicin-induced cognitive impairment (chemobrain) in rats. *Life Sciences* **2021**, *269*, 119078. https://doi.org/10.1016/j.lfs.2021.119078

81. Panahi, N.; Mahmoudian, M.; Mortazavi, P.; Hashjin, G. S. *Effects of berberine on β-secretase activity in a rabbit model of Alzheimer's disease. Archives of Medical Science* **2013**, *9* (1), 146-150. https://doi.org/10.5114/aoms.2013.33354

82. Jung, H. A.; Min, B.-S.; Yokozawa, T.; Lee, J. H-.; Kim, Y. S.; Choi, J. S. Anti-Alzheimer and Antioxidant Activities of *Coptidis Rhizoma* Alkaloids. *Biological and Pharmaceutical Bulletin*, **2009**, *32* (8), 1433-1438. https://doi.org/10.1248/bpb.32.1433

83. Zhang, H.; Zhao, C.; Cao, G.; Guo, L.; Zhang, S.; Liang, Y.; Qin, C.; Su, P.; Li, H.; Zhang, W. Berberine modulates amyloid-β peptide generation by activating AMP-activated protein kinase. *Neuropharmacology* **2017**, *125*, 408-417. https://doi.org/10.1016/j.neuropharm.2017.08.013

84. Zhu, F., Wu, F., Ma, Y.; Liu, G.; Li, Z.; Sun, Y.; Pei, Z. Decrease in the production of beta-amyloid by berberine inhibition of the expression of beta-secretase in HEK293 cells. *BMC Neuroscience* **2011**, *12* (1), 125-132. https://doi.org/10.1186/1471-2202-12-125

85. Brunhofer, G.; Fallarero, A.; Karlsson, D.; Batista-Gonzales, A.; Shinde, P.; Gopi, M. C.; Vuorela, P. Exploration of natural compounds as sources of new bifunctional scaffolds targeting cholinesterases and beta amyloid aggregation: The case of chelerythrine. *Bioorganic & Medicinal Chemistry* **2012**, *20* (22), 6669-6679. https://doi.org/10.1016/j.bmc.2012.09.040

86. He, W.; Wang, C.; Chen, Y.; He, Y.; Cai, Z. Berberine attenuates cognitive impairment and ameliorates tau hyperphosphorylation by limiting the self-perpetuating pathogenic cycle between NF-κB signaling, oxidative stress and neuroinflammation. *Pharmacological Reports* **2017**, *69* (6), 1341-1348. https://doi.org/10.1016/j.pharep.2017.06.006

87. Chen, Y.; Chen, Y.; Liang, Y.; Chen, H.; Ji, X.; Huang, M. Berberine mitigates cognitive decline in an Alzheimer's Disease Mouse Model by targeting both tau hyperphosphorylation and autophagic clearance. *Biomedicine & Pharmacotherapy* **2020**, *121*, 109670. https://doi.org/10.1016/j.biopha.2019.109670

88. Mak, S.; Luk, W. W. K.; Cui, W.; Hu, S.; Tsim, K. W. K.; Han, Y. Synergistic Inhibition on Acetylcholinesterase by the Combination of Berberine and Palmatine Originally Isolated from Chinese Medicinal Herbs. *Journal of Molecular Neuroscience* **2014**, *53* (3), 511-516. https://doi.org/10.1007/s12031-014-0288-5

89. Hošťálkova, A.; Mařiková, J.; Opletal, L.; Korábečný, J.; Hulcová, D.; Kuneš, J.; Nováková, L.; Pérez, D. I.; Jun, D.; Kučera, T; Andrisano, V.; Siatka, T.; Cahlíková, L. Isoquinoline Alkaloids from *Berberis vulgaris* as Potential Lead Compounds for the Treatment of Alzheimer's Disease. *Journal of Natural Products* **2019**, *82* (2), 239-248. https://doi.org/10.1021/acs.jnatprod.8b00592

90. Carradori, S.; D'Ascenzio, M.; Chimenti, P.; Secci, D.; Bolasco, A. Selective MAO-B inhibitors: a lesson from natural products. *Molecular Diversity* **2014**, *18* (1), 219-243. https://doi.org/10.1007/s11030-013-9490-6

91. Fischer, H.; Kansy, M.; Avdeef, A.; Senner, F. Permeation of permanently positive charged molecules through artificial membranes—Influence of physico-chemical properties. *European Journal of Pharmaceutical Sciences* **2007**, *31* (1), 32-42. https://doi.org/10.1016/j.ejps.2007.02.001

92. Wang, X.; Wang, R.; Xing, D.; Su, H.; Ma, C.; Ding, Y.; Du, L. Kinetic difference of berberine between hippocampus and plasma in rat after intravenous administration of *Coptidis rhizoma* extract. *Life Sciences* **2005**, *77* (24), 3058-3067. https://doi.org/10.1016/j.lfs.2005.02.033

93. Baek, S. C.; Ryu, H. W.; Kang, M.-G.; Lee, H.; Park, D.; Cho, M.-L.; Oh, S.-R.; Kim, H. Selective inhibition of monoamine oxidase A by chelerythrine, an isoquinoline alkaloid. *Bioorganic & Medicinal Chemistry Letters* **2018**, *28* (14), 2403-2407. https://doi.org/10.1016/j.bmcl.2018.06.023

94. Tuzimski, T.; Petruczynik, A. Application of HPLC-DAD for In Vitro Investigation of Acetylcholinesterase Inhibition Activity of Selected Isoquinoline Alkaloids from *Sanguinaria canadensis* Extracts. *Molecules* **2021**, *26*, 230. https://doi.org/10.3390/molecules26010230

95. Lee, S.; Kai, M.; Lee, M. Inhibitory effects of sanguinarine on monoamine oxidase activity in mouse brain. *Phytotherapy research* **2001**, *15*, 167-169. https://doi.org/10.1002/ptr.703

96. Amat-ur-Rasool, H.; Ahmad, M.; Hasnain, S.; Ahmed, A.; Carter, W. G. In Silico Design of Dual-Binding Site Anti-Cholinesterase Phytochemical Heterodimers as Treatment Options for Alzheimer's Disease. *Current Issues in Molecular Biology* **2022**, *44*, 152-175. https://doi.org/10.3390/cimb44010012

97. Marasco, D.; Vicidomini, C.; Krupa, P.; Cioffi, F.; Huy, P. D. Q.; Li, M. S.; Florio, D.; Broersen, K.; De Pandis, M. F.; Roviello, G. N. Plant isoquinoline alkaloids as potential neurodrugs: A comparative study of the effects of benzo[c]phenanthridine and berberine-based compounds on β-amyloid aggregation. *Chemico-Biological Interactions* **2021**, *334*, 109300. https://doi.org/10.1016/j.cbi.2020.109300

98. Cahlíková, L.; Opletal, L.; Kurfürst, M.; Macáková, K.; Kulhánková, A.; Hošťálková, A. Acetylcholinesterase and Butyrylcholinesterase Inhibitory Compounds from *Chelidonium Majus* (Papaveraceae). *Natural Product Communications* **2010**, *5* (11), 1751-1754. https://doi.org/10.1177/1934578X1000501110

99. Khanna, A.; Saha, R.; Ahmad, N. National TB elimination programme - What has changed. *Indian Journal of Medical Microbiology* **2023**, *42*, 103-107. https://doi.org/10.1016/j.ijmmb.2022.10.008

100. Zhang, T.; Zhang, J.; Wei, L.; Liang, H.; Zhang, J.; Shi, D.; Wang, Z. The global, regional, and national burden of tuberculosis in 204 countries and territories, 1990–2019. *Journal of Infection and Public Health* **2023**, *16* (3), 368-375. https://doi.org/10.1016/j.jiph.2023.01.014

101. Kremer, L.; Douglas, J. D.; Baulard, A. R.; Morehouse, C.; Guy, M. R.; Alland, D.; Dover, L. G.; Lakey, J. H.; Jacobs, W. R.; Brennan, P. J.; Minnikin, D. E.; Besra, G. S. Thiolactomycin and Related Analogues as Novel Anti-mycobacterial Agents Targeting KasA and KasB Condensing Enzymes in *Mycobacterium tuberculosis*. *Journal of Biological Chemistry* **2000**, *275* (22), 16857-16864. https://doi.org/10.1074/jbc.M000569200

102. Newton, S.M.; Lau, C.; Gurcha, S. S.; Besra, G. S.; Wright, C. W. The evaluation of forty-three plant species for in vitro antimycobacterial activities; isolation of active constituents from *Psoralea corylifolia* and *Sanguinaria canadensis*. *Journal of Ethnopharmacology* **2002**, *79* (1), 57-67. https://doi.org/10.1016/S0378-8741(01)00350-6

103. Jones, R. R.; Harkrader, R. R.; Southard, G. L. The Effect of pH on Sanguinarine Iminium Ion Form. Journal of Natural Products, **1986**, 49 (6), 1109-1111. https://doi.org/10.1021/np50048a025

104. Mitscher, L.A.; Park, Y. H.; Clark, D.; Clark, G. W.; Hammesfahr, P. D.; Wu, W. N.; Beal, J. L. Antimicrobial agents from higher plants. An investigation of *Hunnemannia fumariaefolia* pseudoalcoholates of sanguinarine and chelerythrine. *Lloydia* **1978**. *41* (2), 145-150. https://europepmc.org/article/MED/651561

105. Colombo, M. L.; Bosisio, E. Pharmacological activities of *Chelidonium Majus* L. (Papaveraceae). *Pharmacological Research* **1996**, *33* (2), 127-134. https://doi.org/10.1006/phrs.1996.0019

106. Liu, Y.-X.; Xiao, C.-L.; Wang, Y.-X.; Li, Y.-H.; Yang, Y.-H.; Li, Y.-B.; Bi, C.-W.; Gao, L.-M.; Jiang, J.-D. Song, D.-Q. Synthesis, structure–activity relationship and *in vitro* anti-mycobacterial evaluation of 13-n-octylberberine derivatives. *European Journal of Medicinal Chemistry* **2012**, *52*, 151-158. https://doi.org/10.1016/j.ejmech.2012.03.012

107. Sun, H.; Hou, H.; Lu, P.; Zhang, L.; Zhao, F.; Ge, C.; Wang, T.; Yao, M.; Li, J. Isocorydine inhibits cell proliferation in hepatocellular carcinoma cell lines by inducing G2/M cell cycle arrest and apoptosis. *PLoS One* **2012**, *7* (5), e36808. https://doi.org/10.1371/journal.pone.0036808

108. Chmura, S.; Dolan, M.; Cha, A.; Mauceri, H.; Kufe, D.; Weichselbaum, R. *In vitro* and *in vivo* activity of protein kinase C inhibitor chelerythrine chloride induces tumor cell toxicity and growth delay in vivo. *Clin. Cancer Res.* **2000**, *6* (2), 737-742.

https://aacrjournals.org/clincancerres/article/6/2/737/288010/In-Vitro-and-in-Vivo-Activity-of-Protein-Kinase-C

109. Slaninová, I.; Slunská, Z.; Šinkora, J.; Vlková, M.; Taborska, E. Screening of Minor Benzo(c.)phenanthridine Alkaloids for Antiproliferative and Apoptotic Activities. *Pharmaceutical Biology* **2008**, *45*, 131-139. https://doi.org/10.1080/13880200601113099

110. Zdarilová, A.; Vrzal, R.; Rypka, M.; Ulrichová, J.; Dvorak, Z. Investigation of sanguinarine and chelerythrine effects on CYP1A1 expression and activity in human hepatoma cells. *Food and chemical toxicology* **2006**, *44*, 242-249. https://doi.org/10.1016/j.fct.2005.07.006

111. Ahsan, H.; Reagan-Shaw, S.; Breur, J.; Ahmad, N. Sanguinarine induces apoptosis of human pancreatic carcinoma AsPC-1 and BxPC-3 cells via modulations in Bcl-2 family proteins. *Cancer letters* **2007**, *249*, 198-208. https://doi.org/10.1016/j.canlet.2006.08.018

112. Chang, M.-C.; Chan, C.-P.; Wang, Y.-J.; Lee, P.-H.; Chen, L.-I.; Tsai, Y.-L.; Lin, B.-R.; Wang, Y.-L.; Jeng, J.-H. Induction of necrosis and apoptosis to KB cancer cells by sanguinarine is associated with reactive oxygen species production and mitochondrial membrane depolarization. *Toxicology and applied pharmacology* **2007**, *218*, 143-151. https://doi.org/10.1016/j.taap.2006.10.025

113. Gaziano, R. Antitumor effects of the benzophenanthridine alkaloid sanguinarine: Evidence and perspectives. *World Journal of Gastrointestinal Oncology* **2016**, *8* (1), 30-39. https://doi.org/10.4251/wjgo.v8.i1.30

114. Park, J.-J., Seo, S.-M., Kim, E. J.; Lee, Y.-J.; Ko, Y.-G.; Ha, J.; Lee, M. Berberine inhibits human colon cancer cell migration via AMP-activated protein kinase-mediated downregulation of integrin β1 signaling. *Biochemical and Biophysical Research Communications* **2012**, *426* (4), 461-467. https://doi.org/10.1016/j.bbrc.2012.08.091

115. Kuo, H.-P.; Chuang, T.-C.; Tsai, S.-C.; Tseng, H.-H.; Hsu, S.-C.; Chen, Y.-C.; Kuo, C.-L.; Kuo, Y.-H.; Liu, J.-Y.; Kao, M.-C. Berberine, an Isoquinoline Alkaloid, Inhibits the Metastatic Potential of Breast Cancer Cells via Akt Pathway Modulation. *Journal of agricultural and food chemistry* **2012**, *60*, 9649-9658. https://doi.org/10.1021/jf302832n

116. Vrba, J.; Vrublová, E.; Modrianský, M, Ulrichová, J. Protopine and allocryptopine increase mRNA levels of cytochromes PR350 1A in human hepatocytes and HepG2 cells independently of AhR. *Toxicology letters* **2011**, *203*, 135-141. https://doi.org/10.1016/j.toxlet.2011.03.015

117. Chen, C.-H.; Liao, C.-H.; Chang, Y.-L.; Guh, J.-H., Pan, S.-L.; Teng, C.-M. Protopine, a novel microtubule-stabilizing agent, causes mitotic arrest and apoptotic cell death in human hormone-refractory prostate cancer cell lines. *Cancer letters* **2012**, *315*, 1-11. https://doi.org/10.1016/j.canlet.2011.09.042

118. Slunská, Z.; Gelnarová, E.; Hammerová, J.; Taborska, E.; Slaninová, I. Effect of quaternary benzo[c]phenanthridine alkaloids sanguilutine and chelilutine on normal and cancer cells. *Toxicology in vitro* **2010**, *24*, 697-706. https://doi.org/10.1016/j.tiv.2010.01.012

119. Hošek, J.; Šebrlová, K.; Kaucká, P.; Peš, O.; Taborska, E. The capability of minor quaternary benzophenanthridine alkaloids to inhibit TNF-α secretion and cyclooxygenase activity. *Acta Veterinaria Brno* **2017**, *86*, 223-230. https://doi.org/10.2754/avb201786030223

120. Niu, X.; Fan, T.; Li, W.; Xing, W.; Huang, H. *The anti-inflammatory effects of sanguinarine and its modulation of inflammatory mediators from peritoneal macrophages. European journal of pharmacology* **2012**, *689*, 262-269. https://doi.org/10.1016/j.ejphar.2012.05.039

121. Niu, X.; Zhou, P.; Li, W.-F.; Xu, H.-B. Effects of chelerythrine, a specific inhibitor of cyclooxygenase-2, on acute inflammation in mice. *Fitoterapia* **2011**, 82, 620-625. https://doi.org/10.1016/j.fitote.2011.01.020

122. Šebrlová, K.; Kollar, P.; Zavalova, V.; Taborska, E.; Urbanová, J.; Hošek, J. Investigation of sanguinarine and chelerythrine effects on LPS-induced inflammatory gene expression in THP-1 cell line. *Phytomedicine* **2012**, *19*, 890-895. https://doi.org/10.1016/j.phymed.2012.04.001

123. Saeed, S. A.; Gilani, A. H.; Majoo, R. U.; Shah, B. H. *Anti-thrombotic and anti-inflammatory activities of protopine. Pharmacological Research* **1997**, *36* (1), 1-7. https://doi.org/10.1006/phrs.1997.0195

124. Alam, M. D. B.; Ju, M.-K.; Kwon, Y.-G.; Lee, S.-H. Protopine attenuates inflammation stimulated by carrageenan and LPS via the MAPK/NF-κB pathway. *Food and Chemical Toxicology* **2019**, *131*, 110583. https://doi.org/10.1016/j.fct.2019.110583

125. Opletal, L.; Locarek, M.; Frankova, A.; Chlebek, J.; Smid, J.; Hošťálková, A.; Safratova, M.; Hulcová, D.; Kloucek, P.; Rozkot, M.; Cahlíková, L. Antimicrobial Activity of Extracts and Isoquinoline Alkaloids of Selected Papaveraceae Plants. *Natural product communications* **2014**, *9*, 1709-1712. https://doi.org/10.1177/1934578X1400901211

126. Campo, G. M.; Avenoso, A.; Campo, S.; Nastasi, G.; Traina, P.; D'Ascola, A.; Rugolo, C. A.; Calatroni, A. The antioxidant activity of chondroitin-4-sulphate, in carbon tetrachloride-induced acute hepatitis in mice, involves NF-kappaB and caspase activation. *British journal of pharmacology* **2008**, *155 (*6), 945-956. https://doi.org/10.1038/bjp.2008.338

127. Kodai, S.; Takemura, S.; Minamiyama, Y.; Hai, S.; Yamamoto, S.; Kubo, S.; Yoshida, Y.; Niki, E.; Okada, S.; Hirohashi, K.; Suehiro, S. S-allyl cysteine prevents CCl_4-induced acute liver injury in rats. *Free Radical Research* **2007**, *41* (4), 489-497. https://doi.org/10.1080/10715760601118361

128. Deping, T.; Fang, W.; Jinzhou, T.; Aihong, M., Shiqi, L., Qin, W. *Dicranostiga leptopodu* (Maxim.) Fedde extracts attenuated CCl_4-induced acute liver damage in mice through increasing anti-oxidative enzyme activity to improve mitochondrial function. *Biomedicine & Pharmacotherapy* **2017**, *85*, 763-771. http://dx.doi.org/10.1016/j.biopha.2016.11.097

129. Mao, A.H.; Zhang, Y.; Zhao, Q.; Wang, Q.; Wang, T. P. Protective effect of *Dicranostiga leptodu* (Maxim.) Fedde on immunological live injury in mice. *Chinese Pharmacological Bulletin* **2004**, *20*, 940-943.

130. Jancula, D.; Suchomelová, J.; Gregor, J.; Smutná, M.; Marsálek, B.; Taborska, E. Effects of aqueous extracts from five species of the family Papaveraceae on selected aquatic organisms. *Environmental Toxicology* **2007**, *22*, 480-486. https://doi.org/10.1002/tox.20290

131. Cheung, J.; Gary, E. N.; Shiomi, K.; Rosenberry, T. L. Structures of human acetylcholinesterase bound to dihydrotanshinone I and territrem B show peripheral site flexibility. *Med. Chem. Lett.* **2013**, *4* (11), 1091-1096. https://doi.org/10.1021/ml400304w

132. Nicolet, Y.; Lockridge, O.; Masson, P.; Fontecilla-Camps, J. C.; Nachon, F. Crystal structure of human butyrylcholinesterase and of its complexes with substrate and products. *J. Biol. Chem.* **2003**, *278* (42), 41141-41147. https://doi.org/10.1074/jbc.M210241200

133. Pettersen, E. F.; Goddard, T. D.; Huang, C. C.; Couch, G. S.; Greenblatt, D. M.; Meng, E. C.; Ferrin, T. E. UCSF Chimera--a visualization system for exploratory research and analysis. *J. Comput. Chem.* **2004**, *25* (13), 1605-1612. https://doi.org/10.1002/jcc.20084

134. Sanner, M. F. Python: a programming language for software integration and development. J. Mol. Graph. Model **1999**, *17* (1), 57-61. https://pubmed.ncbi.nlm.nih.gov/10660911/

135. Hanwell, M. D.; Curtis, D. E.; Lonie, D. C.; Vandermeersch, T.; Zurek, E.; Hutchison, G. R. Avogadro: an advanced semantic chemical editor, visualization, and analysis platform. *Journal of Cheminformatics* 2012, *4* (1), 17-33. https://doi.org/10.1186/1758-2946-4-17

136. O'Boyle, N. M.; Banck, M.; James, C. A.; Morley, C.; Vandermeersch, T.; Hutchison, G. R. Open Babel: An open chemical toolbox. *Journal of Cheminformatics* 2011, *3* (1), 33-46. https://doi.org/10.1186/1758-2946-3-33

137. Trott, O.; Olson, A. J. AutoDock Vina: improving the speed and accuracy of docking with a new scoring function, efficient optimization, and multithreading. *J. Comput. Chem.* **2010**, *31* (2), 455-461. https://doi.org/10.1002/jcc.21334

138. Franzblau, S. G.; Witzig, R. S.; McLaughlin, J. C.; Torres, P.; Madico, G.; Hernandez, A.; Degnan, M. T.; Cook, M. B.; Quenzer, V. K.; Ferguson, R. M.; Gilman, R. H. Rapid, low-

technology MIC determination with clinical *Mycobacterium tuberculosis* isolates by using the microplate Alamar Blue assay. *J. Clin. Microbiol.* **1998**, *36* (2), 362-366. https://doi.org/10.1128/jcm.36.2.362-366.1998

139. Schön, T.; Werngren, J.; Machado, D.; Borroni, E.; Wijkander, M.; Lina, G.; Mouton, J.; Matuschek, E.; Kahlmeter, G.; Giske, C.; Santin, M.; Cirillo, D. M.; Viveiros, M.; Cambau, E. Antimicrobial susceptibility testing of *Mycobacterium tuberculosis* complex isolates - the EUCAST broth microdilution reference method for MIC determination. *Clin. Microbiol. Infect.* **2020**, *26* (11), 1488-1492. https://doi.org/10.1016/j.cmi.2020.07.036
140. Miao, F.; Yang, X.-J.; Zhou, L.; Hu, H.-J.; Zheng, F.; Ding, X.-D.; Sun, D.-M.; Zhou, C.-D.; Sun, W. Structural modification of sanguinarine and chelerythrine and their antibacterial activity. *Natural Product Research* **2011**, *25* (9), 863-875. https://doi.org/10.1080/14786419.2010.482055
141. Lee, J.-K.; Cho, J.-G.; Song, M.-C.; Yoo, J.-Su.; Lee, D.-Y.; Yang, H.-J.; Han, K.-M.; Kim, D.-H.; Oh, Y.-J.; Jeong, T.-S.; Baek, N.-I. Isolation of Isoquinoline Alkaloids from the Tuber of *Corydalis turtschaninovii* and their Inhibition Activity on Low Density Lipoprotein Oxidation. *Journal of the Korean Society for Applied Biological Chemistry* **2009**, *52*, 646-654. https://doi.org/10.3839/jksabc.2009.108
142. Sai, C.-M.; Li, D.-H.; Li, S.-G.; Han, T.; Guo, Y.-Z.; Pei, Y.-H.; Bai, J.; Jing, Y.-K.; Li, Z.-L.; Hua, H.-M. Racemic alkaloids from *Macleaya cordata*: structural elucidation, chiral resolution, and cytotoxic, antibacterial activities. *RSC Advances* **2016**, *6* (47), 41173-41180. https://doi.org/10.1039/C6RA05423D
143. Dostál, J.; Táborská, E.; Slavík, J.; Potáček, M.; de Hoffmann, E. Structure of Chelerythrine Base. *Journal of Natural Products* **1995**, *58* (5), 723-729. https://doi.org/10.1021/np50119a010
144. Su, Y.; Li, S.; Li, N.; Chen, L.; Zhang, J.; Wang, J.-R. Seven alkaloids and their antibacterial activity from *Hypecoum erectum* L. *J. Med. Plants. Res*. **2011**, *5* (22), 5428-5432. https://doi.org/10.5897/JMPR.9001127
145. Blanco, O.; Castedo, L.; Cortes, D.; Carmen, V. M. Alkaloids from *Sarcocapnos saetabensis*. *Phytochemistry* **1991**, *30* (6), 2071-2074. https://doi.org/10.1016/0031-9422(91)85069-C
146. Arafa, A.; Mohamed, M.; Eldahmy, S. I. The aerial parts of yellow horn poppy *(Glaucium flavum* Cr.*)* growing in Egypt: Isoquinoline alkaloids and biological activities. *J. Pharm. Sci. & Res.* **2016**, *8*, 323-332. https://www.semanticscholar.org/paper/The-Aerial-Parts-of-Yellow-Horn-Poppy-(Glaucium-in-Arafa-Mohamed/735b53b372cb131be010a88a1f774c4e520ae637
147. Ferreira, M. L. R.; de Pascoli, I. C.; Nascimento, I. R.; Zukerman-Schpector, J.; Lopes, L. M. X. Aporphine and bisaporphine alkaloids from *Aristolochia lagesiana var. intermedia*. *Phytochemistry* **2010**, *71* (4), 469-478. https://doi.org/10.1016/j.phytochem.2009.11.010
148. Nardelli, V.B.; de Souza, C. A. S.; Chaar, J. d. S.; Koolen, H. H. F.; da Silva, F. M. A.; Costa, E. V. Isoquinoline-derived alkaloids and one terpene lactone from the leaves of *Duguetia pycnastera* (Annonaceae). *Biochemical Systematics and Ecology* **2021**, *94*, 104206. https://doi.org/10.1016/j.bse.2020.104206
149. Pacheco, J. C. O.; Lahm, G.; Opatz, T. Synthesis of Alkaloids by Stevens Rearrangement of Nitrile-Stabilized Ammonium Ylides: (±)-Laudanosine, (±)-Laudanidine, (±)-Armepavine, (±)-7-Methoxycryptopleurine, and (±)-Xylopinine. *The Journal of Organic Chemistry* **2013**, *78* (10), 4985-4992. https://doi.org/10.1021/jo400659n
150. Schrittwieser, J. H.; Resch, V.; Wallner, S.; Lienhart, W.-D.; Sattler, J. H.; Resch, J.; Macheroux, P.; Kroutil, W. Biocatalytic Organic Synthesis of Optically Pure (S)-Scoulerine and Berbine and Benzylisoquinoline Alkaloids. *The Journal of Organic Chemistry* **2011**, *76* (16), 6703-6714. https://doi.org/10.1021/jo201056f
151. Kim, J. H.; Ryu, Y. B.; Lee, W. S.; Kim, Y. H. Neuraminidase inhibitory activities of quaternary isoquinoline alkaloids from *Corydalis turtschaninovii* rhizome. *Bioorganic & Medicinal Chemistry* **2014**, *22* (21), 6047-6052. https://doi.org/10.1016/j.bmc.2014.09.004

152. Patel, M. B.; Mishra, S. M. Magnoflorine from *Tinospora cordifolia* stem inhibits α-glucosidase and is antiglycemic in rats. *Journal of Functional Foods* **2012**, *4* (1), 79-86. https://doi.org/10.1016/j.jff.2011.08.002

153. Mishra, S. K.; Tripathi, G.; Kishore, N.; Singh, R. K.; Singh, A.; Tiwari, V. K. Drug development against tuberculosis: Impact of alkaloids. *Eur. J. Med. Chem.* **2017**, *137*, 504-544. https://doi.org/10.1016/j.ejmech.2017.06.005

154. Omosa, L. K.; Nchiozem-Ngnitedem, V.-A; Mukavi, J.; Atieno, O. B.; Ombui, N. H.; Hashim, I.; Obegi, M. J.; Efferth, T.; Spiteller, M. Cytotoxic alkaloids from the root of *Zanthoxylum paracanthum* (Mildbr.) Kokwaro. Nat. Prod. Res. **2021**, *36* (10), 2518-2525. https://doi.org/10.1080/14786419.2021.1913586

155. Rodríguez-Guzmán, R.; Fulks, L. C.; Radwan, M. M.; Burandt, C. L.; Ross, S. A. Chemical constituents, antimicrobial and antimalarial activities of *Zanthoxylum monophyllum. Planta Med.* **2011**, *77* (13), 1542-1544. https://doi.org/10.1055/s-0030-1270782

156. Dostál, J., Slavík, J.; Potáček, M.; Marek, R.; Humpa, O.; Sklenář, V.; Toušek, J.; Hoffmann, E.; Rozenberg, R. Structural Studies of Chelirubine and Chelilutine Free Bases. *Collect. Czech. Chem. Commun.* **1998**, *63*, 1045-1055. https://doi.org/10.1135/cccc19981045

157. Whiteley, C.G.; Daya, S. Protein Ligand Interactions. Part 5: Isoquinoline Alkaloids as Inhibitors of Acetylcholinesterase from Electrophorus Electricus. *Journal of Enzyme Inhibition* **1995**, *9* (4), 285-294. https://doi.org/10.3109/14756369509036557

158. Khorana, N.; Markmee, S.; Ingkaninan, K.; Ruchirawat, S.; Kitbunnadaj, R.; Pullagurla, M. R. Evaluation of a new lead for acetylcholinesterase inhibition. *Medicinal Chemistry Research* **2009**, *18* (3), 231-241. https://doi.org/10.1007/s00044-008-9122-3

159. Nordberg, A.; Ballard, C.; Bullock, R.; Darreh-Shori, T.; Somogyi, M. A review of butyrylcholinesterase as a therapeutic target in the treatment of Alzheimer's disease. *Prim. Care Companion CNS Disord*. **2013**, *15* (2), PCC12r01412. https://doi.org/10.4088/PCC.12r01412

160. Tuzimski, T., Petruczynik, A.; Szultka-Młyńska, M.; Sugajski, M.; Buszewski, B. Isoquinoline Alkaloid Contents in *Macleaya cordata* Extracts and Their Acetylcholinesterase and Butyrylcholinesterase Inhibition. *Molecules* **2022**, *27*, 3606-3601. https://doi.org/10.3390/molecules27113606

161. Cahlíková, L.; Hulová, L.; Hrabinová, M.; Chlebek, J.; Hošťálková, A.; Adamcová, M.; Šafratová, M.; Jun, D.; Opletal, L.; Ločárek, M.; Macáková, K. Isoquinoline alkaloids as prolyl oligopeptidase inhibitors. *Fitoterapia* **2015**, *103*, 192-196. https://doi.org/10.1016/j.fitote.2015.04.004

162. Tarragó, T., Kichik, N.; Claasen, B.; Prades, R.; Teixidó, M.; Giralt, E. Baicalin, a prodrug able to reach the CNS, is a prolyl oligopeptidase inhibitor. *Bioorganic & Medicinal Chemistry* **2008**, *16* (15), 7516-7524. https://doi.org/10.1016/j.bmc.2008.04.067

163. Gupta, M.; Lee, H. J.; Barden, C. J.; Weaver, D. F. The blood–brain barrier (BBB) score. *J. Med. Chem.* **2019**, *62* (21), 9824–9836. https://doi.org/10.1021/acs.jmedchem.9b01220

164. Di, L.; Kerns, E. H.; Fan, K.; McConnell, O. J.; Carter, G. T. High throughput artificial membrane permeability assay for blood–brain barrier. *European Journal of Medicinal Chemistry* **2003**, *38* (3), 223-232. https://doi.org/10.1016/S0223-5234(03)00012-6

165. Okunade, A. L.; Hufford, C. D.; Richardson, M. D.; Peterson, J. R.; Clark, A. M. Antimicrobial properties of alkaloids from *Xanthorhiza simplicissima. J. Pharm. Sci.***1994**, *83* (3), 404-406. https://doi.org/10.1002/jps.2600830327

166. Gentry, E. J.; Jampani, H. B.; Keshavarz-Shokri, A.; Morton, M. D.; Vander, V. D., Telikepalli, H.; Mitscher, L. A.; Shawar, R.; Humble, D.; Baker, W. Antitubercular Natural Products: Berberine from the Roots of Commercial Hydrastis canadensis Powder. Isolation of Inactive 8-Oxotetrahydrothalifendine, Canadine, β-Hydrastine, and Two New Quinic Acid Esters, Hycandinic Acid Esters-1 and -2. *J. Nat. Prod.* **1998**, *61* (10), 1187-1193. https://doi.org/10.1021/np9701889

167. Wijaya, V., Janďourek, O.; Křoustková, J.; Hradiská-Breiterová, K.; Korábečný, J.; Sobolová, K.; Kohelová, E; Hošťálková, A.; Konečná, K.; Šafratová, M.; Vrabec, R.; Kuneš, J.; Opletal, L.; Chlebek, J.; Cahlíková, L. Alkaloids of *Dicranostigma franchetianum* (Papaveraceae) and Berberine Derivatives as a New Class of Antimycobacterial Agents. *Biomolecules* **2022**, *12* (6), 844-856. https://doi.org/10.3390/biom12060844

168. Sobolová, K.; Hrabinová, M.; Hepnarová, V.; Kučera, T.; Kobrlová, T.; Benková, M.; Janockova, J.; Doležal, R.; Prchal, L.; Benek, O.; Mezeiová, E.; Jun, D.; Soukup, O.; Korábečný, J. Discovery of novel berberine derivatives with balanced cholinesterase and prolyl oligopeptidase inhibition profile. *Eur. J. Med. Chem*. **2020**, *203*, 112593. https://doi.org/10.1016/j.ejmech.2020.112593

169. Kim, S. H.; Lee, S. J.; Lee, J. H.; Sun, W. S.; Kim, J. H. Antimicrobial activity of 9-O-acyl- and 9-O-alkylberberrubine derivatives. *Planta Med.* **2002,** *68* (3), 277-281. https://doi.org/10.1055/s-2002-23128

170. Maafi, N.; Mamun, A. A.; Janďourek, O.; Maříková, J.; Breiterová, K.; Diepoltová, A.; Konečná, K.; Hošťálková, A.; Hulcová, D.; Kuneš, J.; Kohelová, E.; Koutová, D.; Šafratová, M.; Nováková, L.; Cahlíková, L. Semisynthetic Derivatives of Selected Amaryllidaceae Alkaloids as a New Class of Antimycobacterial Agents. *Molecules* **2021**, *26* (19), 6023-6043. https://doi.org/10.3390/molecules26196023